PLASMODESMAL REGULATOR *PDLP5* CONNECTS PHYTOHORMONE SIGNALING TO SYMPLASMIC TRANSPORT IN *ARABIDOPSIS THALIANA*

by

Ross Sager

A dissertation submitted to the Faculty of the University of Delaware in partial fulfillment of the requirements for the degree of Doctor of Philosophy in Plant and Soil Sciences

Fall 2017

PLASMODESMAL REGULATOR *PDLP5* CONNECTS PHYTOHORMONE SIGNALING TO SYMPLASMIC TRANSPORT IN *ARABIDOPSIS THALIANA*

by

Ross Sager

Approved: _____
Erik Ervin, Ph.D.
Chair of the Department of Plant and Soil Sciences

Approved: _____
Mark Rieger, Ph.D.
Dean of the College of Agriculture & Natural Resources

Approved: _____
Ann L. Ardis, Ph.D.
Senior Vice Provost for Graduate and Professional Education

I certify that I have read this dissertation and that in my opinion it meets the academic and professional standard required by the University as a dissertation for the degree of Doctor of Philosophy.

Signed: _____

Jung-Youn Lee, Ph.D.
Professor in charge of dissertation

I certify that I have read this dissertation and that in my opinion it meets the academic and professional standard required by the University as a dissertation for the degree of Doctor of Philosophy.

Signed: _____

Harsh Bais, Ph.D.
Member of dissertation committee

I certify that I have read this dissertation and that in my opinion it meets the academic and professional standard required by the University as a dissertation for the degree of Doctor of Philosophy.

Signed: _____

Janine Sherrier, Ph.D.
Member of dissertation committee

I certify that I have read this dissertation and that in my opinion it meets the academic and professional standard required by the University as a dissertation for the degree of Doctor of Philosophy.

Signed: _____

Kim Gallagher, Ph.D.
Member of dissertation committee

ACKNOWLEDGMENTS

First and foremost, I would like to thank my advisor, Dr. Jung-Youn Lee, for pushing me and helping me to "grow up" from a naïve college kid into an *actual* scientist. I would like to thank the members of my Committee, Dr. Harsh Bais, Dr. Janine Sherrier, and Dr. Kim Gallagher, for their suggestions and support of my project. Thank you to all of the professors who taught me during my time at the University of Delaware, for reinforcing my love of science. Special thanks to all of the faculty and staff of the Delaware Biotechnology Institute, including Dr. Jeff Caplan, who was essential for making sure my images were perfect.

Thank you to my former lab members, especially Dr. Sung-Ki Cho, for teaching me, among many things, that patience is the most important lab technique, and Dr. Feng Pan, who acted as a friend and confidant in those tough early years. Thank you so much to my current lab family, Dr. Weier Cui and Xu Wang, for being great friends and scientists I could count on to help me with my questions about pretty much anything.

I'd like to thank A. Murphy, A. Middleton, and D. Wells for helpful and stimulating discussions on our data. I would also like to thank the following for seeds: J. Reed for shy2-2; B. Bartel for iaa281. K.H. and M.J.B. acknowledge the support of the Biotechnology and Biological Sciences Research Council (BBSRC) and Engineering and Physical Sciences Research Council (EPSRC) funding to the Centre for Plant Integrative Biology (CPIB) BB/D019613/1; and K.H. from the BBSRC Professorial Research Fellowship funding to M.J.B. grant BB/G023972/1; and Royal

Society-Wolfson Merit Award to M.J.B. This research was supported by the grants provided partially by the National Science Foundation (IOB 0954931) and by the grants from the IDeA program of the National Institute of General Medical Sciences (P30 GM103519) to J.-Y. L.

Finally, I would like to thank my family, especially my incredibly supportive and patient wife, Melanie, without whom I would be lost.

TABLE OF CONTENTS

LIST OF TABLES

LIST OF FIGURES

ABSTRACT

The characterization of *Plasmodesmata Localized Protein 5* (*PDLP5*) has revealed that it has important connections to two hormone signaling pathways: salicylic acid (SA) basal defense, and auxin-regulated lateral root emergence. *PDLP5* is expressed within the SA defense pathway under control of the genes *EDS1*, *ICS1*, and *NPR1*. *PDLP5* both upregulates, and is upregulated by, SA. Overexpressing *PDLP5* activates SA accumulation and defense signaling genes, stunting plant growth and causing spontaneous lesion formation in the leaves. In roots, *PDLP5* expression is indirectly correlated with the lateral root emergence rate and root branching. *PDLP5* is inducible by auxin, and is expressed in a very specific set of endodermal, cortical, and epidermal cells overlying emerging LRP in an auxin-dependent manner. The timing and location of fluorescent auxin sensors in the LRP-overlying cells increased in *pdlp5-1* and was reduced in *35S:PDLP5*. Using an endodermal tissue-specific promoter expressing diffusible GFP, it was shown that direct upregulation of *PDLP5* by either SA treatment, or *pER8:PDLP5* induction by estradiol, significantly reduced the movement of GFP into neighboring tissue layers. Overall, PDLP5 appears to be an important regulator connecting symplasmic communication to hormone signaling in *Arabidopsis thaliana*.

Chapter 1

LITERATURE REVIEW: A SUMMARY OF THE PLANT HORMONE AUXIN AND ITS FUNCTIONS IN THE PLANT ROOT, WITH A FOCUS ON LATERAL ROOT DEVELOPMENT

1.1 Introduction

Auxin is an essential plant hormone, functioning in the majority of plant growth and developmental processes. Auxin signaling occurs both at the local level, for example during cell wall expansion and cell polarity establishment, as well as in large-scale processes, such as during tissue differentiation and organ formation. To describe every plant function involving auxin is beyond the scope of this chapter, but there are many other reviews providing details on auxin signaling in a variety of plant developmental processes (Teale et al., 2006; Leyser, 2010; Sauer et al., 2013; Enders and Strader, 2015). Instead, this literature review will specifically explore the role of auxin during root growth and development, including its transport into and movement through the root, and its activity within the plant root, with a focus on auxin-regulated lateral root organ development and emergence.

1.2 Auxin is Produced in Green Source Tissues and Moves through the Phloem into Root Sink Tissues

Almost all of the auxin in plants is first synthesized in the green tissues. A series of enzymatic reactions in the chloroplasts, starting with chorismate, eventually lead to the creation of the amino acid tryptophan (Zhao, 2010; Mano and Nemoto, 2012; Zhao, 2014). Tryptophan has long been established as the major auxin

precursor; studies have shown that the majority of radiolabeled tryptophan is converted into radiolabeled indole-3-acetic acid (IAA, the most common natural form of auxin within the plant) (Sherwin and Purves, 1969). Tryptophan is exported into the cytosol, where it becomes the substrate for *Tryptophan Aminotransferase of Arabidopsis* (*TAA*) enzymes, converting it into indole-3-pyruvic acid (IPA) (Won et al., 2011). IPA then becomes the substrate of *Yucca* (*YUC*) enzymes, which convert it into IAA (Mashiguchi et al., 2011). The Tryptophan→IPA→IAA pathway seems to be the main synthesis pathway for the IAA that functions in growth and developmental processes (Zhao, 2012).

The IAA produced in the green tissues is next loaded into the phloem for long-distance transport. One of the critical proteins involved was found to be a type of auxin transport protein, called *Auxin Resistant 1* (*AUX1*) (Marchant et al., 2002). *AUX1* is expressed in the vascular elements of leaves. In *aux1* mutants, the amount of IAA significantly increases, but only in the shoot tissues. Furthermore, root morphology in *aux1* is altered, with few to no lateral roots emerging; treating the roots with auxin rescued lateral root emergence. These results demonstrated that AUX1 is essential for loading the IAA into the phloem to be transported into the root.

Once IAA is loaded into the phloem, non-directional bulk flow carries it into sink tissues across the plant, especially the root tips. Yet bulk flow alone cannot bring auxin to the many spatially-distinct tissues and organ developmental sites within the root where it is required. For this, specialized auxin transport proteins are expressed in a tissue-specific manner to guide root growth and organogenesis.

1.3 Auxin Transport Proteins Control the Movement and Redistribution of Auxin in the Roots

1.3.1 The Chemiosmotic Model of Transcellular Auxin Transport

During bulk flow transport, auxin moves through the sieve pores of phloem elements, a type of symplasmic transport. However, in order for enough auxin to leave the vasculature and reach other tissues, a different type of transport, called "transcellular" transport, is needed. Transcellular transport occurs when a molecule is exported/diffuses from the cytosol into the extracellular space, then is imported/diffuses into the cytosol of another cell (Robert and Friml, 2009). Although transcellular transport utilizes the extracellular space, it differs from apoplastic transport in that the molecules only diffuse short distances before moving back into the intracellular space of the next cell.

Based on the existing chemical data about IAA (Rubery and Sheldrake, 1974; Raven, 1975), the "chemiosmotic model" was created that best describes how auxin moves via the transcellular pathway (Goldsmith, 1977). In a neutral environment, the weak acid IAA is typically in the negatively charged form, IAA-. IAA- is membrane-impermeable, trapping it inside the neutral (~ pH 7) cytosol of plant cells. However, in an acidic environment, IAA is protonated (IAA-H), a form which can diffuse through membranes. Thus, in the extracellular space (~ pH 5.5), IAA-H can diffuse freely between cell walls and membranes until it enters the cytosol of another cell, when IAA- becomes trapped again. Thus, by using proteins that export IAA- into the extracellular space, plant cells can keep auxin moving transcellularly.

1.3.2 Auxin Gradients May Influence the Polarity of Both Individual Plant Cells and Whole Tissues

The chemiosmotic model explains how auxin can move transcellularly, but the directional targeting of auxin to precisely where it is needed depends on the polar arrangement of auxin-exporting and –importing proteins on the plasma membrane (Dhonukshe, 2009). Multiple mechanisms have been implicated in controlling cell polarity and the polar localization of proteins in plants, including: polar endocytosis; polar secretion; and cell wall properties (Dettmer and Friml, 2011; Korbei and Luschnig, 2011; Langowski et al., 2016). Polar endocytosis describes the process by which endocytic machinery recycles the proteins within a highly specific polar plasma membrane domain, then targets the recycled proteins back to the same domain (Kleine-Vehn et al., 2011); this type of regulation will be explored more in the PIN section of this chapter. For polar secretion, the newly-synthesized or recycled proteins are specifically targeted to certain polar plasma membrane domains. This was explored by tagging polar proteins with fluorescent markers like GFP, then photobleaching the cells in which they are expressed and measuring their Fluorescent Recovery After Photobleaching (FRAP). The results of mathematical models showed that the recovery rates of polar proteins at their designated plasma membrane domains were significantly faster than those of non-polar proteins, strongly suggesting that polar secretion is a factor controlling polar protein localization (Langowski et al., 2016). Finally, two recent studies revealed that mutational or chemical disruption of cell wall components like cellulose, as well as reduction or elimination of plasma membrane/cell wall connections, strongly reduced or eliminated the polar localization of auxin transport proteins, implicating the cell wall as a major factor regulating protein polarity (Feraru et al., 2011; Martiniere et al., 2012).

All of the above mechanisms appear to be mostly required for *maintaining* polarity; the initial establishment of polarity in plant cells is still mysterious. However, there is evidence to suggest that an intracellular auxin gradient may be the crucial early step for initial plant cell polarity establishment (Tanaka et al., 2006). In this scenario, auxin-sensing proteins within an individual plant cell detect the variation in auxin levels between each end of the cell, then regulate intracellular development differently at each end in response, leading to a polarized cell (van Berkel et al., 2013). At present, these hypothetical auxin-sensing proteins involved in the initial establishment of plant cell polarity have not been uncovered.

Auxin gradient-induced plant cell polarity is an important part of the "canalization hypothesis," which was developed to describe how an entire tissue(s) might develop in a polar manner via auxin regulation (Sachs, 1991). The canalization hypothesis states that, during the earliest stages of tissue development, the initial gradient of auxin establishes a polarity in individual cells, including polarity in the localization of auxin transport proteins. The polar transport of auxin through these proteins further reinforces the auxin gradient, affecting the cells in the direction of auxin flow, but not the surrounding cells (Sachs, 1986). The positive feedback of cell polarity and polar auxin transport eventually creates an entire polar tissue, with cell shapes and intracellular components designed to maximize transport in a certain direction. The canalization hypothesis was based on observations of vascular element formation (Sachs, 1981), though it could be applied to other plant tissues as well.

The reinforcement of the auxin gradient by polar auxin transporter localization is a key aspect of the canalization hypothesis, and indeed there is evidence that an intracellular auxin gradient induces polar distribution of auxin transport proteins

(Sauer et al., 2006). In this study, exogenous auxin treatments were sufficient to redirect the localization of polar auxin transport proteins within certain cell types towards the area of auxin application (Sauer et al., 2006). Importantly, the repolarization of these auxin transport proteins induced new tissue growth in the direction of auxin export, and was even required for the formation of lateral roots (an aspect that will be described more in later sections of this chapter). Though these results are promising, the cellular components involved in connecting the initial intracellular auxin gradient to the polarization of the auxin transport proteins are currently unknown.

In contrast to the many undiscovered components of early auxin-based plant cell polarization, the types and behaviors of numerous auxin transport proteins themselves have been well-documented. Three general subtypes exist: Auxin Efflux Carriers, Auxin Influx Carriers, and ATP-Binding Cassette transporters (Zazimalova et al., 2010). The first two subtypes will be highlighted in this review due to their major functions in lateral root emergence (aspects that will be explored in later sections).

1.3.3 The PIN Family of Polar Auxin Efflux Carriers

The *Pin-formed* (*PIN*) family derives its name from the phenotype of the first mutant discovered, *pin1*, which has an inflorescence completely devoid of side branches or apical buds, giving it a pin-like appearance (Křeček et al., 2009). The first indication that these proteins were involved in polar auxin transport came when a study of wild type (WT) plant growth on media containing polar auxin transport-inhibiting compounds revealed they had a very similar inflorescence phenotype to *pin1* mutants grown on normal media (Okada et al., 1991). The authors compared the

movement of radiolabeled IAA through cut inflorescence stems and found that, not only did IAA movement in WT progress in a basipetal direction, even against gravity, but that IAA movement was reduced by up to 93% in *pin1* mutants compared to WT (Okada et al., 1991). Several years later, *PIN1* was identified and cloned, and immunofluorescent imaging of *Arabidopsis* stem tissue sections revealed that PIN1 was located specifically at the basal end of parenchymal xylem and cambial cell plasma membranes (Galweiler et al., 1998). The results from these two studies proved that PIN1 is a polar auxin transport protein.

The other PIN genes were soon uncovered based on their homology to PIN1. *Arabidopsis* currently has eight identified PIN proteins, all of which are auxin efflux carriers, meaning they transport IAA out of plasma membrane compartments (Petrasek and Friml, 2009). The characteristics shared by all members of the *Arabidopsis* PIN family include two transmembrane hydrophobic regions, one on either side of an intracellular hydrophilic region called the "loop" due to its shape (Habets and Offringa, 2014). The loop portion of the protein can be short or long, and this difference signifies the function of the PIN; "short PINs" almost always localize within the endoplasmic reticulum membrane, while "long PINs" are all polar auxin efflux carriers that localize to the plasma membrane. The exact functions of the short PINs—PIN5, PIN6, and PIN8—are unclear, but they seem to reduce the cytosolic pool of IAA by sequestering it in the endoplasmic reticulum, so it has been suggested that in certain cases they may act to modulate the cytosolic auxin concentration (Habets and Offringa, 2014). The long PINs—PIN1, PIN2, PIN3, PIN4, and PIN7—are responsible for the polar auxin flux that controls tissue development, organ

emergence, gravitropism, and other functions (Kovrizshnykh et al., 2015), and they will be the focus of this section.

Several components responsible for maintaining long PIN polar localization have been identified (Qi and Greb, 2017). While it was originally shown that PIN secretion to the plasma membranes occurred in a non-polar manner prior to relocalization to plasma membrane subdomains, failed attempts to get these results consistently have thrown this data into question (Dhonukshe et al., 2008, 2014). What has been proven is that a process called (clathrin-mediated) polar endocytosis ensures that PIN localization is maintained at the proper membrane domain (Kitakura et al., 2011). It was first discovered that the mutant of an *ADP-Ribosylation Factor for G-proteins-GDP/GTP Exchange Factor* called *GNOM* (*GNOM ARF-GEF*), a vesicle budding regulator, showed a strong loss of PIN1 polar localization in *A. thaliana* embryos (Steinmann et al., 1999). Furthermore, inhibiting GNOM-ARF-GEF-mediated vesicle formation by treating roots with Brefeldin A (BFA) also eliminated basal PIN polarization (Geldner et al., 2001). Finally, a transgenic GNOM-ARF-GEF line insensitive to BFA did not lose PIN polarization (Geldner et al., 2003). These results combined proved that PIN1 endocytic recycling via GNOM-ARF-GEF is required for its polar localization.

The phosphorylation status of PINs is another factor controlling their polar localization (Armengot et al., 2016). Much of this research has focused on PIN1, which localizes to the basal side of root stele cells under normal conditions. First, it was found that knocking out the serine/threonine protein kinase *PINOID* (*PID*) caused a *pin1*-like phenotype in plants (Christensen et al., 2000). However, when PID was overexpressed, PIN1 localization significantly increased at the apical end of these cells

instead (Christensen et al., 2000; Dhonukshe et al., 2010; Huang et al., 2010). In contrast, *Protein Phosphatase 2 subunit A* (*PP2A*) loss-of-function mutants have the PIN1 basal-to-apical polarity shift (Michniewicz et al., 2007). PID and PP2A colocalize with PIN proteins at the plasma membrane, competing to phosphorylate/dephosphorylate several major conserved serine/threonine sites (Weller et al., 2017), especially Ser337 and/or Thr340 (Zhang et al., 2010a), along the PIN central hydrophilic loop (Michniewicz et al., 2007; Kleine-Vehn et al., 2009).

The results from the findings above provide a basic model for PIN polarity regulation. PINs phosphorylated by PID (and similar kinases) preferentially localize to the apical side of plant cells, while PINs dephosphorylated by PP2A (and similar phosphatases) favor the basal side. GNOM-ARF-GEF, essential for recycling and redistributing the PINs to the basal plasma membrane, likely has a preference for dephosphorylated PINs (Kleine-Vehn et al., 2009), and thus maintains PIN basal polarity through polar endocytosis; a currently unknown, but likely similar mechanism to GNOM-ARF-GEF, would maintain polarity of apical PINs. An imbalance between any of these factors leads to PIN mislocalization and faulty auxin distribution, causing severe growth phenotypes.

1.3.3.1 PINs Function Together to Create an Auxin Maximum in Primary and Lateral Root Tips

The auxin-mediated maintenance of the meristematic zone in the primary and lateral root tips is vital for the continued growth and differentiation of the plant root (Prasad and Dhonukshe, 2013). Bulk flow through the phloem may bring auxin from the shoot into the root tip, but this alone would not provide the precise targeting of

auxin to the meristematic cells. For this, the polar auxin carriers of the long PIN subfamily are needed to target and recirculate auxin into the root tips.

Each of the long PINs has a specific role in recirculating auxin in root tips (Feraru and Friml, 2008). PIN1 specifically localizes to only the basal sides of the root stele cells (Xu et al., 2006), and so it is crucial for focusing the acropetal transport of auxin towards the root tip. PIN2 actually has dual polar localizations in the root tip: it localizes to the apical sides of the lateral root cap and epidermal cells, but the basal side of immature cortical cells (Muller et al., 1998). PIN3 and PIN7 are basally localized in the stele, acting redundantly with PIN1, and though they are both also expressed in the columella, they have non-polar localization there (Friml et al., 2002a; Blilou et al., 2005; Bruno et al., 2017). PIN4 can localize in both a non-polar and basal fashion in the columella and quiescent center (Friml et al., 2002b; Blilou et al., 2005).

Combining the effects of these efflux carriers: basal PIN1 (and to a lesser extent PIN3/PIN7) in the stele transports auxin acropetally from the phloem directly into the quiescent center and surrounding meristematic cells to maintain the "stemness" of these cells. PIN3, PIN4 and PIN7 draw auxin from the columella and move it back into the surrounding lateral root cap and epidermal cells, where apical PIN2 directs auxin basipetally towards the shoot. However, basal PIN2 in the immature cortical cells of the root tip also works to recirculate some of this auxin acropetally again, reinforcing the PIN1/PIN3/PIN7 stele flux. This model explains how auxin is kept concentrated, yet balanced, in such a fashion as to guide meristem growth and differentiation (Blilou et al., 2005). Importantly, once lateral roots have developed and grown enough, the same model applies to their outward growth.

1.3.4 The AUX/LAX Family of Auxin Influx Carriers

Hormones in plant cells often must reach a certain threshold before they activate downstream signaling, and in the case of auxin, this intracellular concentration increase is often dependent on the Auxin Influx Carrier family of proteins (Swarup and Peret, 2012). *AUX1* was discovered first, followed by three members called *Like-Aux1 1* (*LAX1*), *LAX2*, and *LAX3*, found based on their homology to AUX1 (Peret et al., 2012b). The AUX1 protein was found to be purified along with membrane fractions from root cells, and through fluorescent tagging was found to colocalize with membrane markers at the plasma membrane (Swarup et al., 2004). To determine the protein structure, the authors designed multiple transgenic AUX1-YFP lines, attaching a pH-sensitive YFP to various predicted AUX1 protein subdomains. The pH-sensitive YFP would be repressed in a low pH environment such as the apoplastic space, so it could be determined by the presence or absence of fluorescence in each of the different AUX1-YFP lines whether a certain subdomain was intracellular or extracellular. In this way, AUX1 was found to have eleven transmembrane domains, a cytoplasmic N-terminal and extracellular C-terminal (Swarup et al., 2004).

1.3.4.1 AUX/LAX Proteins in Root Tips Enable Auxin Maximum to Promote Meristematic Cell Growth

In contrast to the polar localization of PINs, the AUX/LAX proteins in roots are not typically polar, so their expression within a cell promotes auxin influx from all directions. This is essential for keeping an auxin maximum within the columella, quiescent center, and other required cells in the primary and lateral root tips (Eckardt, 2014). AUX1 was described previously in this chapter as necessary for loading auxin into the phloem in leaves and shoot tissue (Marchant et al., 2002); however, it was

found to also be important for unloading IAA in the roots. *AUX1* is expressed in the root columella and protophloem, and *aux1* mutants showed a marked reduction in IAA at the root tips (Swarup et al., 2001). LAX2 and LAX3 have distinct expression patterns in root tips; LAX2 is expressed in the columella, while LAX3 is weakly expressed in the columella but strongly in the root stele (Peret et al., 2012b). Mutations in *LAX2* had no adverse effects on root growth however, while *lax3* and *aux1* showed abnormalities in lateral root emergence and gravitropic responses (Swarup et al., 2005; Swarup et al., 2008). The roles of AUX1 and LAX3 in lateral root emergence will be explored in later sections of this chapter.

1.4 Auxin Control of Lateral Root Development

Almost every aspect of lateral root (LR) growth is controlled by auxin signaling (Overvoorde et al., 2010; Van Norman et al., 2013; Atkinson et al., 2014). The following sections describe the major components contributing to auxin-sensitive gene upregulation and auxin transport during the process of lateral root primordium (LRP) formation, development, growth and emergence.

1.4.1 LRP Founder Cell Specification

The initial cells that develop into lateral roots lie within the xylem pole pericycle (XPP) tissue. The process of XPP growth into LRP is not continuous; the first step is the specification of what are called the lateral root founder cells (FCs), which remain undivided for a brief period before they truly begin the LRP growth process. The following key studies have better defined the role of auxin and other signals in the process of FC specification.

1.4.1.1 Oscillating Gene Expression in the Root Basal Meristem, Regulated by Unknown Signal Pulses, Creates the "Pre-Branch Sites" that Become FCs

Experiments using the artificial auxin-sensing promoter DR5 (Ulmasov et al., 1997) demonstrated that auxin plays an important role in determining the point where XPP cells are first modified into FCs. The root basal meristem was known to be a zone of auxin-driven cellular differentiation (Swarup et al., 2005), so one group, who hypothesized that this area could have a major role in LR formation, transferred *DR5:GUS* seedlings to auxin-containing medium and observed when and where new auxin maxima first formed (De Smet et al., 2007). They found that after only 20 minutes, new auxin maxima formed in a very specific set of XPP cells in the basal meristem. They proceeded to grow *DR5:GUS* seedlings and harvest some of them every five hours, and found that this XPP auxin maxima in the basal meristem formed and dissipated at regular intervals. By marking the root tips of growing seedlings with toner ink particles at times corresponding to when the XPP auxin maxima were detected, they showed that these maxima correlated highly with where LRP eventually developed along the root (De Smet et al., 2007). This was corroborated using a live imaging time series to directly follow the fates of presumptive FCs in the *DR5:GFP* marker line (Dubrovsky et al., 2008). All *DR5:GFP*-expressing XPP cells in the basal meristem became FCs, which eventually developed into LRP; in contrast, zones without *DR5:GFP* expression never developed LRP (Dubrovsky et al., 2008).

Later experiments proved that while auxin is important for the process of FC specification, it is not sufficient on its own. Researchers used the DR5 promoter expressing luciferase (*DR5:Luc*) to detect oscillating waves of auxin along the length of living roots, with strong pulses in what they deemed the "oscillation zone," the same basal meristem region where FC specification was hypothesized to occur

(Moreno-Risueno et al., 2010). They dissected the oscillation zones of multiple roots at times corresponding to either the maximum or minimum intensity of the *DR5:Luc* pulse to perform microarray analyses; many genes fluctuated with the presence and absence of the pulse within the oscillation zone, including those related to the cell division, auxin responsive-transcription, and more. As the root continued to grow, the areas where the intensity of the pulse peaked eventually developed lateral roots; these "pre-branch" sites were marked by a lingering *DR5:Luc* signal in the XPP after the *DR5:Luc* pulses. All these cells developed into FCs, corroborating the results from Dubrovsky et al. (2008). However, when the group attempted to correlate the timing of *DR5:Luc* pulses with expression of endogenous auxin-responsive promoters, they found little overlap (Moreno-Risueno et al., 2010). Furthermore, auxin treatments of the oscillation zone during the time between *DR5:Luc* pulses showed that auxin could not designate a pre-branch site without the oscillating signal. These results suggested that while auxin may be needed for the eventual development of FCs into LRP at the pre-branch sites, it is not the source of the *DR5*-activiting signal pulses in the oscillation zone.

Intriguingly, newer studies have found that a carotenoid(s) is a necessary component downstream of the oscillating pulses that designate pre-branch sites. Researchers found that treatment of *A. thaliana* seedlings with carotenoid inhibitors caused diminished-LRP phenotypes (Van Norman et al., 2014). By studying the roots of multiple carotenoid biosynthesis mutants, as well treatments with carotenoid inhibitors, they found that repressing the *Carotenoid Cleavage Dioxygenases* (*CCDs*) of the beta-carotenoid pathway led to diminished-LRP phenotypes. The results suggested that the partially-redundant CCDs synthesize the carotenoid(s) involved in

correct pre-branch site formation (Van Norman et al., 2014), however the identity of the carotenoid(s) remains to be uncovered.

1.4.1.2 Auxin Produced in Root Cap Contributes to Pre-Branch Site Formation and FC Specification

The majority of the auxin controlling LRP development and LR emergence is produced in the shoot tissue before being transported into the root via the phloem, the root apex being a major sink tissue (Robert and Friml, 2009). It has been shown repeatedly that shoot removal and polar auxin transport inhibitors severely impair LR emergence (Reed et al., 1998; Casimiro et al., 2001; Bhalerao et al., 2002). However, recent research has proven that a root-based source of auxin is also required for the proper formation of the pre-branch sites that become the FCs (Van Norman, 2015).

The first study began by screening 10,000 auxin-like compounds for the ability to stimulate LRP formation, specifically by measuring the staining intensity of the cell division marker *Cyclin B1;1 (CYCB1;1)pro:GUS* in the XPP (De Rybel et al., 2012). The authors discovered naxillin, which upregulates a significant number of FC specification-related genes within the same root domain as the oscillation zone. They then screened a population of EMS-mutagenized seedlings for naxillin resistance, and found a mutation in *Indole-3-Butyric Acid Response 3* (*IBR3*), a biosynthesis gene for the auxin precursor indole-3-butyric acid (IBA) (Zolman et al., 2007). *IBR3*, and similar genes that convert IBA→IAA, had highly-specific expression in the root cap cells, and treating the roots of shoot-removed *Arabidopsis* seedlings with IBA significantly enhanced LRP formation and emergence. These results demonstrated that IAA produced in the root cap from IBA plays a significant role in FC specification (De Rybel et al., 2012).

In a follow-up study, the authors further tested if auxin perception controlled any aspect of the pre-branch site creation (Xuan et al., 2015). The auxin perception genes *Transport Inhibitor Response 1* (*TIR1*) and *Auxin-Related F-Box 2* (*AFB2*) (Parry et al., 2009) were found to be highly expressed in the oscillation zone; *tir1afb2* double mutants were severely hindered in lateral root formation, but not primary root growth. Furthermore, when *DR5:Luc* was expressed in the *tir1afb2* mutant, the bioluminescent expression was strongly reduced. Loss-of-function mutants of *IBR3* and other IBA→IAA biosynthesis enzymes also had repressed *DR5:Luc* bioluminescence, suggesting a diminished response to the oscillating pulse, and fewer LRP. *In silico* analyses for genes upregulated in the oscillation zone during the pulse and also responsive to IBA revealed *Membrane-Associated Kinase-Regulator 4* (*MAKR4*), which is expressed in pre-branch sites and FCs; *makr4-1* loss-of-function mutants had significantly fewer LRP. The authors conclude that root cap-produced IAA from IBA is required for the perception of the oscillating pulse, creating FCs via MAKR4 in the oscillation zone (Xuan et al., 2015).

1.4.1.3 Auxin-Responsive Genes in the XPP Control FC Specification

A critical piece of the genetic pathway controlling FC specification was discovered by performing a meta-analysis of existing data on auxin-upregulated genes expressed in xylem pericycle cells (De Rybel et al., 2010). One of the candidates was *GATA Transcription Factor 23* (*GATA23*). *GATA23pro:GUS* seedlings showed staining within XPP cells of the basal meristem and pre-branch sites. Importantly, when groups of seedlings germinated simultaneously with *DR5:GUS* seedlings were collected and stained in five-hour intervals, the timing of *GATA23* expression oscillated in pattern closely correlating to the *DR5:GFP* and *DR5:Luc* patterns

described in the previous section (De Smet et al., 2007; Dubrovsky et al., 2008; De Rybel et al., 2010; Moreno-Risueno et al., 2010). A *GATA23* RNAi line had greatly reduced lateral root formation, as did a gain-of-function mutant line of the transcriptional repressor *Indole-3-Acetic Acid Inducible 28* (*IAA28*) (Rogg et al., 2001). *GATA23pro:GUS* was not detectable when expressed in either the *iaa28-1* mutant background, or in a double mutant of two transcription factors under the control of IAA28, *Auxin Response Factor 7* (*ARF7*) and *ARF19* (De Rybel et al., 2010).

The combined results from this and the previous sections outline the major pathway for how FC identity is determined in *Arabidopsis* seedlings (Laskowski and ten Tusscher, 2017). In summary, oscillating pulses of an unknown signal move through the root and form periodic maxima within the basal meristem oscillation zone. Root cap-produced IBA→IAA perceives the signal, and triggers pre-branch site formation. IAA also represses IAA28, which activates ARF7 and ARF19, thereby upregulating GATA23 in the pre-branch sites and priming them to become FCs.

1.4.2 Lateral Root Initiation

At a later point during root growth, the FCs are stimulated into the first divisions of LR formation (Vermeer and Geldner, 2015). The divisions of the pericycle cells that act as the hallmark of lateral root initiation (LRI) had been observed for many years, but the genetic pathway controlling the process was unknown until recently (Dubrovsky et al., 2000).

1.4.2.1 The Genetic Pathway Controlling LRI in the Root Pericycle

The major players of LRI were discovered by analyzing mutants with severely impaired root development phenotypes. One such mutant led to the gene being dubbed *Solitary Root* (*SLR*), due to the total loss of LR formation; this was revealed to be a gain-of-function mutation in *IAA14* (Fukaki et al., 2002). The cell division marker line *CYCB1;1:GUS* revealed that in *slr-1* mutants, the initial divisions of LRI were not detected. *IAA14pro:GUS* was expressed along the length of the root in the vasculature, but was strongly upregulated in the FCs during LRI (Fukaki et al., 2002). The group designed a dexamethasone-inducible stabilized version of IAA14 (IAA14-GR) and expressed it under the *IAA14* promoter as well as an XPP-specific enhancer trap line expressing *IAA14-GR*, and found that induction led to the same repression of FC cell division and loss of LR as the mutant *slr-1* (Fukaki et al., 2005). Importantly, they found that IAA14 interacted with ARF7 and ARF19 in yeast, and when IAA14-GR was expressed under those promoters, the transgenic plants pheno-copied *arf7arf19* double mutants, which also lack LR formation (Fukaki et al., 2005; Wilmoth et al., 2005). Overexpressing cell cycle-progression regulators led to increased pericycle division but could not stimulate LR development in the *slr-1* background (Vanneste et al., 2005). These combined results reveal what is now generally agreed-upon to be one of the most important pathways for LRI: the auxin-triggered degradation of IAA14 in the pericycle, allowing ARF7 and ARF19 to upregulate genes controlling the differentiation of the FCs into a new LRP. In recent years, targets of auxin-regulated ARF7/19 during this process have been found, like *Lateral Organs Boundaries Domain 1*6 (*LBD16*), which is responsible for the first asymmetric divisions of the FCs that form the basis of the LRP (Okushima et al., 2007; Goh et al., 2012a).

1.4.2.2 Regulation of LRI from the Root Endodermis

Despite the majority of the steps during LRI taking place within the pericycle, there also seems to be a genetic pathway within the endodermal layer regulating the process. It had previously been discovered that *Short Hypocotyl 2* (*SHY2*), also called *IAA3*, had gain-of-function mutants with strongly-reduced LR emergence, suggesting that it acts as a transcriptional inhibitor (Tian and Reed, 1999). *SHY2* is expressed in the endodermal cells overlying LRP (Swarup et al., 2008), and plays an important part during LRP emergence, as will be discussed in later sections. However, it was found that the *shy2* gain of function mutants had an increased amount of auxin, LR initiation sites, and *LBD16* expression in the pericycle, even though no LRP developed (Goh et al., 2012b). As previously mentioned, *LDB16* is under the control of the *IAA14* and *ARF7/19* pathway during LRI, suggesting that SHY2 normally acts to inhibit auxin buildup within the pericycle and suppresses excess LRP formation; thus its inactivity promotes FC formation and LRI (Goh et al., 2012b).

Intriguingly, reactive oxygen species (ROS) have recently emerged as a possible signal for activating LRI. ROS can stimulate the activation of pre-branch sites and emergence of LRP (Orman-Ligeza et al., 2016). Not only can exogenous H_2O_2 treatment override the reduced LRP phenotype of *aux1lax3* double mutants, but cell wall remodeling enzymes were upregulated by treatments as well. Clearly, while auxin is critical for LRI, there are likely underlying signals, like ROS, working together with auxin, that have yet to be discovered.

1.4.3 LRP Development and Emergence

1.4.3.1 Polar Auxin Transport Guides Growth and Emergence of the LRP

The bulk flow of auxin through the phloem into the basal meristem is required for FC specification and LRI, but when the LRP is ready to begin outward growth, auxin must be targeted to both the LRP and the overlying cells in order for emergence to occur properly (Peret et al., 2009). The targeting of auxin to specific cells is carried out by auxin influx or efflux carriers (Robert and Friml, 2009), the latter of which are often expressed in a polar manner to establish the auxin gradients necessary for directional growth and specific cell differentiation in the developing lateral root tips (Feraru and Friml, 2008; Tanaka et al., 2013).

At first, how the auxin moving through the phloem from the shoot was targeted to sites of LRP development was unclear. Researchers studying a mutant of *AUX1* found that LR development was hindered, and when they created an *AUX1pro:GUS* line they found that this auxin influx carrier was expressed as early as in the FCs during LRI (Marchant et al., 2002). Furthermore, mutant *aux1* had severely hindered auxin movement into the root, and the combined results led them to conclude that AUX1 likely acted to transport shoot-derived auxin from the phloem into the young LRP, to promote division and differentiation (Marchant et al., 2002). AUX1 is assisted by PIN1, which is also expressed in early LRP and, as the dome forms, moves into a column within the center, directing auxin movement into the LRP apex to drive growth (Benkova et al., 2003; Omelyanchuk et al., 2016).

The polar auxin efflux transporter PIN3 is also expressed in the endodermis overlying the FCs during the initial divisions of the LRP. Researchers monitoring *PIN3pro:PIN3-GFP* expression during root development discovered that it is

transiently expressed within the earliest dividing cells of the LRP, as well as within the overlying endodermal cells (Marhavy et al., 2013). By expressing PIN3-GFP under the Scarecrow (SCR) promoter in the endodermis, then treating the roots with auxin, they discovered that PIN3 polarizes solely to the inner side of the endodermal tissue, meaning it normally transports auxin back towards the LRP. Furthermore, the *pin3* knockout mutant had decreased LRP emergence but increased FCs. They concluded that targeted auxin efflux from the endodermis into the FCs (or rather "reflux" since the source of the auxin is the FCs themselves) allows them to retain the specific auxin maximum required in those cells to grow and differentiate into an LRP (Marhavy et al., 2013).

During lateral root development, the auxin influx carrier LAX3 transports auxin into the cortical and epidermal cells above the developing LRP (Swarup et al., 2008). *LAX3pro:GUS* is specifically expressed in the LRP-overlying cortical and epidermal cells during emergence, and its expression there is dependent upon the auxin-based IAA14 and ARF7/19 pathway (Swarup et al., 2008). *LAX3* knockout mutants had a decreased LR emergence rate, but increased FC formation, compared to WT. Importantly, the expression of auxin-sensitive cell wall remodeling (CWR) enzymes, which modify the walls connecting the cells above the primordium so they separate cleanly (Peret et al., 2009), was greatly reduced in the *lax3* mutant background (Swarup et al., 2008). In a different study, the LRP apex was found to be the source of auxin driving *LAX3* expression in overlying cortical cells (Peret et al., 2013). Furthermore, the researchers used a mathematical model, combined with observation of *PIN3pro:GFP*, to demonstrate that *PIN3* polar auxin efflux out of the LRP-overlying cortical cells into the epidermal cells is essential for maintaining the

proper targeting of LAX3 to only the several most-overlying cortical cells. Therefore, LAX3 influx and PIN3 efflux of auxin maintain the exact balance in the specific overlying cortical and epidermal cells that leads to cell wall remodeling enzyme upregulation there, and thus cell separation (Peret et al., 2013).

1.4.3.2 Mechanical Changes in the Overlying Tissues Allow LRP Emergence

While the direction of auxin transport and upregulation of developmental pathways stimulates the growth of the LRP, certain mechanical changes must occur in the overlying cells if the LRP has any chance of emerging. One of the earliest essential events in allowing the progression of LRP development takes place in the overlying endodermis (Vermeer et al., 2014). Because the Casparian strip tightly connects the endodermal layer, the overlying cells cannot be easily separated. Instead, the cells undergo extensive volume loss and intracellular component shifting, as observed by various membrane markers for the vacuole, tonoplast, and plasma membrane; the volume loss suggested a great reduction in turgor pressure in the endodermal cells (Vermeer et al., 2014). By developing an endodermis-specific auxin-insensitive line called *CASP1pro:shy2-2*, they found that the LRP-overlying endodermal cells remained turgid longer. Importantly, this turgidity eliminated LRP growth and emergence in the transgenic line. The conclusion was that the LRP can mechanically sense the pressure of the overlying endodermal cells, and an auxin-controlled pathway under SHY2 leads to the necessary loss of turgidity and volume for it to emerge; however, if the LRP senses that it will not be allowed to emerge through the overlying endodermal layer, it is aborted early in development (Vermeer et al., 2014).

Aquaporins, water-transporting proteins that move water across membranes, have been found to impact LRP emergence. By observing the expression patterns of

several plasma membrane-localizing aquaporins in the LRP and overlying tissues, one group created a mathematical model predicting water flow directionality and its impact on the turgor pressure of cells (Peret et al., 2012a). Their model predicted that aquaporin-based lowering of turgor pressure in the overlying tissue was one of the most important factors driving the timely emergence of the LRP, and indeed when they tested the knockout mutants of several auxin-responsive aquaporins, they found delayed LRP emergence rates, as their model predicted (Peret et al., 2012a). Recently, another group proved that tonoplast-localized aquaporin activity also drives LRP emergence (Reinhardt et al., 2016). Analyzing the expression patterns of the tonoplast aquaporins revealed that many were found at the base of the LRP. Knockout mutants of these aquaporins had significantly delayed LRP emergence, leading to the prediction that aquaporins may be directing water flow from the vasculature into the LRP to increase its turgor pressure and drive outward growth (Reinhardt et al., 2016).

Finally, an intriguing study proved that auxin can influence a previously unseen type of signaling during LRP emergence: that of small peptide communication between tissue layers (Kumpf et al., 2013). Knockout mutations of the peptide, called *Inflorescence Deficient in Abscission* (*IDA*), or its receptors HAESA-LIKE and HAESA-LIKE 2 (HAE and HSL2), delayed LRP emergence and led to odd separations of the overlying cell layers. The expression of these components was LRP-overlying cell specific and relied on auxin-induced *LAX3*. Importantly, these components appear to be involved in upregulating the cell wall degradation required for overlying cells to separate (Kumpf et al., 2013).

1.5 Auxin and Plasmodesmata

1.5.1 A Brief Summary of Plasmodesmata

This literature review has focused mainly on the transcellular movement of auxin through plant tissues. However, as a small, diffusible molecule that is stable in the cytosol, IAA could move cell-to-cell symplasmically—that is, directly between cytoplasms of neighboring cells—in the proper conditions. Symplasmic communication occurs via plasmodesmata (PD), small pores connecting the cytoplasms of neighboring cells through the rigid cell walls. All multicellular plants require plasmodesmata to grow and survive (Xu and Jackson, 2010; Burch-Smith et al., 2011; Sevilem et al., 2015; Brunkard and Zambryski, 2016).

The typical PD pore is lined along the outside with plasma membrane from the two neighboring cells, while a tightly-appressed strand of cortical endoplasmic reticular (ER) membrane stretches between each cell along the middle of the pore, forming a membrane-lined channel through which the cytoplasms are shared (Hepler, 1982; Oparka, 1993; Bel and Kesteren, 1999; Ehlers and Kollmann, 2001); there are likely finer details of PD structure that remain unknown due to the difficulty of imaging intact PD and extracting PD proteins. The simple basic structure of PD belies the fact that they are actually dynamic, adaptable channels, not only allowing passive diffusion of small molecules, like nutrients, but also playing a very active role in the selection and passage of macromolecules, like transcription factors, between cells (Kragler, 2013; Sager and Lee, 2014; Yadav et al., 2014). Most PD are able to modify their permeability in response to a variety of environmental or endogenous signals, but as techniques for viewing PD structural changes and measuring cell-to-cell transport

have advanced, the influence of plant hormone signaling on PD control has been given more attention (Sager and Lee, 2014).

1.5.2 Connections between Auxin-Controlled Developmental Processes and Regulation of Intercellular Communication via Plasmodesmata

There is surprisingly little data on how auxin influences PD regulation, and vice versa. A recent study has made some headway into this knowledge gap by discovering that symplasmic communication between the quiescent center and surrounding cells regulates auxin biosynthesis in the root tip (Liu et al., 2017). Using an inducible callose over-producing mutant system called *icals3m* under an inducible promoter specific to the quiescent center cells (*pWOX5:icals3m*), they found that PD closure via callose deposition in the quiescent center cells caused the surrounding meristem cells lose their meristematic capacity and become differentiated. Furthermore, while the intensity of the auxin maximum in the columella was greatly weakened in induced *pWOX5:icals3m* lines, the polar localization of the PINs in this area was unaffected. Ultimately, they created GUS lines under the promoters of several key auxin biosynthesis genes expressed in the root tip, and found their expression was significantly repressed upon closure of the PD in the quiescent center. Taken together, the authors concluded that the quiescent center cells must be in constant symplasmic communication with the surrounding cells to regulate the local auxin biosynthesis that maintains the stemness of these cells (Liu et al., 2017).

There has been scarce research into the movement of auxin itself through PD. In one of the few previous attempts, researchers found that IAA in both low (30 nM) and high (100 nM) concentrations did not impact solute flux through root meristem PD after either 2 or 24 hours, as measured by carboxyfluorescein dye movement into

photobleached cells of the root meristem, though other treatments known to affect PD permeability showed significant changes (Rutschow et al., 2011). However, they never addressed the possibility that different tissues might have different symplasmic responses to auxin treatments.

In a recent study, one group tested the idea that PD closure via callose deposition was responsible for maintaining the auxin gradient needed for the hypocotyl phototropic response (Han et al., 2014). The group was studying a knockout mutant of the *GSL8* (*CALS10*) gene, *gsl8*, which has a significantly reduced phototropic response. After finding that *gls8* mutants almost completely lacked basal PD callose deposition in the shoots, they used a dexamethasone-inducible RNAi for the *GSL8* to observe the phototropic response when basal hypocotyl callose was reduced. They observed a loss of the phototropic response when GSL8-RNAi was induced prior to photostimulation. They reasoned that, with the PD open due to callose loss, perhaps the auxin required to bend the shoot diffused out of the cells through open PD. They tested auxin diffusion directly, by injecting the radio-labeled synthetic auxin 2,4-dichlorophenoxyacetic acid (2,4-D) into dex-induced GSL8-RNAi hypocotyls; the rate of auxin diffusion significantly increased throughout the hypocotyl compared to non-dex-induced control seedlings. This was backed by crossing *DR5:GUS* into the dex:GSL8-RNAi lines and comparing the extent of GUS staining when IAA was loaded onto clipped hypocotyl ends; when induced prior to IAA loading, the GSL8-RNAi allowed a greater spread of the auxin compared to un-induced controls, as shown by enhanced GUS staining (Han et al., 2014). Though these results imply that PD closure via callose deposition is required to maintain the local auxin accumulation driving the phototropic bending, the authors did not test in

the *gsl8* mutant whether PIN protein localization/expression was altered—which can be a side-effect of cell fate changes caused by altered symplasmic communication (Wu et al., 2016)—and so no strong conclusions can be formed until this is addressed.

Though the above process of detecting the influence of PD on auxin has not yet been applied to roots, several studies gave the first hints that symplasmic isolation might play a role in LRP growth. First, researchers found that a phloem-loaded symplasmic tracer was temporarily prevented from moving into LRP during an early stage (Oparka et al., 1995). This result was supported years later when it was found that transient callose deposition at PD within the LRP enables its proper development (Benitez-Alfonso et al., 2013). Immunofluorescent detection of callose showed that the timing of its accumulation within the LRP correlated with a loss of symplasmic GFP movement. The authors identified two *Plasmodesmal-Localized β-1,3-Glucanases* (*PdBG1* and *2*) which, when mutated, resulted in higher callose accumulation in growing lateral root primordia. Furthermore, prevention of symplasmic movement of signals from the phloem increased lateral root initiation and density in the mutant lines (Benitez-Alfonso et al., 2013). Considering the importance of auxin transport to all stages of LRP development and growth, it seems possible that symplasmic regulation by PD callose deposition could play a role in controlling the movement and/or accumulation of auxin in the LRP and overlying cells.

Chapter 2

PDLP5 FUNCTIONS WITHIN A SALICYLIC ACID DEFENSE PATHWAY FEEDBACK LOOP

2.1 Background

2.1.1 The Salicylic Acid Defense Pathway Protects Against Biotrophic Pathogens

Plants have a wide variety of signals that are propagated during defense, including small, diffusible hormones that trigger many downstream changes within plant cells. A plant defense hormone can be newly synthesized, released from an inactive isoform, or both, within cells after initial pathogen recognition (An and Mou, 2011). Which hormone is propagated is often dependent on the pathogen type, although multiple hormonal pathways may intersect to form a complete response (Spoel and Dong, 2008; An and Mou, 2011). Defense hormone accumulation can lead to different responses, like upregulation of defense genes and reinforcement of the cellular architecture (Spoel and Dong, 2008; Voigt and Somerville, 2009).

Here, the focus will be the salicylic acid (SA) pathway during the basal immune response against biotrophic pathogens (Vidhyasekaran, 2015). The basal immune pathway begins with the binding of a pathogen-associated molecular pattern (PAMP) to a pathogen recognition receptor (PRR); this triggers a mitogen-activated protein kinase (MAPK) cascade and a burst in reactive oxygen species (ROS), that initiate a wide range of downstream defense reactions (Shamrai, 2014; Wu et al.,

2014). Following these initial reactions, the key components of SA defense are activated.

2.1.1.1 EDS1 and PAD4 Upstream Signaling Node in SA Defense

Two genes, *Enhanced Disease Susceptibility 1* (*EDS1*) and *Phytoalexin Deficient 4* (*PAD4*), comprise part of an essential signaling node in SA-dependent defense responses during basal immunity against biotrophic pathogens (Wiermer et al., 2005). *EDS1* and *PAD4* were separately discovered as mutants with strongly-deficient defense responses to pathogens (Glazebrook et al., 1996; Parker et al., 1996); the two proteins were soon found to interact with each other (Feys et al., 2001). Structurally, both share some homology with eukaryotic lipases, though they have no known enzymatic activity (Falk et al., 1999; Jirage et al., 1999); in fact, little is understood about the actual protein functionality of EDS1 and PAD4 (Gao et al., 2015). However, much has been uncovered about how their behavior and localization affects plant basal immune responses: for instance, though the main partner of EDS1 had always been considered PAD4 during basal immunity, a different component, *Senescence Associated Gene 101* (*SAG101*), can bind to EDS1 alone or in a ternary complex with PAD4 to upregulate basal defense signaling (Feys et al., 2005; Zhu et al., 2011). The distinct heteromeric complexes involving EDS1, PAD4, and SAG101 could potentially cooperate with each other to respond to and regulate immunity in different ways (Wagner et al., 2013).

One of the more important discoveries about EDS1 is that it moves between the nucleus and cytoplasm (Garcia et al., 2010). Transgenic lines expressing an enhanced-nuclear export version (EDS1-YFP-NES), as well as a dexamethasone-inducible nuclear-import version of EDS1 (EDS1-YFP-GR), were treated with

virulent Pst DC3000 bacteria. In both cases, it was found that EDS1 retention in the cytoplasm increased plant susceptibility to the bacteria, meaning EDS1 must be present to some extent within the nucleus to properly promote the basal immune response (Garcia et al., 2010). Within the nucleus, ESD1 directs transcriptional reprogramming of its partner PAD4, as well as SA biosynthesis genes. The exact nature of EDS1 control over transcription is unknown, although it seems likely that EDS1, alone or part of an EDS1/PAD4 complex, may interact with certain transcriptional activators or repressors (Garcia et al., 2010). Importantly, cytoplasmically-sequestered EDS1 still conferred partial resistance from pathogens when transformed into in *eds1* mutants. Thus, it may be that for a fully-developed defense response, the proper balance of nuclear and cytoplasmic EDS1 complexes is required.

2.1.1.2 SA Biosynthesis Genes

In most cases, the key SA biosynthesis gene for basal immunity is *Isochorismate Synthase* (*ICS1*), which plays a critical role in defensive SA biosynthesis by converting the compound chorismate into isochorismate, a precursor to SA, during defense responses (Wildermuth et al., 2001). The majority (~90%) of SA that accumulates during basal immunity is synthesized from the isochorismate synthase pathway (Garcion et al., 2008). Plants lacking *ICS1* are unable to accumulate SA levels high enough to fully resist pathogen infection (Wildermuth et al., 2001).

There are other SA biosynthesis genes that, while they often play a smaller role in defense, can in certain cases be critical for a complete basal immune response. For example, the *Phenylalanine Ammonia Lyase* (*PAL*) family of enzymes, which converts phenylalanine to the SA precursor cinnamate, also contributes a certain amount of SA

to defense responses (Chen et al., 2009). In *A. thaliana* plants, if PAL is inhibited by 2-aminoindan-2-phosphonic acid (AIP), certain pathogens like downy mildew can successfully grow on the plant even if ICS1 is still intact (Mauch-Mani and Slusarenko, 1996). Furthermore, silencing PAL in tobacco plants leads to susceptibility to Tobacco Mosaic Virus (TMV) (Pallas et al., 1996). These results demonstrate PALs can be critical for complete resistance to specific pathogens.

HopW1-1 Interacting 3 (*WIN3*) (also known as *avrPphB Susceptible 3* (*PBS3*)) is a Gretchen Hagen 3 (GH3)-like protein that can conjugate amino acids to 4-substituted benzoates (Okrent et al., 2009). First discovered as auxin-responsive genes, GH3 proteins are now known to have myriad functions. WIN3 itself contributes to the biosynthesis of SA during plant defense responses: *win3* mutants are more susceptible to certain bacterial pathogens (Warren et al., 1999), a phenotype which can be rescued by exogenous SA application (Jagadeeswaran et al., 2007). Furthermore, when crossed with the SA hyper-accumulating mutant *Accelerated Cell Death 6* (*acd6*), *win3* contributed additively with *sid2* (a knockout mutant of *ICS1*) in reducing the cell death phenotype and total SA accumulation (Wang et al., 2011). Recent results suggest the possibility that WIN3 does not directly lead to SA synthesis, but rather creates a pool of conjugated benzoates that are potential SA precursors (Westfall et al., 2016).

2.1.1.3 NPR1 Controls Transcription of SA Defense Genes

Non-expressor of Pathogenesis-Related Genes 1 (*NPR1*) is an essential regulator of SA signaling. Many of its critical functions arise from downstream signaling. For example, the expression of critical pathogen response genes, including *Pathogenesis-Related Protein 1* (*PR1*) (Grant and Lamb, 2006) are regulated by

NPR1. Prior to SA activation, NPR1 exists as an oligomer in the cytosol, however upon accumulation of SA, the redox potential in the cell changes; NPR1 is reduced and released as monomers (Mou et al., 2003). Monomeric NPR1 can be activated by phosphorylation and imported into the nucleus, where it is responsible for PR gene expression and signaling leading to systemic acquired resistance (SAR). Activated monomeric NPR1 does not directly bind to DNA itself, but instead forms complexes with transcription factors like the TGA family in the nucleus to control the transcription of downstream pathogenesis related genes (Pape et al., 2010). In order for transcription by NPR1 to continue, the dephosphorylated inactive NPR1 must be degraded by the proteasome and cleared from the nucleus to be replaced with more of the active form (Spoel et al., 2009). This supports a model in which NPR1 is "used up" and must be degraded and replaced with fresh phosphorylated NPR1 monomers to stimulate further transcription (Spoel et al., 2009).

The NPR1 protein acts as a receptor for SA *in vivo* (Wu et al., 2012; Manohar et al., 2014), establishing it among other SA binding proteins during defense (Kuai et al., 2015). The binding site was found to be two cysteines, Cys521 and Cys529, which interacted with SA via the transition metal copper, and when mutated caused NPR1 inactivation (Wu et al., 2012). Furthermore, the authors found that SA binding is the actual trigger of the disassociation of the NPR1 oligomer, not reducing conditions alone; in other words, while the accumulation of SA during defense leads to reducing intracellular conditions, the binding of SA itself is the key factor for NPR1 activation (Wu et al., 2012).

2.1.1.4 SA Defense is Regulated by Feedback Loops

In order to maintain a response to pathogens, while minimizing damage to the plant, each step of the SA basal defense pathway is controlled by feedback loops. For example, application of exogenous SA upregulates EDS1 and PAD4 expression, which in turn upregulate ICS1, indicating a positive feedback loop between SA and these genes (Feys et al., 2001; Chandra-Shekara et al., 2004). This ensures that the plant produces a sustained defense response, although since EDS1/PAD4 have been implicated as functioning in other, non-SA-related defense pathways, the feedback loop could also allow these genes to diversify the defense response by triggering other pathways as they accumulate.

It has been shown that NPR1 is required to suppress ICS1 expression and hyperaccumulation of SA during pathogen infection (Zhang et al., 2010b). By designing an NPR1 construct that was constrained to the cytoplasm by the loss of its nuclear localization signal, the group found that plants lost the ability to tolerate growth in a high-SA medium, meaning NPR1 also stimulates the transcription of genes required to protect the plant from the harmful effects of high SA build-up (Zhang et al., 2010b). ICS1 transcripts and SA also accumulated to a level much higher in these ΔnlNPR1 plants than wild-type (Zhang et al., 2010b). As with EDS1, this suggests that feedback loops within the SA pathway are essential for an efficient defense response; in this case, an essential downstream component, NPR1, acts in a negative feedback loop to limit the build-up of SA biosynthesis enzyme ICS1, thus preventing detrimental overaccumulation of SA. Adding to this, WIN3 is inhibited by salicylate, the downstream product of the SA biosynthesis pathway—another negative feedback loop preventing SA from becoming too high (Okrent et al., 2009). As more

is learned about the proteins in the SA pathway, our knowledge about feedback regulation at every level will continue to develop.

2.1.2 The Impact of PDLP5 on the SA Defense Pathway

The *Plasmodesmata-Located Protein* (*PDLP*) family in *Arabidopsis thaliana* was initially identified by sequence homology based on PDLP1, the first member isolated from a proteomics study (Thomas et al., 2008). The PDLP family has eight members, *PDLP1-8*, all with similar structural domains. Each has two extracellular Domains of Unknown Function 26 (DUF26) in their N-terminal-to-mid protein regions; a conserved transmembrane domain closer to the C-terminal end; and a short, cytoplasmic C-terminal region (Thomas et al., 2008). Fluorescent tagging of all eight PDLP members found that they localize along the cellular perimeter in the epidermal cells of *A. thaliana* leaves, in a pattern strongly suggesting plasmodesmal (PD) localization (Thomas et al., 2008).

Functional studies of several PDLP family members connected their expression to PD closure. For example, *Arabidopsis* knock-out plants containing double/triple mutations in *PDLP1*, *2*, and *3* showed increased intercellular movement of free GFP compared to wild-type plants. Conversely, overexpressing *PDLP1* under the control of the 35S promoter reduced GFP cell-to-cell trafficking significantly, demonstrating that PDLP1 plays a role in restricting cell-to-cell transport (Thomas et al., 2008). Online bioinformatics data, and fluorescent tagging of PDLP proteins expressed under their native promoters, have shown that PDLP members often have distinct areas of expression—for example, *PDLP2* and *PDLP3* are both expressed in the shoot apical meristem, but only in partially-overlapping cellular zones (Bayer et al., 2008). These results suggest that PDLP family members may act non-redundantly,

to regulate intercellular transport in differing tissues in response to developmental or environmental stimuli.

Our lab had independently investigated PD-enriched cell wall material in search of putative PD proteins, based on a previous protocol using *A. thaliana* seedlings cultured in liquid media (Lee et al., 2003). This analysis identified PDLP5, which according to the expression data available in the online databases Genevestigator™ and Arabidopsis eFP Browser is predicted to be upregulated by pathogen infection. Furthermore, one study found *PDLP5* transcript is highly upregulated in *A. thaliana* infected by *Pseudomonas syringae* expressing the effector HopW1-1 (Lee et al., 2008). The apparent connection between PDLP5 and plant defense evoked the exciting possibility that PD are regulated during defense, and made examining the defense genes regulating *PDLP5* expression a priority. Thus, to elucidate the biological function of PDLP5 and determine the factors regulating *PDLP5* expression in *Arabidopsis*, I pursued the following research objectives for Chapter 2 of my Thesis.

2.1.3 Research Objectives

Objective 1: Describing the morphological phenotypes associated with altered levels of *PDLP5* expression. To this end, a transgenic line constitutively overexpressing *PDLP5* (*35S:PDLP5*), and a mutant knock-down line having a T-DNA insertion in the *PDLP5* gene (*pdlp5-1*), were compared to the wild type (WT) Col-0 plants, to find any differences in their growth patterns and morphology.

Objective 2: Expression profiling of *PDLP5* transgenic lines. To this end, RT-PCR was performed with tissue from WT, *35S:PDLP5*, and *pdlp5-1*, to find changes in salicylic acid defense and cell death pathway genes, which had been connected to PDLP5 through bioinformatics data mining.

Objective 3: Determining the genetic pathway controlling *PDLP5* expression. To this end, RT-PCR was performed for *PDLP5* expression on mutants of the salicylic acid defense pathway and WT plants after salicylic acid treatment, to further elucidate the relationship between *PDLP5* and the salicylic acid pathway.

2.2 Materials and Methods

2.2.1 Cultivation of Plants in Soil

Plants were grown in soil or on agar media as described in Appendix A1 and A2, respectively. Plant genotypes used in this study are described in Appendix Table A6. Crosses were made by dissecting the unopened buds of the mutant plants (maternal lines) under a light microscope, and spreading the pollen of the transgenic plants (paternal lines) onto the unpollinated stigma of the dissected bud. Genotyping for mutant homozygosity was performed using the primers and PCR program described in Appendix Tables A2 and A4. Plant transformations were performed using the standard *Agrobacterium* floral dip methods (Clough and Bent, 1998).

2.2.2 Plant Treatments

To treat Arabidopsis, plants of the desired age were either sprayed with hormones diluted to the necessary concentration in autoclaved nano-purified water and 0.01% Silwett-77 (as a surfactant), or hormones were mixed into autoclaved MS media after cooling to a temperature that was tolerable to hold with bare hands. For stock and treatment concentrations, see Appendix Table A8.

2.2.3 Design of the Estradiol-Inducible PDLP5 Construct

Blunt-ended PCR product PDLP5 was amplified from template plasmid "PDLP5 in pdGN" using Phusion® DNA polymerase (New England Biolabs). The

PCR program used was 1 cycle of 94°C for 30 sec; followed by 30 cycles of 94°C for 30 sec, 62°C for 20 sec, and 72°C for 15 sec; followed by a final extension of 72°C for 7 min.

PCR product was gel-purified and extracted using a NucleoSpin Extract II Kit (Clontech Labs, Inc). Concentration of purified PCR product DNA was measured using a NanoDrop ND-1000 Full Spectrum UV/Vis Spectrophotometer. The blunt-ended PCR product of the coding sequence for PDLP5 was then inserted into the StrataClone Blunt PCR Cloning Vector "pSC-B-amp/kan" according to the kit instructions. DH5alpha bacteria harboring the plasmids "pER8" and "PDLP5 in pSC-B-amp/kan" were cultured in LB liquid media overnight, and plasmids were extracted using manual miniprep technique (Serghini et al., 1989). Digestions and ligations were performed using XhoI and SpeI restriction enzymes (NEB), CIP (Fisher), and T4 DNA ligase (NEB), according to the protocols of each company. When necessary, products were gel-purified and extracted using a NucleoSpin Extract II Kit.

2.2.4 Microscopy

Soil-grown plants and plant parts were documented using a Nikon D3100 digital camera. Imaging of leaf close-ups and seedlings was performed on a Zeiss Stemi SV 11 Apo Stereoscope under direct lighting, using a Zeiss AxioCam with AxioVision software.

2.3 Results

2.3.1 *PDLP5* Overexpression Causes a Dwarf, Hypersensitive Response-like Lesion-Mimic Phenotype in *Arabidopsis*

To determine whether altering *PDLP5* expression could affect *Arabidopsis* plant morphology, transgenic plants ectopically expressing *PDLP5* under control of the Cauliflower Mosaic Virus 35S promoter (*35S:PDLP5*), and a severe *PDLP5* knockdown line with a SAIL T-DNA insertion in the first intron (*pdlp5-1*), were grown along with WT (Col-0) in soil, to compare phenotypes. 1.5 weeks after cotyledon emergence, the *35S:PDLP5* plants began to show noticeable phenotypic differences from the WT and *pdlp5-1* plants—leaf tissue was chlorotic, and the rosette diameter was reduced. At 4 weeks old, the *35S:PDLP5* plants (Fig 2.1B) were significantly smaller than the WT and *pdlp5-1* plants (Fig 2.1A and C), which appeared to have no phenotypic differences from each other at the aerial tissue level. Furthermore, unlike the WT and *pdlp5-1* leaves (Fig 2.1D and F), the leaves of *35S:PDLP5* plants developed small patches of spontaneous, HR-like cell death (Fig 2.1E). Plants with these characteristics are said to have a "dwarf lesion-mimic" phenotype (Lorrain et al., 2003).

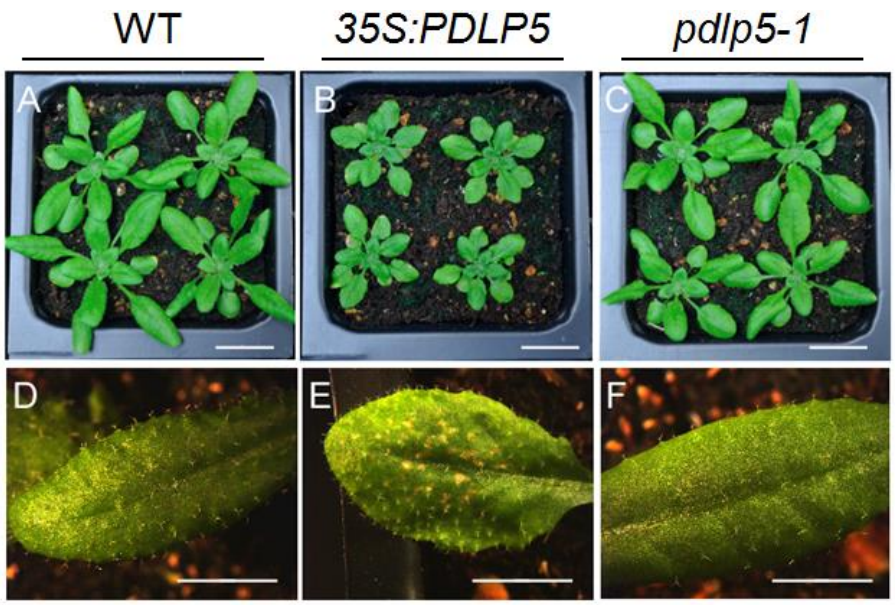

Figure 2.1: *35S:PDLP5* plants have a dwarf, lesion-mimic phenotype. **A-C**, phenotypes of whole plants at 28 days old. **D-F**, magnified images of mature leaves from 28 day old plants; in **E**, yellow spots are regions of spontaneous cell death. Scale bar, 2.5 cm in **A-C**; 1 cm in **D-F**.

2.3.2 *PDLP5* Overexpression Upregulates Salicylic Acid Defense Pathway Signaling

Many lesion-mimic mutants are defective in genes regulating the accumulation of salicylic acid (SA), a plant defense hormone (Bruggeman et al., 2015). The hyper-accumulation of SA in these mutants triggers downstream defense reactions, including spontaneous cell death, in the absence of pathogens. To test the possibility that *PDLP5* expression could influence the accumulation of SA and activate cell death signaling pathways, RT-PCR was used on *35S:PDLP5*, *pdlp5-1*, and WT leaf tissue, to detect the transcript levels of several downstream marker genes: two important SA pathway defense markers, *Pathogenesis-Related Protein 1* (*PR1*) and *2* (*PR2*), as well as two markers for cell death, *WRKY6* (from a family of transcription factors with a conserved WRKY protein sequence) and *Senescence-Associated Gene 13* (*SAG13*).

The transgenic plant line *NahG*, which ectopically expresses a salicylate hydroxylase gene that degrades the SA hormone, served as a SA-negative control. It was found that the basal levels of all tested marker genes were significantly higher in the *35S:PDLP5* plants, while there were no significant differences between WT and *pdlp5-1* in the expression of the tested markers (Fig 2.2); *NahG* had lower levels of SA markers *PR1* and *PR2*, as expected. These results suggested that high *PDLP5* expression increased the amount of SA accumulation within the plant; this was confirmed when leaf extracts from WT, *35S:PDLP5*, and *pdlp5-1* were analyzed using high-performance liquid chromatography, and it was found that the level of SA did significantly increase in the *35S:PDLP5* background (Wang et al., 2013).

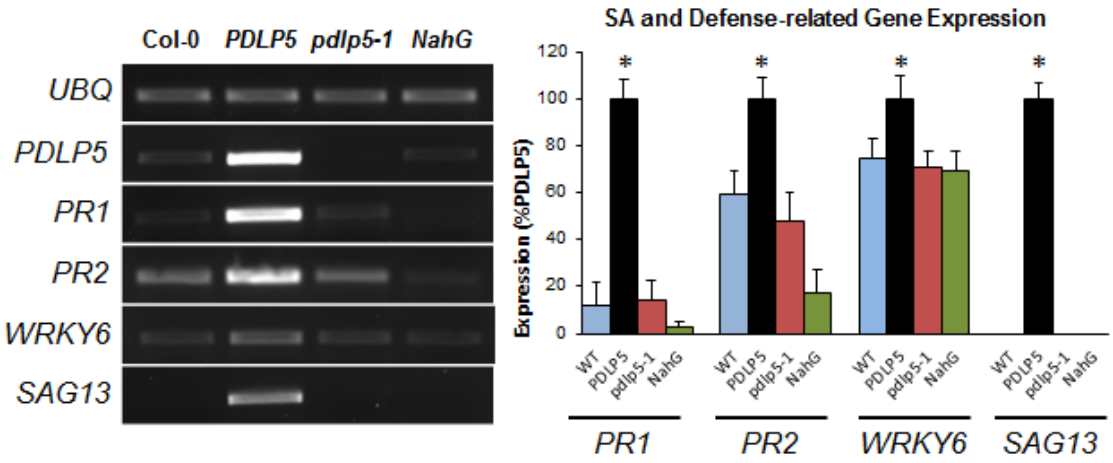

Figure 2.2: *PDLP5* overexpression plants have significantly increased levels of defense and death markers.
Graph shows expression standardized to the level of each marker in *35S:PDLP5* (shortened to "*PDLP5*" here); in WT, *pdlp5-1*, and *NahG*, markers were either not detectable or ranged from about 5-75% of the level in *35S:PDLP5*. UBQ used as loading control. Asterisks indicate that the increased expression of the markers in *35S:PDLP5* was statistically significant compared to the other backgrounds ($p<0.05$). Image-J was used to quantify intensities of gel bands.

The key components in the SA defense pathway include the upstream protein partners *Enhanced Disease Susceptibility 1* (*EDS1*) and *Phytoalexin Deficient 4* (*PAD4*), which trigger SA accumulation in response to pathogen infection; *Isochorismate Synthase 1* (*ICS1*), an essential part of the SA biosynthesis pathway; and *Nonexpressor of Pathogenesis-Related genes 1* (*NPR1*), a major downstream transcriptional regulator activated by SA. To determine whether *PDLP5* expression could alter the transcript levels of any of these major SA defense pathway genes, RT-PCR was performed on leaf tissue from WT, *35S:PDLP5*, and *pdlp5-1* plants. It was found that transcripts of *PAD4* and *ICS1* increased significantly in the *35S:PDLP5* background (Fig 2.3), proving that *PDLP5* expression leads to upregulation of certain parts of the SA defense pathway.

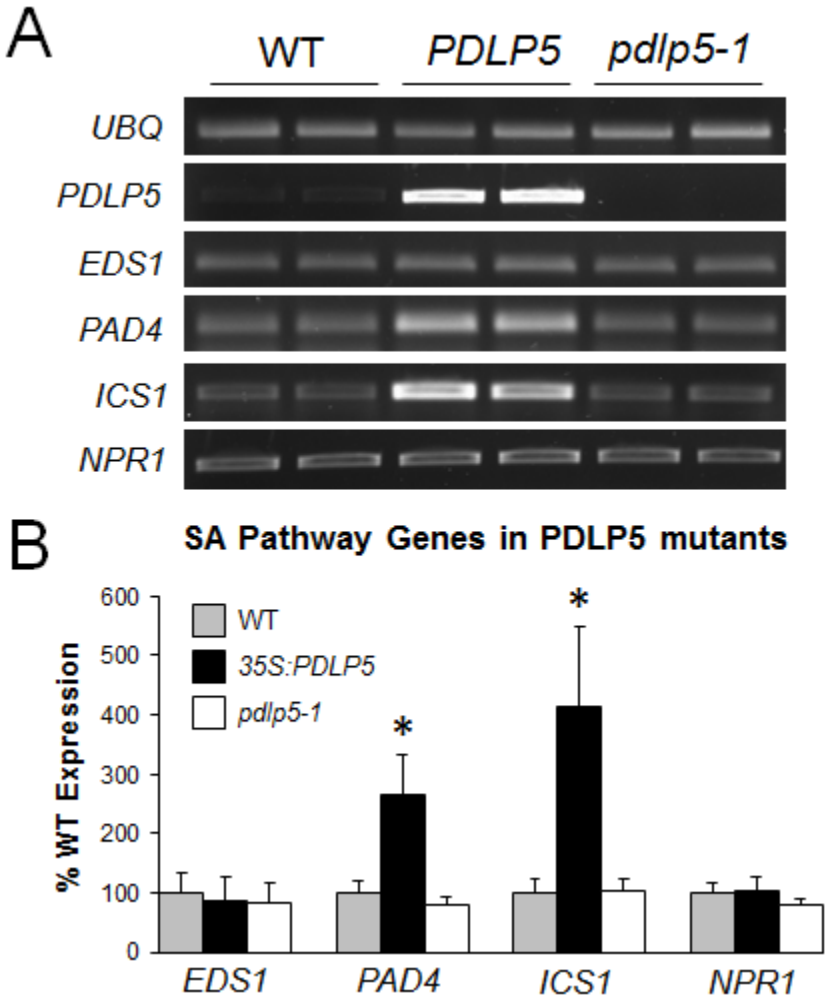

Figure 2.3: Transcripts of SA defense pathway genes *PAD4* and *ICS1* are significantly higher in the *35S:PDLP5* background.
A, The gel results were semi-quantified using Image J software. **B**, The graph representing the results, standardized against the level of each gene in WT. *UBQ* was used as loading control. The expression levels of *PAD4* and *ICS1* were significantly higher ($p<0.05$) in *35S:PDLP5* compared to WT.

2.3.3 Eliminating SA Accumulation via the *NahG* Transgene Fully Rescues the *35S:PDLP5* Dwarf Lesion-Mimic Phenotype

To determine whether the *35S:PDLP5* dwarf lesion-mimic phenotype could be rescued by preventing the hyper-accumulation of SA hormone, *35S:PDLP5* was

crossed into the *NahG* background. The *NahG* transgene effectively degrades almost all SA within plant tissue. *NahG x 35S:PDLP5* crosses had the *NahG* parental line phenotype (Fig 2.4A). Furthermore, the high *PR1* accumulation seen in *35S:PDLP5* plants was eliminated (Fig 2.4B). These results showed that the dwarf lesion-mimic phenotype in *35S:PDLP5* plants is dependent upon the hyper-accumulation of SA, and suggested that *PDLP5* requires SA to upregulate cell death-promoting functions.

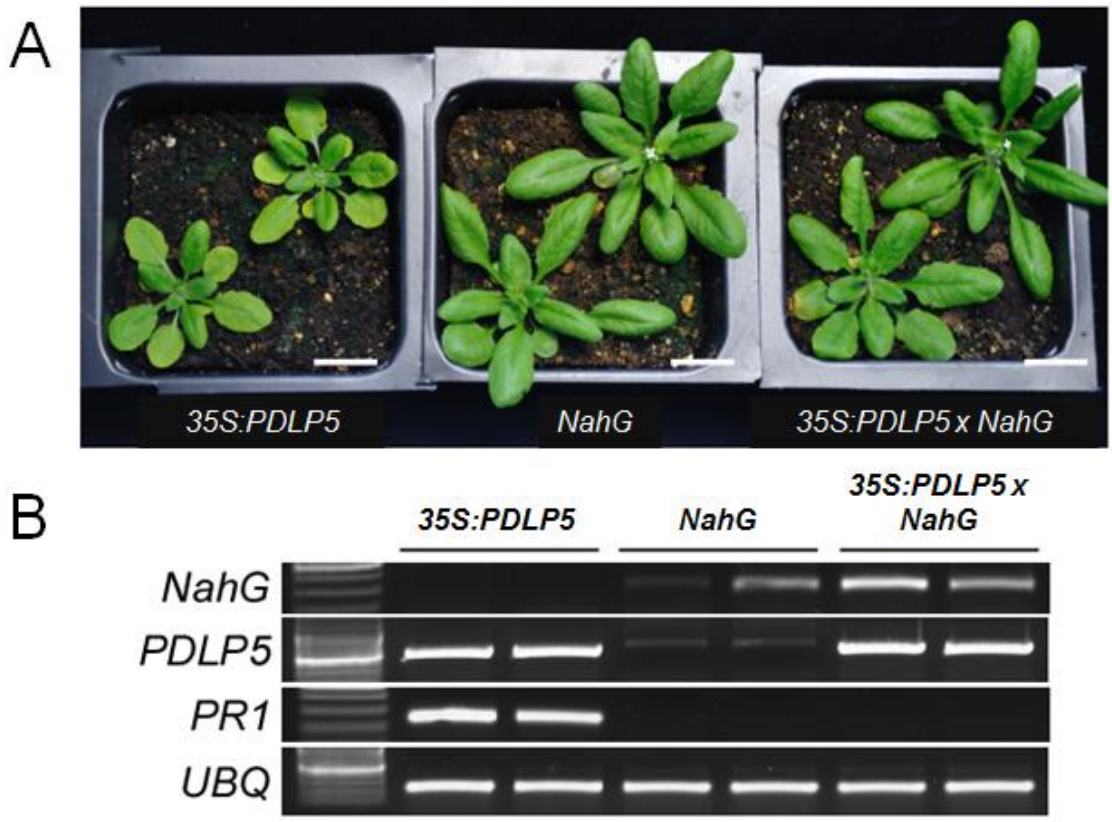

Figure 2.4: *NahG*-based degradation of SA in *35S:PDLP5* plants rescues stunted growth and eliminates spontaneous death and ectopic SA marker expression.
A, growth phenotypic comparison of 4-week old NahG x 35S:PDLP5 plants (F2 generation) versus parental lines *NahG* and *35S:PDLP5*. **B**, RT-PCR results for NahG, PDLP5, and PR1 in the crosses and parental lines; UBQ used as loading control. Scale bars, 2 cm in **A**.

2.3.4 Crossing *35S:PDLP5* with SA Defense Pathway Knockout Mutants *eds1*, *ics1*, and *npr1* Eliminates HR-like Lesions, but Retains the Dwarf Phenotype

To determine which parts of the SA defense pathway were required for the *35S:PDLP5* phenotype, crosses were made between *35S:PDLP5* and nonfunctional mutants of the critical SA pathway genes, *eds1*, *ics1*, and *npr1* (Fig. 2.5). In each of the double-homozygous crossed lines, the SA pathway mutation eliminated the spontaneous lesion formation seen on the *35S:PDLP5* parental line (Fig 2.5B). However, the stunted growth was still present in all crosses (Fig 2.5A). Therefore, while SA accumulation and signaling controlled by *EDS1*, *ICS1*, or *NPR1* is required for the spontaneous cell death phenotype, none of them is fully responsible for controlling the dwarfing caused by *PDLP5* overexpression.

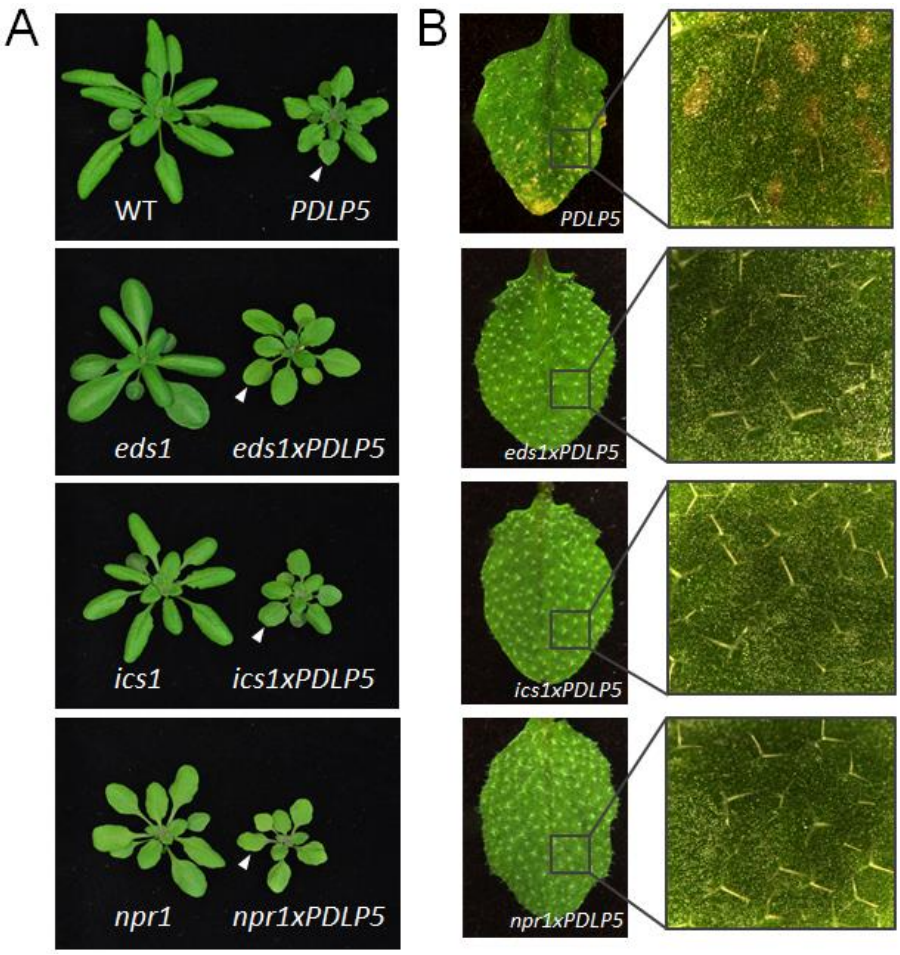

Figure 2.5: Mutations in critical SA defense pathway genes *EDS1*, *ICS1*, and *NPR1* eliminate spontaneous lesion formation in *35S:PDLP5* background.
Double-mutant homozygosity was confirmed prior to study (**Appendix B1**). **A**, whole-plant phenotypic comparison of crosses of *35S:PDLP5* (shortened to "*PDLP5*" in the above figure) and SA pathway mutants, demonstrating the retention of the dwarfism seen in the parental *35S:PDLP5* plants. Arrowheads in **A** point to the fourth rosette leaf, shown in **B**, along with a magnified leaf surface picture, to demonstrate how the SA mutant backgrounds eliminate the spontaneous lesion formation seen when *35S:PDLP5* is expressed in WT.

2.3.5 SA Defense Pathway Mutants *eds1*, *ics1*, and *npr1* Partially or Fully Reduce Ectopic SA Defense Marker Expression in the *35S:PDLP5* Background

To determine which parts of the SA defense pathway were required for downstream transcriptional regulation induced by *PDLP5*, leaf tissue from *35S:PDLP5* crossed into the *eds1*, *ics1*, and *npr1* mutant backgrounds was analyzed by RT-PCR, with the parental lines as controls. It was found that the SA pathway mutant backgrounds did lower defense and cell death marker gene expression caused by *35S:PDLP5* (Fig 2.6). For example, although *WRKY6* transcript was high when *35S:PDLP5* was expressed in the WT background, when *35S:PDLP5* was expressed in the SA pathway mutant backgrounds, *WRKY6* expression was reduced to the basal levels of the mutant parental lines (Fig 2.6, lower left graph). *PR2* was higher in the *35S:PDLP5* crosses than in the SA mutant parental lines, but still lower than *PR2* in the *35S:PDLP5* parental line (Fig 2.6, upper right graph). Finally, the *ics1* and *npr1* mutations completely eliminated both *PR1* and *SAG13* expression in the *35S:PDLP5* crosses, while a small amount of these markers was still upregulated in the *eds1* cross (Fig 2.6, upper left and lower right graphs). These results prove that the *35S:PDLP5*-based transcriptional upregulation of SA defense and cell death marker genes is at least partially dependent on the SA defense pathway.

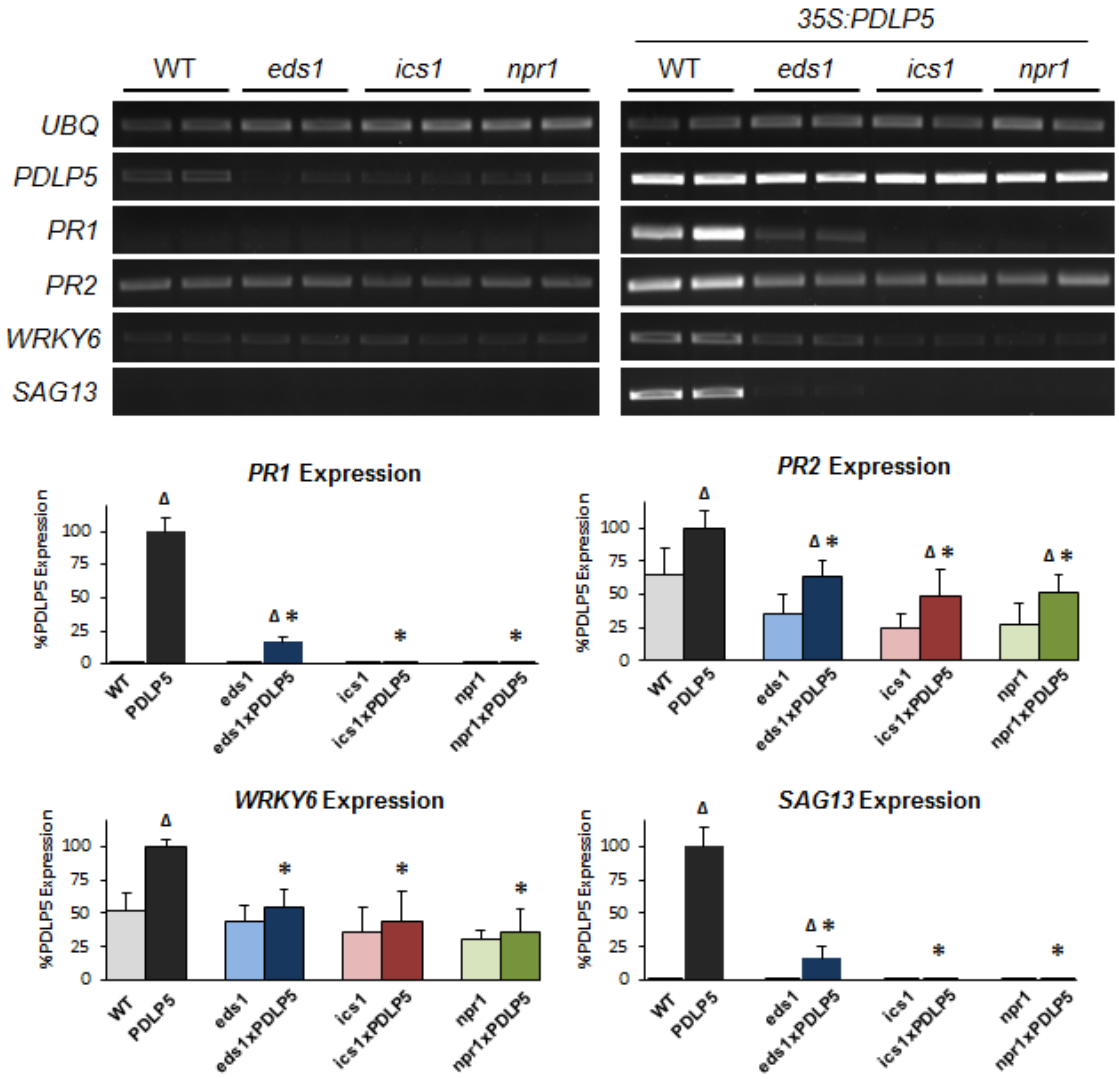

Figure 2.6: SA pathway mutations partially or fully reduce ectopic defense and cell death marker accumulation in the *35S:PDLP5* background.
Graphs show data standardized to *35S:PDLP5* expression. The delta symbol (Δ) indicates that the expression of the marker is significantly higher ($p<0.05$) when *35S:PDLP5* is expressed compared to the basal expression level of that marker in the WT or SA mutant parental line. The asterisk (*) indicates that the expression of the marker is significantly lower ($p<0.05$) in each SA mutant crossed with *35S:PDLP5*, compared to the *35S:PDLP5* parental line in the WT background.

2.3.6 The *PDLP5*-Overexpression Phenotype is Not a Side Effect of the 35S Promoter

Expressing genes artificially under the 35S promoter can sometimes give misleading results. Depending on where in the genomic DNA the transgene is inserted, the 35S promoter may increase expression of nearby native genes unrelated to the transgene itself; furthermore, having high ectopic expression of the transgene starting from germination and continuing throughout the plant's lifecycle may lead to severe developmental anomalies that are not reflective of the actual purpose of the gene under its own native promoter. To prove that the plant phenotypes and marker gene upregulation observed from high *PDLP5* expression were not due to side effects of the 35S promoter, a construct was designed expressing *PDLP5* under the estradiol-inducible promoter pER8 (*pER8:PDLP5*). Estradiol induction mimics the upregulation of *PDLP5* during an actual defense response more closely than the constitutive expression under the 35S promoter.

The construct *pER8:PDLP5* was transformed into WT, *eds1*, *pad4*, *ics1*, *npr1*, and *NahG* plants. Transgenic seedlings germinated on normal MS agar media were transferred to 10 μM estradiol-containing media at 3 dpg. In WT and each SA mutant background except *NahG*, estradiol-induced *pER8:PDLP5* caused stunted growth and chlorosis in seedlings (Fig 2.7A). Furthermore, estradiol treatment of adult *pER8:PDLP5* transgenic lines showed that transcript of the SA marker *PR1* was as highly induced by *PDLP5* induction as it was by SA treatment in the WT background, while the SA pathway mutant backgrounds reduced or eliminated *PDLP5*-based *PR1* expression to a similar extent as in the *35S:PDLP5* crosses (Fig 2.7B). These results prove that *PDLP5* itself is responsible for stunted growth and SA marker induction when it is highly expressed, rather than these being side effects of the 35S promoter.

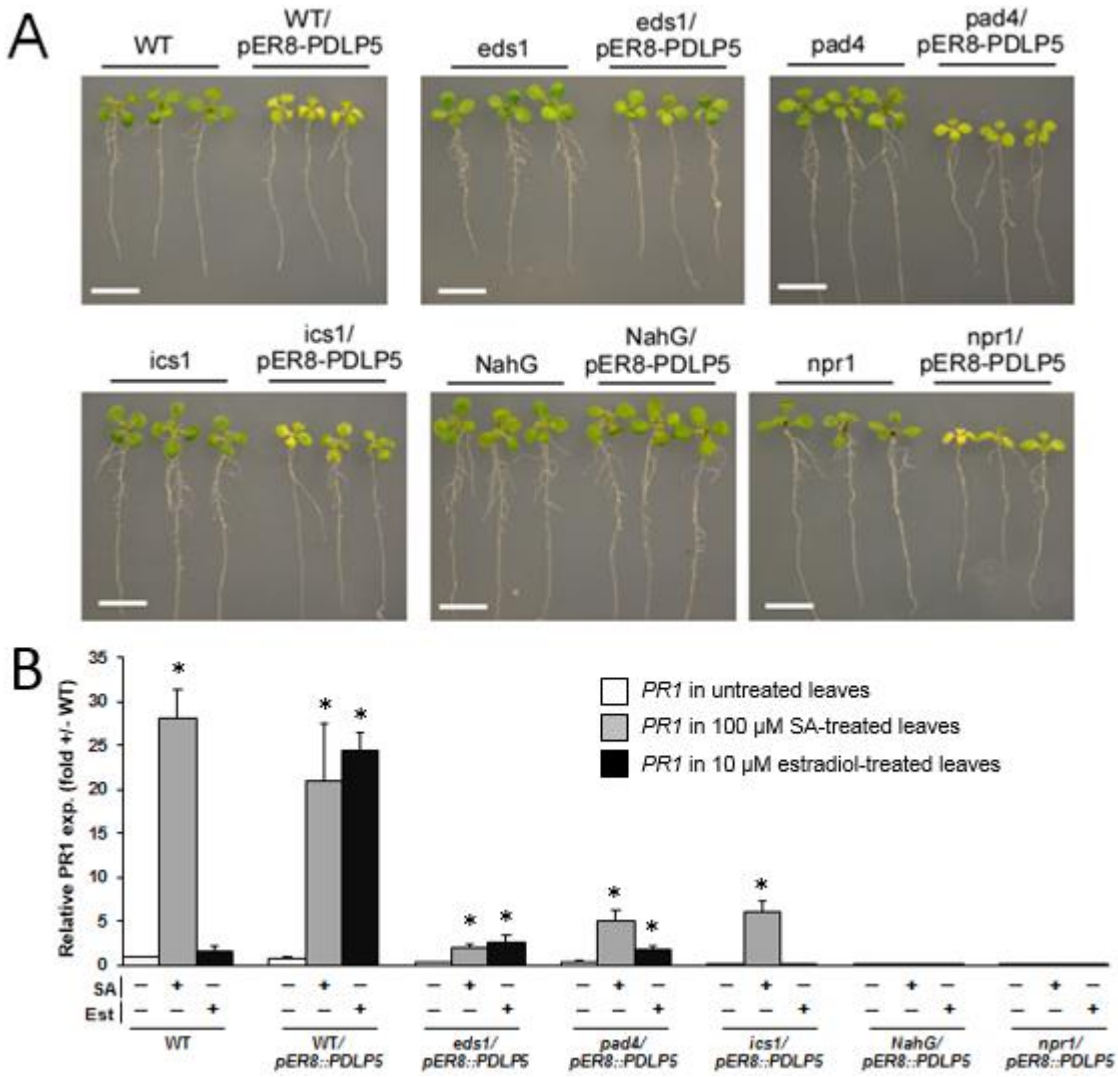

Figure 2.7: Strong *PDLP5* induction via the pER8 promoter in SA defense pathway mutant backgrounds leads to varying degrees of stunted growth, chlorosis, and SA marker upregulation.
A, Phenotypes of transgenic seedlings of WT, *eds1*, *pad4*, *ics1*, *NahG*, and *npr1* plants expressing an estradiol-inducible *PDLP5* construct (*pER8:PDLP5*), compared to parental lines, transferred at 3 dpg to 10 µM estradiol media for 10 days. **B**, RT-PCR results for *PR1* in 4-week old leaves of the above transgenic plants, both mock-treated and treated with either 100 µM SA or 10 µM estradiol for 24 hours. Each column is standardized to untreated WT (-/-WT); *UBQ* used as loading control (see **Appendix B2** for representative gel). Asterisks (*) indicate values significantly higher ($p<0.05$) than each line untreated. Scale bars, 1 cm in **A**.

2.3.7 *PDLP5* Upregulation is Controlled by the SA Defense Pathway

Results from a previous study (Lee et al., 2008), along with information gathered from the online database Genevestigator™, supported the idea that *PDLP5* could be upregulated by SA accumulation during innate immunity. To determine if *PDLP5* expression could be induced by the SA hormone, RT-PCR was performed on SA-treated and mock-treated WT leaves. It was found that WT plants treated with 100 µM SA had a 3-fold increase in *PDLP5* expression compared to mock treatment with water, demonstrating that SA can upregulate *PDLP5* transcript (Fig 2.8A). To further support this, a computational analysis of conserved cis-regulatory elements within the *PDLP5* promoter was performed using the PlantCARE online resource [http://bioinformatics.psb.ugent.be/webtools/plantcare/html/]. The *PDLP5* promoter was found to contain cis-acting elements that are common for many SA-responsive defense genes (Fig 2.8B), including one binding site for WRKY transcription factors, called a W-box, as well as two types of binding sites for TGA transcription factors, called a TGA-box and as-1-like elements (Garner et al., 2016). Together, these results strongly support that SA-activated transcription factors control *PDLP5* upregulation during stress responses.

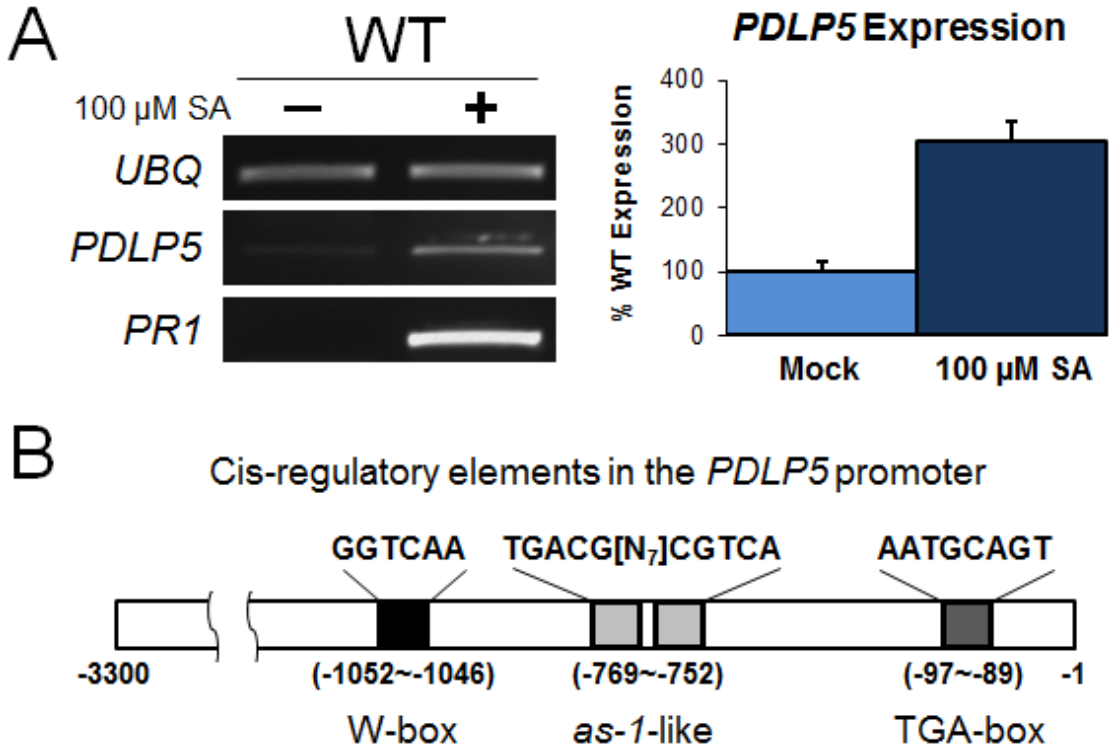

Figure 2.8: SA treatment upregulates *PDLP5* expression.
A, RT-PCR results for *PDLP5* expression in WT 3-week old leaves, treated with water or 100 µM SA for 24 hours; *UBQ* used as loading control, *PR1* used as positive control for SA treatment. Graph shows expression standardized to the level of *PDLP5* in mock-treated WT. Quantified by comparing gel band intensities using Image-J software. **B**, a graphical representation of the type and position of stress response cis-regulatory elements in the *PDLP5* promoter.

To determine which SA pathway defense genes are required for SA-induced *PDLP5* expression, RT-PCR expression profiling of *PDLP5* transcript in the SA pathway mutants *eds1*, *ics1*, and *npr1* was performed. Not only was the SA-induced expression of *PDLP5* significantly reduced in all SA pathway mutants compared to WT plants, but the basal level of *PDLP5* in each mutant was reduced as well (Fig 2.9). These results indicated that even in non-stressed growth conditions, basal *PDLP5* expression is partially dependent on SA pathway genes.

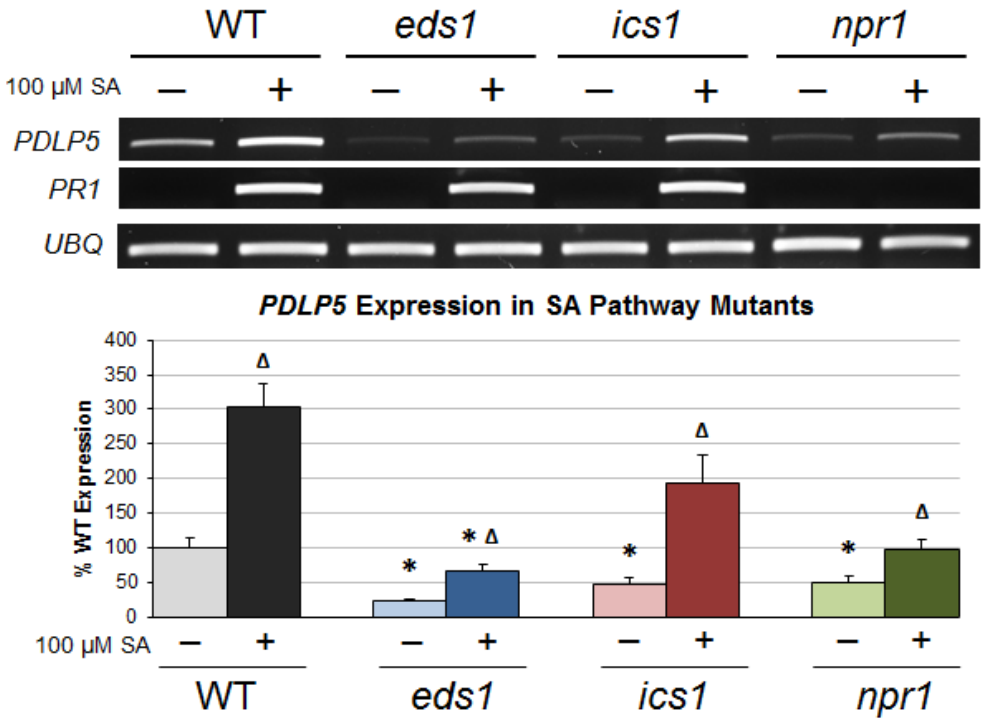

Figure 2.9: Mutations in the SA defense pathway reduce *PDLP5* expression. RT-PCR results for *PDLP5* in WT, *eds1*, *ics1*, and *npr1* 3-week old leaves, either mock-treated or treated with 100 µM SA; *UBQ* used as loading control, and *PR1* was used to confirm the effectiveness of SA treatment. Results were quantified by comparing band intensities using Image-J software. Graph shows data standardized to expression in mock-treated WT. The asterisk (*) indicates that the basal or SA-induced expression of *PDLP5* is significantly lower ($p<0.05$) in the SA pathway mutant background compared to the mock-treated WT background. The delta symbol (Δ) indicates that the SA-induced expression of *PDLP5* in WT or each mutant background is significantly higher ($p<0.05$) compared to its basal expression level in the same background.

In summary, when *PDLP5* is strongly expressed in *Arabidopsis*, it leads to high SA accumulation, spontaneous cell death, and the induction of SA-based defense and cell death genes. *PDLP5*-induced SA accumulation, defense signaling, and cell death are dependent on a functional SA defense pathway. In turn, basal and induced expression of *PDLP5* itself is also dependent upon the SA defense pathway.

2.4 Discussion

It is intriguing that the *ics1* mutation cannot fully rescue the dwarf phenotype caused by *35S:PDLP5*, while *NahG* can (see Fig 2.4 and 2.5). The *ICS1* biosynthesis pathway controls about 90% of SA produced during most innate immune responses (Wildermuth et al., 2001; Garcion et al., 2008). This means that there would still be about 10% SA produced in *ics1 x 35S:PDLP5,* compared to no accumulation in *NahG x 35S:PDLP5*. It seems unlikely that this small difference in SA concentration is attributable to the residual growth defect in the *ics1 x 35S:PDLP5* plants. Thus, it seems possible that *PDLP5* could upregulate the SA pathway through means other than ICS1.

I speculate that the best candidate gene for a potential PDLP5-dependent, ICS1-independent SA biosynthesis pathway could be *WIN3*, also called *PBS3*. *WIN3/PBS3* is part of the Gretchen Hagen 3 (GH3) family of enzymes, which conjugate amino acids to 4-substituted benzoates (Okrent et al., 2009), and studies have shown that *WIN3/PBS3* contributes to some amount of SA accumulation during defense (Warren et al., 1999; Jagadeeswaran et al., 2007). Importantly, bioinformatics data collected from the online resource ATTED-II (http://atted.jp) show that this gene is co-expressed with *PDLP5* (see App Table B1), and when WIN3/PBS3 is targeted by the bacterial effector HopWin1, *PDLP5* transcript is very highly induced (Lee et al., 2008). These characteristics make WIN3/PBS3 a strong candidate for PDLP5-dependent, ICS1-independent SA biosynthesis during an innate immune response. This hypothesis could be tested by introducing *35S:PDLP5* into *win3* and *win3/ics1* mutant backgrounds, and comparing plant growth to *ics1 x 35S:PDLP5*, to determine if *win3* and *ics1* act additively to reduce the stunted growth phenotype.

Alternatively, PDLP5-dependent, ICS1-independent stunted growth could be caused by SA-precursors or similar benzoate compounds with some bioactive defense properties. Recent studies into GH3 family proteins like WIN3/PBS3 have revealed that they might enhance SA production during defense responses by creating an SA-precursor pool of conjugated benzoate compounds (Westfall et al., 2016), which could be converted to SA through ICS1-independent pathways (Widhalm and Dudareva, 2015). Relatively little is known about the defensive properties of these ICS1-independent SA-precursors and similar benzoates, but if they can both alter plant defense responses and act as substrates for *NahG*, it would explain why *NahG* fully rescues the *35S:PDLP5* phenotype, while *ics1 x 35S:PDLP5* still retains stunted growth (Fig 2.4 and 2.5). This alternative hypothesis could be tested by metabolic profiling to measure for abnormal accumulations of such chemical compounds in *35S:PDLP5*, then comparing the results to the metabolic profiles from *35S:PDLP5* crossed with *win3*, *ics1*, or *NahG*, to find which SA-precursors or similar benzoates are reduced in each mutant background.

Our model for the role of PDLP5 during innate immunity is shown below (Fig 2.10). A virulent pathogen activates the SA pathway through the upstream components EDS1 and PAD4, upon which these work together to upregulate SA biosynthesis via the ICS1 enzyme. SA accumulation triggers downstream expression of innate immune defense genes via NPR1, including PDLP5, which itself activates SA accumulation via an unknown mechanism, creating a positive feedback loop that boosts immunity. PDLP5 may also work through an ICS1-independent pathway, like through PBS3/WIN3-dependent SA or SA-precursor biosynthesis, to boost innate immunity. Whether PDLP5 can impact innate immunity through pathways besides SA, and

whether PD closure itself may have some effect on innate immune signaling, remains to be uncovered. Given the importance of PD to multicellular plant growth and development, it would not be surprising to find that other proteins guard PD during defense as well.

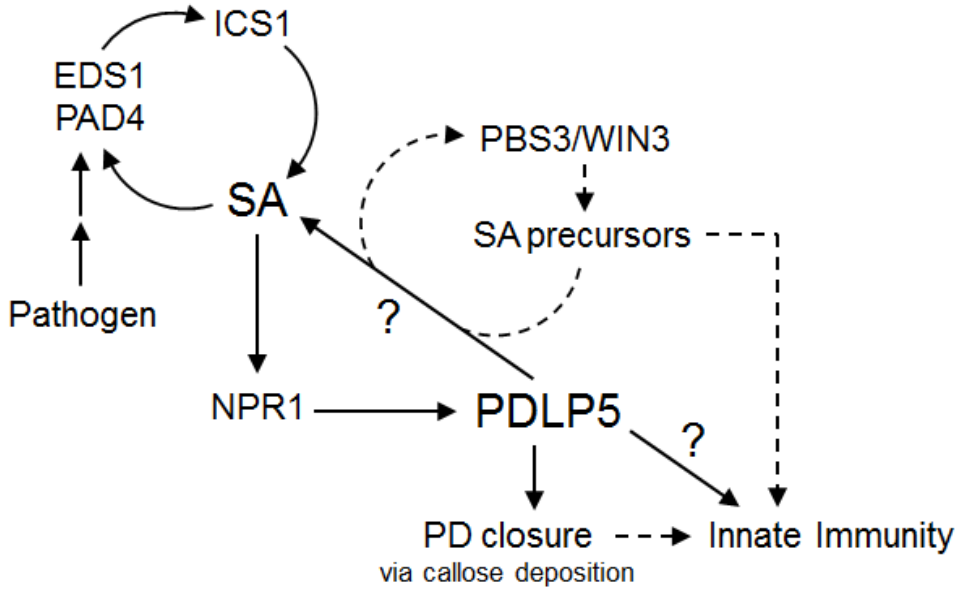

Figure 2.10: Hypothetical model of a PDLP5 and SA-dependent innate immune pathway.
Solid arrows indicate proven connections between components of the pathway, and those with question marks indicate that how one component regulates the other is unknown. Dashed arrows indicate speculated but as yet unproven connections between components of the pathway.

Our lab has since gone on to prove that PDLP5 is required for innate immunity to virulent bacterial pathogens (Lee et al., 2011), and that during an innate immune response, PDLP5 and SA are both required together to close PD via callose deposition, in an NPR1-dependent pathway (Wang et al., 2013). Excitingly, this SA- and PDLP5-dependent PD callose is regulated by a particular *Callose Synthase* (*CALS*), *CALS1*, a

protein that has been known to be upregulated during basal defense responses (Cui and Lee, 2016). The likely reason for this would be protection against plant viruses, which require PD as they move from infected to healthy cells, and indeed we have proven that *PDLP5* upregulation can prevent the spread of some viruses (Lee et al., 2011). Thus, a complete pathway, from biotrophic bacterial attack to PD closure via callose, has been outlined.

The research into the PDLP5/SA defense connection described in this chapter prompted other research into PDLPs and defense. Intriguingly, PDLP1 has been discovered to work together with PDLP5 to control the movement of SAR signals during plant defense. *PDLP5* and *PDLP1* overexpression was found to restrict the symplasmic movement of the SAR signals Defective in Induced Resistance 1 (DIR), azelaic acid (AzA) and glycerol-3-phosphate (GP3), while SA itself moves via an apoplastic pathway (Carella et al., 2015; Lim et al., 2016). Even though SAR signal movement is impaired, functional *PDLP5* and *PDLP1* are still required for the SAR response in distal leaves (Lim et al., 2016). Collectively, it seems plausible to me that PDLP5 evolved separate but essential functions in basal immunity and SAR: the initial, localized SA upregulation and PD closure during basal immunity that may be required to prevent intercellular pathogen movement or the cell-to-cell spread of pathogenic molecules; followed by control of SAR signal intercellular movement and the perception of SAR signals in distal leaves. It also seems possible that the level of PD closure versus PDLP SAR signal transmission acts in a gradient fashion: PD are tightly restricted via PDLP-induced callose deposition in the area of infection, but less so farther out from the infection site, instead shifting to the SAR recognition function

at PD. Clearly, the correct balance of PD restriction/transmission of SAR signals is required for a whole-plant defense response.

The salicylic acid pathway has long been known to control many important defense-building reactions within the plant, though only recently has the relationship between SA accumulation and PD regulation begun to be explored in more detail. With further research, other PD-regulating proteins will likely be found, each connected to specific hormone signals or downstream CALS for different environmental or defense responses. It would be exciting if future research proved that other pathogen types, like bacteria and fungi, somehow attempted to hijack PD in order to enhance their virulence, which SA-induced PDLP5-dependent callose deposition could prevent. In fact, some promising results with pathogenic fungi targeting PD have come out recently (Kankanala et al., 2007; Faulkner et al., 2013).

Chapter 3

PDLP5 REGULATES LATERAL ROOT DEVELOPMENT

3.1 Background

3.1.1 The Role of Auxin in Lateral Root Emergence

The plant hormone auxin plays an essential role in controlling lateral root growth and development (Vilches-Barro and Maizel, 2015). Auxin is first synthesized in the shoot and transported via bulk flow through the phloem into the root, where it accumulates within the primary and lateral root apices, driving their growth (De Smet et al., 2007; Ingram et al., 2011). Specialized extracellular transmembrane proteins called auxin influx or efflux carriers, depending upon whether they transport auxin into or out of a cell, respectively (Robert and Friml, 2009), allow for targeted auxin accumulation within the specific cells involved in lateral root development.

Auxin accumulation within two zones is required for lateral root development and emergence: the developing lateral root itself, and the overlying tissue. Development begins when auxin is targeted to specific xylem pole pericycle cells called founder cells (FCs), where it stimulates the first cellular divisions that will become the new lateral root, a process called lateral root initiation (LRI); after LRI, the immature lateral root is called a lateral root primordium (LRP) (Fig 3.1A). The auxin that propels LRP growth also moves into the overlying root tissue, where it activates tissue-specific pathways that lead to separation of the overlying cells, allowing the LRP to emerge. LRP development and emergence progresses through

nine stages, each representing the size of the LRP and where its apex has reached within the overlying tissue: in stage 0, LRI occurs; in stages I-III, LRP outgrowth begins and moves through the separating endodermal cells; in stages IV-VI, the LRP grows through the separating cortical cells; and in stage VII-VIII, the LRP grows through the separating epidermal cells, before finally emerging (Fig 3.1A).

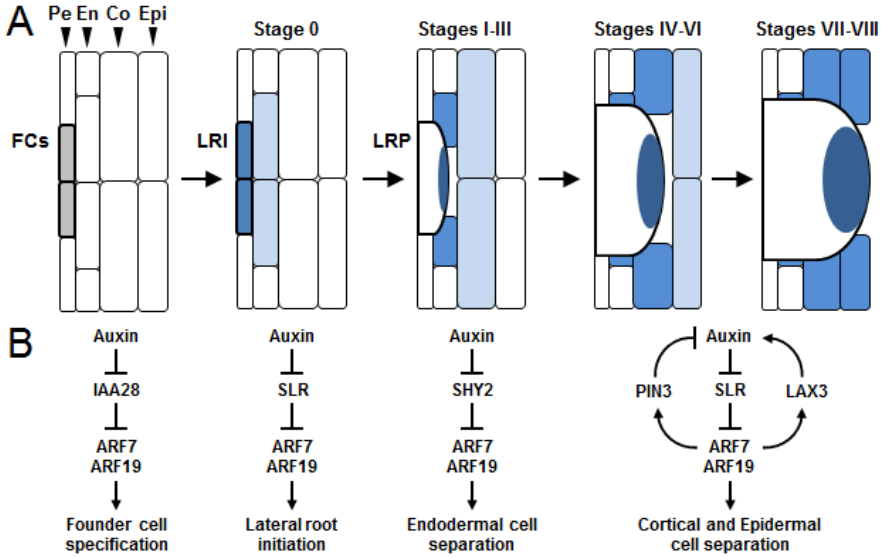

Figure 3.1: Model of LRP development, with representative examples of various stages before emergence.
A, auxin controls the formation of founder cells (FCs, gray), which are later stimulated by auxin to divide during LRP initiation (LRI); auxin transported from the LRP apex accumulates within the overlying cells to control LRP emergence (light to dark blue indicates increasing auxin). LRP initiate in the pericycle (Pe) (stage 0), and grow outward through the overlying endodermal (En) (stages I-III), cortical (Co) (stages IV-VI), and epidermal (Epi) (stages VII-VIII) layers before emerging. **B**, different auxin-dependent factors control each stage of LRP development and emergence.

Recent work has uncovered many of the auxin-dependent factors controlling LRP development and emergence (Fig 3.1B). For example, auxin causes the degradation of transcriptional repressor *Indole-Acetic Acid Inducible 28* (*IAA28*) in the

pericycle, allowing the transcription factors *Auxin Response Factor 7* (*ARF7*) and *ARF19* to upregulate the process that designates the FCs (De Rybel et al., 2010). After FC specification, auxin targeted to these cells leads to the degradation of the transcriptional repressor *Solitary-Root* (*SLR*), which upregulates *ARF7* and *ARF19* to activate LRI (Fukaki et al., 2002; Fukaki et al., 2005). Auxin-regulated *Short Hypocotyl 2* (*SHY2*), an endodermis-specific repressor of *ARF7* and *ARF19*, controls the LRP-overlying endodermal cell separation process (Goh et al., 2012b; Vermeer et al., 2014), while the separation of the LRP-overlying cortical and epidermal layers occurs through a *SLR* and *ARF7/19*-regualted pathway (Swarup et al., 2008). The correct balance of auxin controlling the LRP-overlying cortical and epidermal cell separation is sustained by the auxin influx carrier *Like Auxin-Resistant-1 3* (*LAX3*), which draws auxin from the developing LRP to concentrate it within these cells, and the auxin efflux carrier *Pin-Formed 3* (*PIN3*), which lowers the auxin level within the cells and is necessary to maintain the flow of auxin from inner to outer tissue (Swarup et al., 2008; Peret et al., 2013; Perrine-Walker and Jublanc, 2014). Eventually, the high auxin level that builds in the LRP-overlying cells upregulates cell wall-remodeling enzymes, which degrade the middle lamella and other cell wall components holding the two cells together, allowing them to separate with minimal cellular damage (Peret et al., 2009).

Auxin influx and efflux carriers have so far been the major focus of research into how cells create and retain an auxin maximum in LRP-overlying root tissue (van Berkel et al., 2013), but the role of plasmodesmata (PD) in auxin accumulation has been largely ignored. Excitingly, I have found that *PDLP5* expression in *Arabidopsis thaliana* roots is highly specific to the cells overlying LRP. Auxin is a small molecule

that could potentially diffuse from auxin-accumulating cells through PD, and we hypothesized that *PDLP5* has an important function in maintaining auxin maxima during LRP emergence by closing PD to prevent auxin diffusion. To test this hypothesis, I pursued the following research objectives.

3.1.2 Research Objectives

Objective 1: Determining the root phenotypes associated with PDLP5 gain-of-function and loss-of-function mutants. To this end, seedlings of WT, *pdlp5-1*, and *PDLP5OE* (*35S:PDLP5*) were grown vertically on agar plates, lateral roots were counted, primary and lateral roots were measured, and the rate of LRP emergence was compared.

Objective 2: Determining the spatiotemporal expression pattern of *PDLP5*. To this end, histochemical staining was performed on seedlings of *PDLP5pro:GUS*.

Objective 3: Determining whether auxin and other hormones regulate *PDLP5* expression in roots. To this end, *PDLP5pro:GUS* seedlings were subjected to various plant hormone treatments, as well as hormone-repressing treatments, then stained for GUS activity.

Objective 4: Uncovering which auxin signaling pathway is responsible for *PDLP5* expression in the roots. To this end, *PDLP5pro:GUS* was crossed into mutants of various auxin-regulated genes in the lateral root emergence pathway.

Objective 5: Identifying the subcellular domains and timing of *PDLP5* expression during LRP development. To this end, *PDLP5pro:PDLP5-GFP Arabidopsis* transgenic lines were produced and examined using confocal microscopy.

Objective 6: Determining the function of *PDLP5* in LRP-overlying cells. To this end, *pdlp5-1* and *PDLP5OE* were crossed with auxin fluorescent marker lines

DR5:3VENUS and *LAX3pro:LAX3-YFP*, to detect differences in the diffusion of auxin into overlying root cells.

Objective 7: Examining the role of *PDLP5* in root PD regulation. To this end, GFP was expressed under the root endodermis-specific promoter of *Casparian Strip Membrane Protein 1* (*CASP1*), and *PDLP5* was induced to observe changes in GFP PD trafficking.

3.2 Materials and Methods

3.2.1 Plant Growth Conditions

Plants were grown in soil or on agar media as described in Appendix A1 and A2, respectively. Plant genotypes used in this study are described in Appendix Table A7. Crosses were made by dissecting the unopened buds of the mutant plants (maternal lines) under a light microscope, and spreading the pollen of the transgenic plants (paternal lines) onto the unpollinated stigma of the dissected bud. Plant transformations of Col-0 were performed using the standard *Agrobacterium* floral dip method (Clough and Bent, 1998).

3.2.2 Plant Treatments

To treat Arabidopsis, plants of the desired age were either sprayed with hormones diluted to the necessary concentration in autoclaved nano-purified water and 0.01% Silwett-77 (as a surfactant), or hormones were mixed into autoclaved MS media after cooling to a temperature that was tolerable to hold with bare hands. For stock and treatment concentrations, see Appendix Table A8.

3.2.3 Creation of PDLP5 and Tissue-Specific Promoter PDLP5 and Fluorescent Marker Lines

To clone tissue-specific promoter *CASP1*, Arabidopsis Col-0 genomic DNA was extracted according to standard protocol, and used as the template for PCR amplification with Phusion® High-Fidelity DNA Polymerase (Thermo Scientific™). Plasmid DNA of PDLP5pro:GUS in pRita was used as a template to clone the PDLP5 promoter; plasmid DNA of pdYC was used as a template to clone ER-YFP; plasmid DNA of P30 TMV-MP-GFP in pdGN was used as a template to clone TMV-MP-GFP (for primers and PCR program, see Appendix Tables A3 and A5).

The PCR products were purified using a Zymo Research DNA (PCR) Clean & Concentrator™ kit. Digestions and ligations were performed using New England Biolabs® Inc. (NEB) restriction enzymes and T4 DNA ligase, following the company's protocols.

All digestion products were gel-purified and extracted using a Zymoclean™ Gel DNA Recovery Kit (Zymo Research). Ligation products were transformed into electrocompetent DH10 bacteria and stored as glycerol stocks.

3.2.4 Histochemical Staining for β-Glucuronidase (GUS) Activity

Seedlings were removed from agar media, then submerged in GUS staining solution (100 mM sodium phosphate buffer pH 7.0, 10 mM EDTA pH 8.0, 0.5 mM each potassium ferrocyanide and potassium ferricyanide, 1.24 mM X-Gluc, and 0.1% Triton X-100). The GUS solution was vacuum-infiltrated into plant tissue for five minutes, then removed from vacuum and incubated in 37°C for 30 min or up to 16 hrs, followed by a series of 70% ethanol clearing. Stained tissues were imaged using light microscope and software (see below).

3.2.5 Microscopy

Root counting was performed using a Zeiss Axioskop 2 microscope. LRP were quantified by counting both the emerged LR and unemerged LRP, as determined by DR5:GUS staining of the primordia, under a dissecting microscope (1.2X magnification). LRP stages were determined by examining ethanol-cleared, GUS-stained tissue using a 40X water lens.

To image using a confocal, seedlings were mounted in nano-pure water and placed in a Nunc™ chamber under a glass slide coverslip. For PDLP5pro:PDLP5-GFP localization, seedlings were stained for 10-15 min in 5 μg/mL propidium iodide at 7 dpg. Imaging was performed on a Zeiss AxioObserver Z1 inverted light microscope using a LSM 710 scanhead. For DR5:3VENUS imaging, a LD LCI Plan-Apochromat 25x/0.8 Imm Korr DIC objective was used, with a 514 nm excitation laser and 515-550 nm (for VENUS) and a 585-758 nm (for propidium iodide) emission filters. For PDLP5pro:PDLP5-GFP, a C Apochromat 40x/1.20 W Korr objective was used, with a 488 nm excitation laser and 500550 (GFP) emission filter, and detected with a BiGaAsP (Bi Gallium Arsenide Phosphide) Detector. Image brightness, contrast and gamma were adjusted to enhance the images via ZEN 2011 software. The 3D model of PDLP5pro:PDLP5-GFP in overlying cells was created using Amira 5.6 software to render separate channels, highlighting GFP signal and interpolating root cell shape from the propidium iodide outline. For counting LAX3pro:LAX3-YFP cells, a 25x/0.8 mm Korr DIC objective was used, with a 514 nm excitation laser and a 575-610 nm BP filter (YFP) and a 543-735 nm BP filter (propidium iodide), and YFP was detected with the BiGaAsP Detector. For monitoring the timing of LAX3pro:LAX3-YFP expression, the cortical cell fluorescence at the root bend was monitored at different time points using a Zeiss LSM 780 confocal upright light microscope using a W Plan-

Apochromat 20x/1.0 DIC M27 75mm objective and the 415-nm excitation line of an argon laser with 520-550nm band pass emission filter. Images are presented as 3-D composites of 30 µm-thick z-stacks.

3.3 Results

3.3.1 *PDLP5* is Required for Normal Lateral Root Branching

To determine the role of *PDLP5* in root development, seedlings of WT (Col-0), *pdlp5-1*, and *PDLP5OE* lines were grown vertically side-by-side on agar plates. By 10-days post-germination (dpg), compared to WT, the *pdlp5-1* line seemed to have a small increase in root branching, while root branching was reduced in *PDLP5OE*, compared to WT. To better quantify the impact of *PDLP5* expression levels on lateral root branching, *pdlp5-1* and *PDLP5OE* lines were crossed with the *DR5:GUS* reporter line. The DR5 promoter is artificially engineered from several auxin-response promoter elements (Ulmasov et al., 1997). As such, the *DR5:GUS* line is useful to visually locate LRPs, as stains the auxin maxima that form in the tips of LRPs from their earliest stages of development. The total number of secondary, tertiary, and quaternary roots in the WT, *pdlp5-1*, and *PDLP5OE* backgrounds were counted at 8 and 11 dpg (Fig 3.2A and B). The *pdlp5-1* background had significantly higher numbers of tertiary roots (50% more at 8 dpg, Fig 3.2A ; 70% more at 11 dpg, Fig 3.2B) and quaternary roots (200% more at 11 dpg, Fig 3.2B) compared to WT, though the number of secondary roots remained similar. In contrast, the *PDLP5OE* background had significantly fewer secondary roots (33% fewer at 8 dpg, Fig 3.2A; 23% fewer at 11 dpg, Fig 3.2B) and tertiary roots (67% fewer at 8 dpg, Fig 3.2A; 50%

fewer at 11 dpg, Fig 3.2B) compared to WT. These results revealed a negative correlation between *PDLP5* expression levels and lateral root branching.

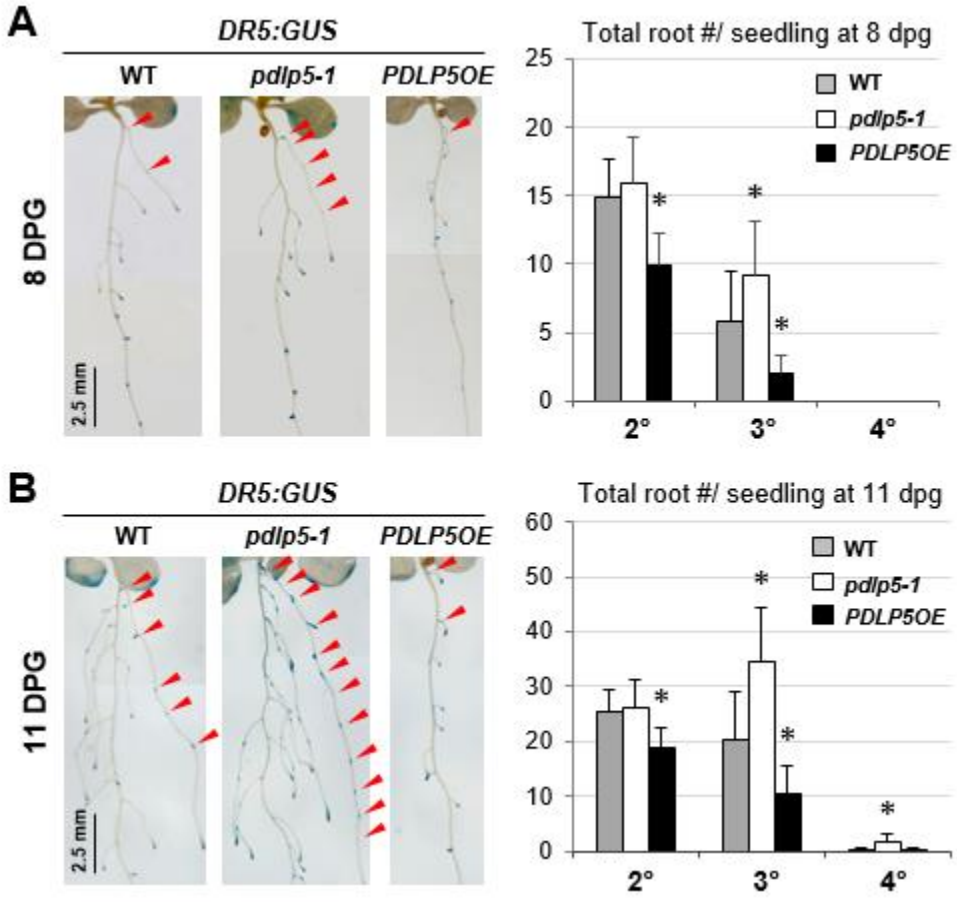

Figure 3.2: *PDLP5* expression indirectly correlates with lateral root branching. Lateral root development and quantification in WT, *pdlp5-1*, and *PDLP5OE* expressing *DR5:GUS*, at 8 dpg (**A**) and 11 dpg (**B**). In the images, arrowheads indicate the growth of tertiary roots along the length of a representative secondary root(s) in each background. In the graphs, quantification of total secondary [2°], tertiary [3°], and quaternary [4°] roots was done with n≥30 per seedlings per line. Bars, standard deviation. Asterisks, significance determined by student T-test (P<0.01).

Next, the lengths of *pdlp5-1* and *PDLP5OE* primary and secondary roots were measured. It was found that *PDLP5OE* had reduced primary root length (31% shorter) and repressed secondary root emergence (49% fewer emerged) compared to WT (Fig 3.3A and B). Average primary root length and total number of secondary root number were comparable between WT and *pdlp5-1* backgrounds (Fig 3.3A and B). However, the average secondary root length per seedling was 29% longer in *pdlp5-1* seedlings than in WT, while the tertiary root density remained similar between these backgrounds (Fig 3.3C and D). These results suggested that longer secondary roots in *pdlp5-1* allow more tertiary roots to develop compared to WT seedlings.

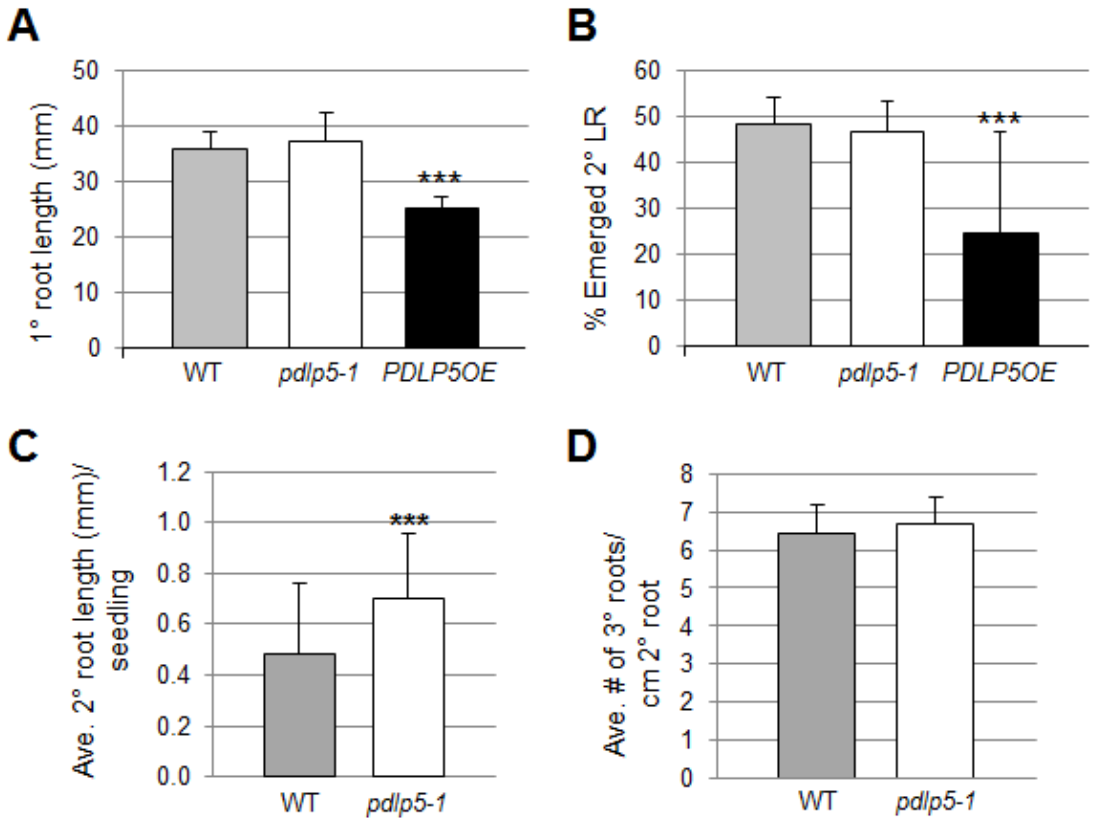

Figure 3.3: Differing expression levels of *PDLP5* leads to changes in root phenotype.

A, total primary root length is similar in WT and *pdlp5-1*, but reduced in *PDLP5OE*. **B**, the percent of emerged secondary roots per seedling was similar in WT and *pdlp5-1*, but reduced in *PDLP5OE*. **C**, average secondary root length per seedling was higher in pdlp5-1 than in WT. **D**, the tertiary root density is similar between WT and *pdlp5-1* backgrounds. **A** and **B**, seedlings 10 dpg, n=30 per line; **C** and **D**, seedlings 7 dpg, n>20 per line.

3.3.2 *PDLP5* is Required for Normal Progression of Lateral Root Emergence

The changes in secondary root length (Fig 3.3) suggested that the dynamics of LRP emergence might differ between the *PDLP5* backgrounds. Thus, a gravitropic assay (Peret et al., 2012a) was used to compare the LR emergence rates of WT, *pdlp5-1*, and *PDLP5OE*. To perform this assay, vertically-grown seedlings are rotated 90° by turning the agar plate, causing the roots to bend toward the new gravitropic vector. The auxin accumulation required to bend the root also triggers a new LRP to form at the bend, providing a known initial time-point for observing LRP from the onset of development. Three time-points post-gravitropism were chosen based on the LRP progression timing of WT (Peret et al., 2012a): 18 hours post-gravitropism (hpg), when the LRP would be between I-III stages; 42 hpg, when LRP would be between V-VIII stages, and 48 hpg, when the majority of LRP should have fully emerged (Fig 3.1).

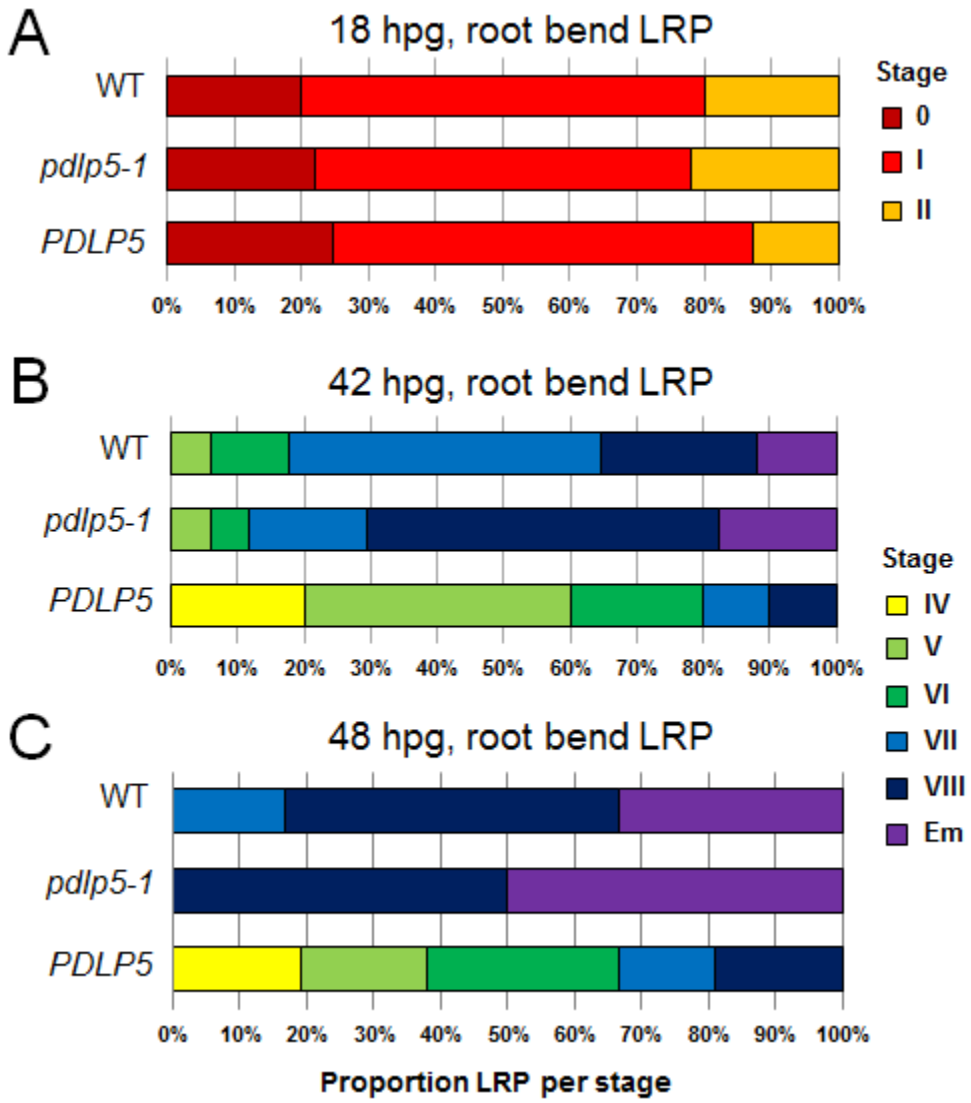

Figure 3.4: *PDLP5* expression affects the rate of LRP emergence.
Graphs of different time-points post-gravistimulation, showing the proportion of total root bend LRP at certain stages of emergence in WT, *pdlp5-1*, and *PDLP5OE*. **A**, 18 hpg is a representative time-point of the LRP initiation and organization phase; here, root bend LRP of all *PDLP5* backgrounds showed similar levels of development. **B** and **C**, 42 and 48 hpg are representative time-points of late-stage LRP emergence; here, root bend LRP of *pdlp5-1* were farther along in the progression of LRP emergence than WT, while *PDLP5OE* lagged behind. At each time-point, n>20 seedlings.

WT, *pdlp5-1*, and *PDLP5OE* backgrounds were grown vertically on 1% agar plates for four days before being turned 90°. At 18 hpg, LRP in the root bend area were at similar stages of development in WT, *pdlp5-1*, and *PDLP5OE* (Fig 3.4A). However, during later development, clearer differences among the three genotypes became apparent. At 42 hpg, 32% more pdlp5-1 root bend LRP had reached stage VIII (Fig 3.4B), and by 48 hpg, 17% more LRP had fully emerged (Fig 3.4C), compared to WT. In contrast, *PDLP5OE* was severely restricted in LRP emergence; no LRP had emerged by 42 or 48 hpg, and a majority of seedlings (67-80%) were still in earlier stages (IV-VI), compared to WT (Fig 3.4B and C). These data suggest that *PDLP5* expression is essential for modulating the rate of LRP emergence, but not the initial development of these organs.

To determine whether *PDLP5* expression could alter LRP and root tip growth rates, which could account for differences in the LRP emergence rates and LR lengths in *PDLP5* mutants, the level of cell division in the root tips of WT and *pdlp5-1* was examined. *CYCB1;1:GUS*, a marker for cell division used previously to find enhanced cell division and increased root growth (Ferreira et al., 1994), was crossed into *pdlp5-1*, and compared to *CYCB1;1:GUS* in WT as a control. No changes were found in the amount of root tip cell division between WT and *pdlp5-1* (see Appendix C1). Thus, the faster LR emergence of the *pdlp5-1* mutant is not attributable to an increased rate of root tip growth.

3.3.3 *PDLP5* Expression is Induced in Cells Overlying Lateral Root Primordia

Previous studies on *Arabidopsis* mutants with altered LRP emergence rates showed that several auxin regulators were expressed within endodermal, cortical, and/or epidermal root cells overlying the emerging LRP (Neuteboom et al., 1999;

Vissenberg et al., 2005; Gonzalez-Carranza et al., 2007; Swarup et al., 2008). To examine whether PDLP5 expression followed similar spatiotemporal patterns to these auxin regulators, the proximity of *PDLP5* expression to LRP was determined by using the transcriptional reporter *PDLP5pro:GUS* in the Col-0 WT background.

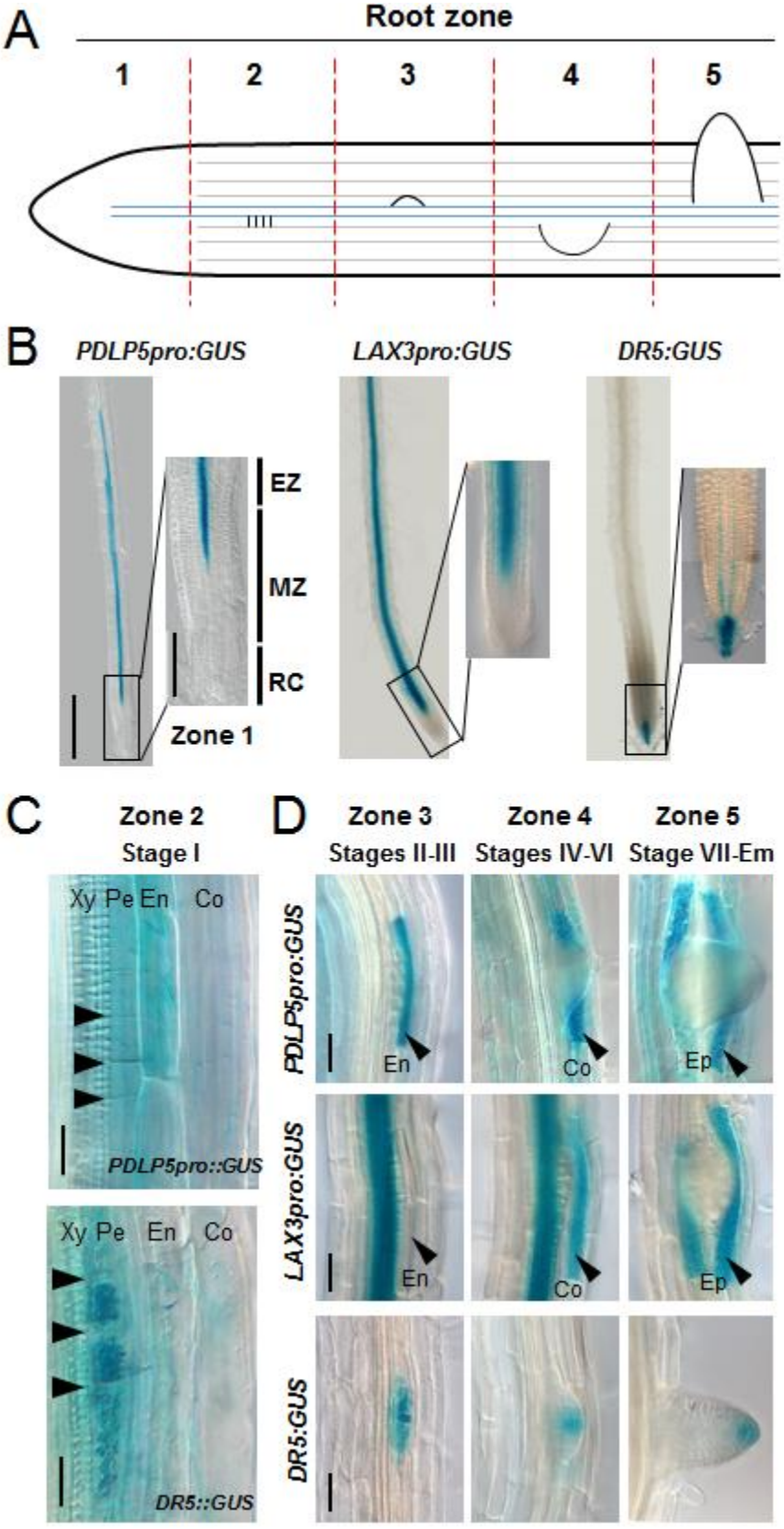
A
Root zone
1
2
3
4
5
B
PDLP5pro:GUS
LAX3pro:GUS
DR5:GUS
EZ
MZ
RC
Zone 1
C
Zone 2
Stage I
Xy Pe En Co
PDLP5pro::GUS
Xy Pe En Co
DR5::GUS
D
Zone 3
Stages II-III
Zone 4
Stages IV-VI
Zone 5
Stage VII-Em
PDLP5pro:GUS
LAX3pro:GUS
DR5:GUS
En
Co
Ep

Figure 3.5: Spatiotemporal expression of *PDLP5* in overlying cells during LRP development.
A, simple root model, representing different developmental zones (**Zones 1-5**) along the root that correspond to where the images were taken; each of the five zones is separated by dashed red lines. **B**, representative images of the lower roots of *PDLP5pro:GUS*, *LAX3pro:GUS*, and *DR5:GUS*, encompassing the root cap (RC), meristematic zone (MZ), and elongation zone (EZ) (**Zone 1**). **C**, close-up representative images of dividing pericycle cells in first stage (I) of LRP development (arrowheads indicate first divisions) (**Zone 2**). **D**, representative images of LRP at different developmental stages, corresponding to growth through the endodermis (stages II-III), cortex (stages IV-VI), and epidermis (stages VII-Em) (**Zones 3-5**). Xy, xylem; Pe, pericycle; En, endodermis; Co, cortex; Ep, epidermis. Scale bars, 10 µm. Scale bars, 50 µm.

Histochemical staining revealed that *PDLP5* promoter activity was visible in LRP-overlying cells at all stages of emergence (Fig 3.5). Starting from stages I-III, *PDLP5pro:GUS* was visible within the overlying endodermal cells (Fig 3.5 columns 2-3). As the LRP progressed into later stages of emergence and pushed through the overlying tissue, GUS-staining became visible in the overlying cortical and epidermal cells (Fig 3.5 columns 4-5). This expression pattern closely matched *LAX3*, a known regulator of LRP emergence (Swarup et al., 2008) (Fig 3.5 columns 4-5). Furthermore, *PDLP5pro:GUS* is excluded from inside LRP and the tips of primary and lateral roots, unlike *DR5:GUS*, which stains the auxin maxima that form in the root cap and meristematic zones (Fig 3.5 row 1 and columns 2-5).

3.3.4 Auxin Controls *PDLP5* Expression in LRP-Overlying Cells

The known LRP-emergence regulator *LAX3*, expressed in a very similar pattern to *PDLP5* (Fig. 3.5), was previously shown to be dependent on shoot-derived auxin (Swarup et al., 2008). To test if a shoot-derived signal, possibly auxin, could be responsible *PDLP5* expression within LRP-overlying cells, *PDLP5pro:GUS*,

LAX3pro:GUS, and *DR5:GUS* were grown vertically on plates for five days, then shoot tissue was cut off at the hypocotyl/root junction, and the roots were GUS-stained after two more days of post-shoot growth on the plates. Post-shoot removal, GUS staining was greatly reduced in all genotypes: *PDLP5pro:GUS* and *LAX3pro:GUS* were almost completely eliminated from the LRP-overlying tissues, and *DR5:GUS* staining was eliminated from the LRP tips (Fig 3.6). These results indicated that *PDLP5* expression in LRP-overlying cells is likely reliant on shoot-derived auxin.

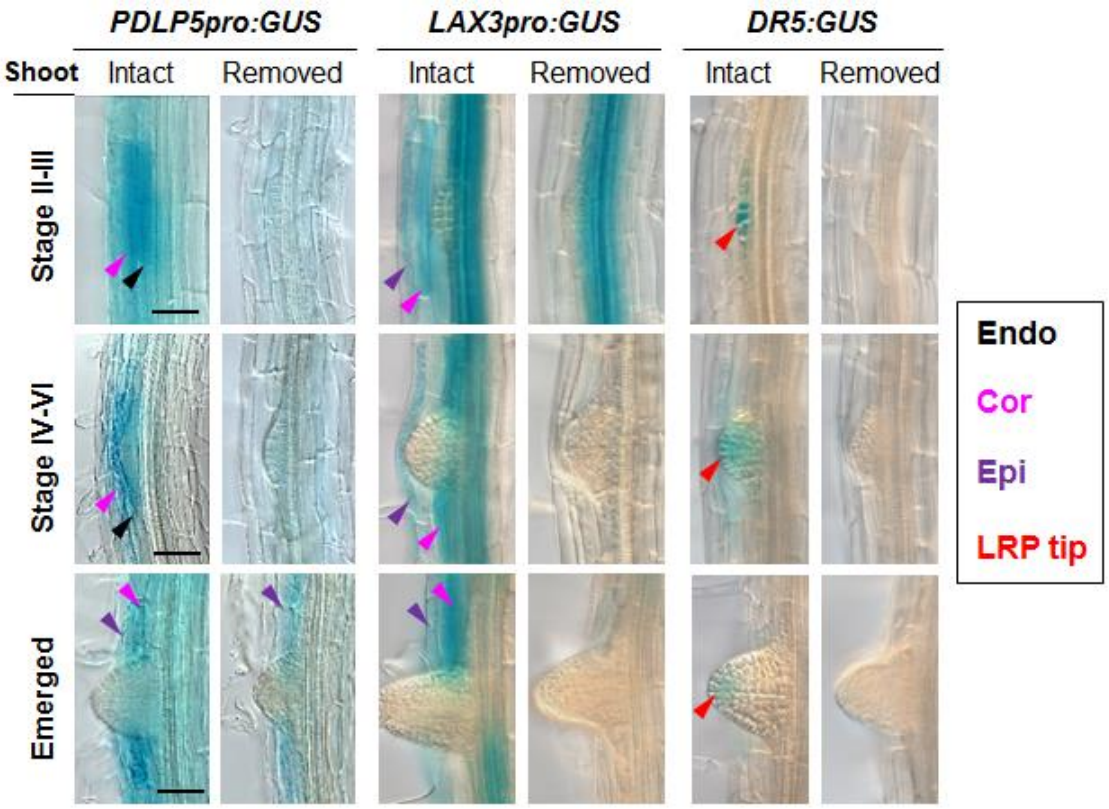

Figure 3.6: The LRP-overlying cell expression pattern of *PDLP5* depends on shoot-derived auxin.
PDLP5pro:GUS, *LAX3pro:GUS*, and *DR5:GUS* were grown for five days on agar plates, then shoots were either removed or left intact, and seedlings were grown for

two more days before GUS staining. Arrowheads indicate where GUS-staining occurs in each line, and their colors correspond to tissue (see legend at right).

To directly test whether auxin regulates *PDLP5* expression in roots, PDLP5pro:GUS seedlings were treated with two concentrations of the membrane-permeable auxin analog 1-napthalene acetic acid (NAA). The lower auxin concentration (0.1 µM NAA) induced *PDLP5pro:GUS* strongly and specifically in the overlying cells above both endogenous and auxin treatment-stimulated LRP (Fig 3.7A). At a higher auxin concentration (1 µM NAA), *PDLP5pro:GUS* was indiscriminately induced throughout the root, except within the root cap and meristematic zones (Fig 3.7A). At 1 µM NAA, *DR5:GUS* staining was also saturated, including the root tips (Fig 3.7B). Salicylic acid (SA), which induces *PDLP5* expression in shoots (Lee et al., 2011), also strongly induced *PDLP5pro:GUS* in the roots except for the root cap and meristematic zones, similar to auxin-induced *PDLP5* expression (Fig 3.7A). By contrast, *DR5:GUS* was unaffected by SA treatment (Fig 3.7B). Other hormones were tested, but these did not affect *PDLP5* promoter activity (Fig 3.7).

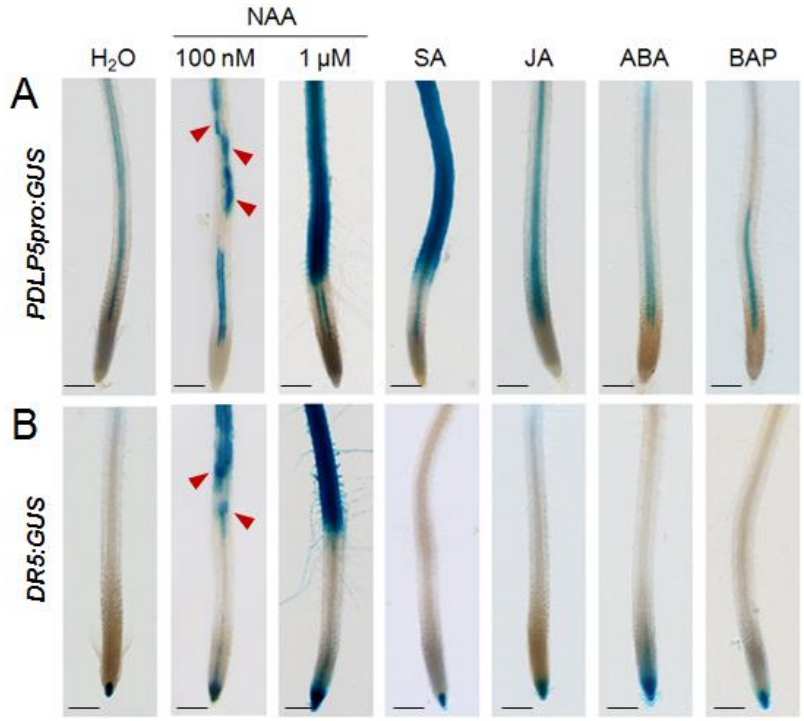

Figure 3.7: Exogenous auxin treatment induces *PDLP5pro:GUS* expression in the root.
Seven-day-old *PDLP5pro:GUS* (**A**) or *DR5:GUS* (**B**) seedlings grown on MS plates were mock-treated with water drops or treated with the indicated hormones in drops. Nine hours post treatment, the seedlings were GUS-stained for 3 hrs. Concentrations: SA, 100 µM; JA, 50 µM; ABA, 10 µM; 6-BAP, 1 µM. n=10 per treatment for each line. Representative images are shown. Scale bar, 100 µm.

To confirm that auxin-induced *PDLP5* promoter activity was tied to an upregulation of *PDLP5* transcript, RT-PCR was used on auxin-treated and untreated whole-root tissue. *PDLP5* transcript did increase by 50% in the roots upon NAA treatment (Fig 3.8A). Conversely, root treatment with polar auxin transport inhibitor 1-N-naphthylphthalamic acid (NPA) suppressed *PDLP5pro:GUS* induction in all root tissues (Fig 3.8B). Collectively, these results show that endogenous auxin stimulates *PDLP5* expression in the LRP-overlying cells.

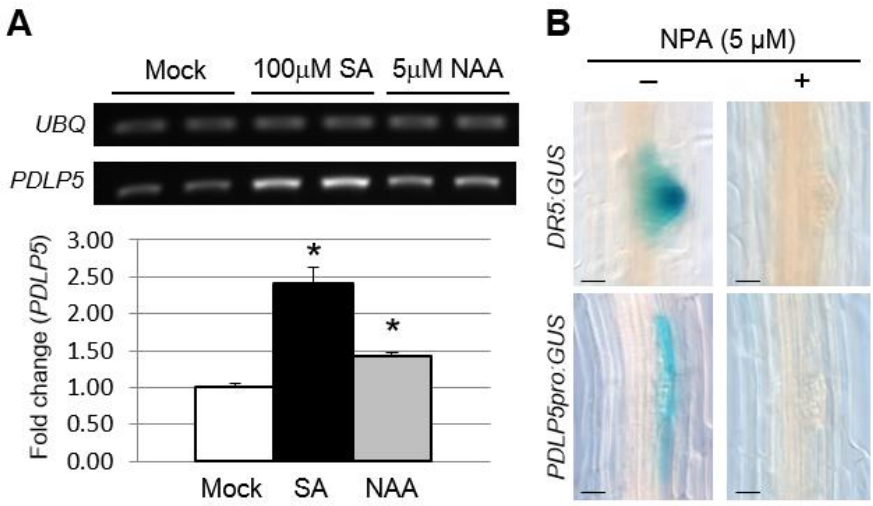

Figure 3.8: Auxin increases, while auxin inhibitor decreases, *PDLP5* root expression. **A**, Nine-day-old Arabidopsis WT seedlings were mock-treated with water or sprayed with the indicated hormones for 4 hours, then roots were excised, frozen, and RNA collected for RT-PCR. Relative band intensity was quantified with Image-J and standardized against ubiquitin. Concentrations: 100 μM SA, 5 μM NAA. Three biological and two technical repeats were performed. **B**, GUS-stained seedlings of *PDLP5pro:GUS* and *DR5:GUS*, transferred at 5 dpg to media lacking (-) or containing (+) 5 μM NPA, and grown for a further 24 hrs. Scale bars, 25 μm.

3.3.5 Auxin-Dependent Genes in the LRP Emergence Pathway Control PDLP5 Expression

To determine whether *PDLP5* expression in LRP-overlying cells is under the control of an auxin-dependent genetic pathway, *PDLP5pro:GUS* was crossed into auxin-insensitive mutants of early regulators of LRP development and emergence. A gain-of-function mutant of *SHY2*, called *shy2-2*, was tested first. In *shy2-2*, a negative auxin feedback loop is repressed, leading to abnormally high auxin levels in the LRP-overlying endodermis and nearby cells (Goh et al., 2012b); endodermal cell separation is strongly hindered (Vermeer et al., 2014); and while many LRP form, they fail to emerge and are aborted in early development (Tian and Reed, 1999). Compared to normal WT expression (Fig. 3.9, top row), the *PDLP5* promoter is highly active in the

shy2-2 root. *PDLP5pro:GUS* is strongly concentrated in the endodermal cells overlying the many aborted LRP in the *shy2-2* background (Fig 3.9, middle row), with some also detectable in the surrounding cells. Thus, *PDLP5* expression in LRP-overlying endodermal cells can occur through a *SHY2*-independent pathway, though due to the direct correlation between the high level of *PDLP5* promoter activity and the auxin increase in *shy2-2*, it seems likely that its expression is still auxin-dependent.

Next, *iaa28-1*, a gain-of-function mutant of *IAA28*, was explored. In *iaa28-1*, founder cell specification is severely hindered, resulting in only a few, underdeveloped LRP forming along the primary root (Rogg et al., 2001). Compared to the WT background, *PDLP5pro:GUS* staining was reduced in the endodermal cells overlying the few, underdeveloped LRP that formed in this background (Fig 3.9, bottom row). Thus, normal expression of *PDLP5* in LRP-overlying tissues requires *IAA28*-controlled LRP formation and initiation.

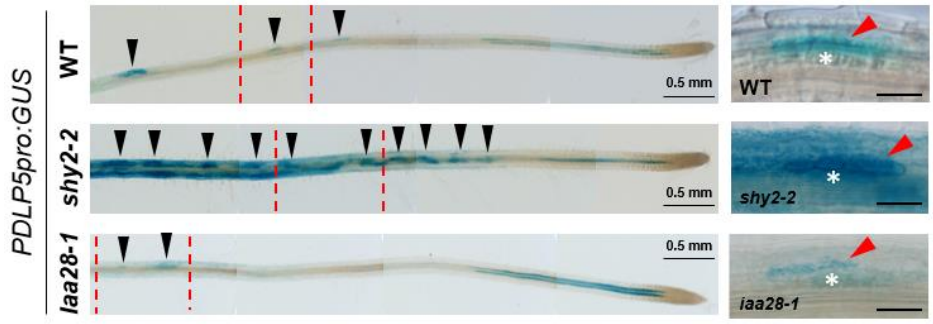

Figure 3.9: Lateral root mutants alter *PDLP5* root expression.
PDLP5pro:GUS expressed in 7 dpg WT, shy2-2, and iaa28-1 mutant backgrounds, showing the changes in staining pattern and intensity. Black darts, LRP-forming or aborted regions. Red dashes border the location along the root where stage II-III LRP (magnified images at right) first start to appear in each genetic background; stage II-III LRP were selected for closer focus because the majority of LRP in *iaa28-1* and *shy2-2* are aborted at or before stage III. Red darts in the higher magnification images point to

overlying endodermal cells of stage II-III LRP (LRP tips marked with white asterisks), showing the differing intensity of auxin-stimulated *PDLP5:GUS* expression.

Further exploration of the auxin-dependent pathway controlling *PDLP5* expression in LRP-overlying tissues was performed by crossing *PDLP5pro:GUS* with the double knockout mutant *arf7arf19,* which is severely hindered in LRP foundation, initiation, and emergence, resulting in no LRP formation (Wilmoth et al., 2005). No GUS staining was detected in aborted LRP-overlying cells of the *arf7arf19* mutants (see Appendix C2). Finally, *PDLP5pro:GUS* was crossed into the gain-of-function mutant *slr-1,* which is severely hindered in the process of LRP initiation (Fukaki et al., 2002). In older seedlings of *slr-1,* the process of LRP initiation seems to be attempted; intriguingly, this attempt appears to be enough to stimulate some *PDLP5pro:GUS* expression in the overlying endodermal cells (see Appendix C2). These results indicate that *PDLP5* expression in LRP-overlying cells is induced by an auxin-dependent SLR→ARF7/ARF19-dependent pathway, starting from the earliest stages of LRP development, and that *PDLP5* is upregulated only when this pathway is active and not from any other spatiotemporal changes in auxin maxima.

3.3.6 PDLP5 is Targeted to Plasmodesmata within LRP-Overlying Cells

To determine the subcellular location of PDLP5 in LRP-overlying cells, *PDLP5pro:PDLP5-GFP* lines were created in both WT and *pdlp5-1* plants. *PDLP5pro:PDLP5-GFP* in *pdlp5-1* complemented the LRP emergence phenotype, proving the functionality of PDLP5-GFP in roots (see Appendix C3). In both WT and *pdlp5-1* roots, PDLP5-GFP was visible as puncta within the cell walls of the endodermal (En), cortical (Co), and epidermal (Epi) layers overlying LRP, indicating that PDLP5 does localize to PD within these cells (Fig 3.10, Appendix C3).

Further study of *PDLP5pro:PDLP5-GFP* was conducted in WT to examine whether PDLP5-GFP accumulates preferentially at a particular cell-cell junction during LRP emergence. 3D modeling software was used with confocal z-stack images to automatically map PDLP5-GFP sites in LRP-overlying cells based on a set fluorescent intensity threshold (Fig 3.10A). Within the emerged-LR area used for the model, the majority of PDLP5-GFP-marked puncta with fluorescent intensity higher than the detection threshold were at the Epi-Co junctions, though several puncta were still visible at the Co-En and Epi-Epi junctions (Fig 3.10A).

To monitor PDLP5-GFP localization patterns in overlying cells during LRP development, a series of images was taken using *PDLP5pro:PDLP5-GFP* seedlings. Consistent with the *PDLP5pro:GUS* results, *PDLP5pro:PDLP5GFP* showed specific spatiotemporal expression patterns in LRP-overlying cells at all stages of emergence (Fig 3.10B). A number of images appeared to show a strong build-up of PDLP5-GFP at the cell junctions separating in response to LRP growth, yet PDLP5-GFP was hardly ever detected within the cell walls that had already separated (Fig 3.10B). These two observations suggest that PD may be modified or even degraded at the separating cell junction during and after cell separation. A model of PDLP5 localization to PD during the course of LRP emergence is shown in Fig 3.10C.

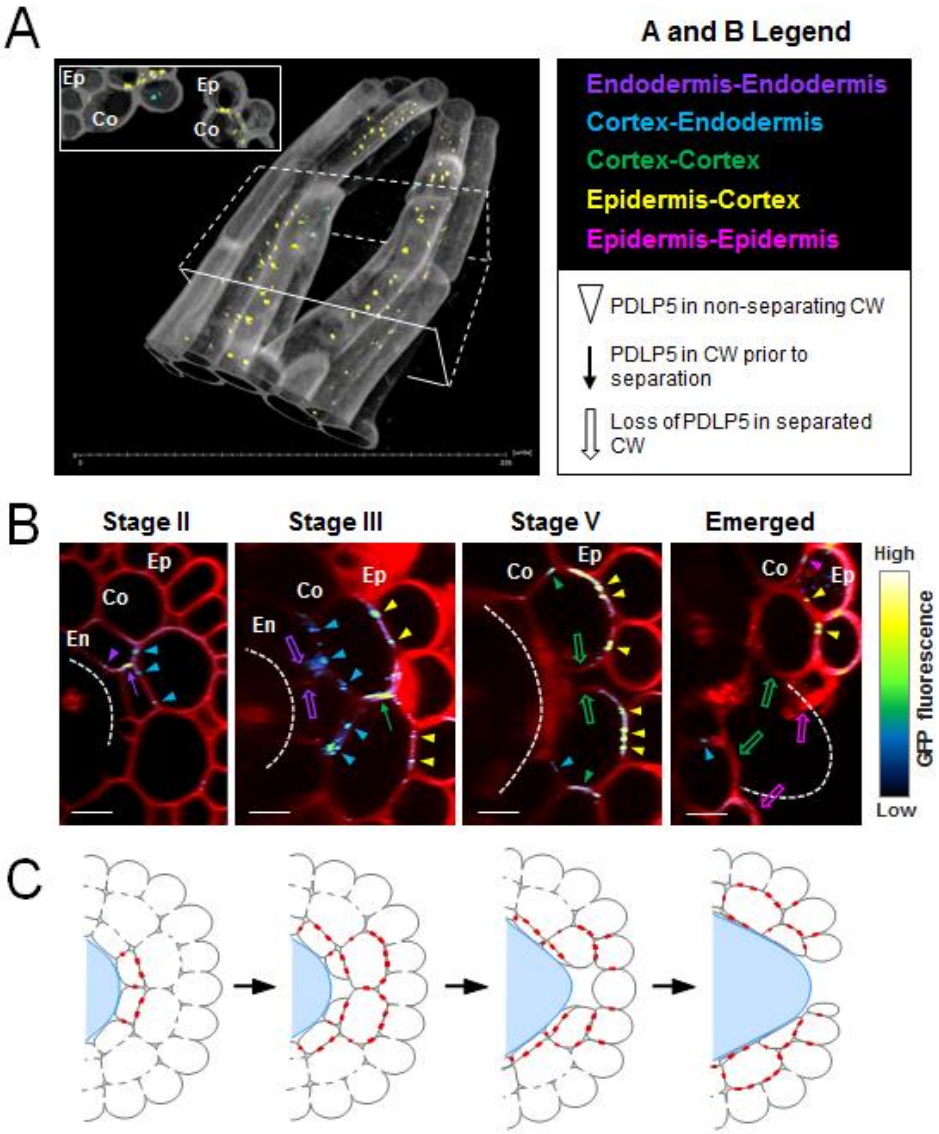

Figure 3.10: PDLP5 localizes to PD in LRP-overlying cells.
A, The confocal z-stack image of an emerged lateral root in *PDLP5pro:PDLP5-GFP* was modeled in 3D using Amira 5.6 software. An intensity threshold value was set to highlight PDLP5-GFP signal at PD junctions, and PD within these junctions were colored according to each specific cell-cell boundary (see **A** and **B** Legend). The upper left corner inset represents a 3D cross-section of the area encased in the dashed white box, to better visualize the increased frequency of PD pit fields at the Epi-Co junction. **B**, Confocal images showing PDLP5-GFP during progressing stages lateral root emergence. Images are 2D maximum intensity projections of 10 μm-thick z-stack cross-sections. Propidium iodide was used to stain the cell walls of the root tissue red. PDLP5-GFP can be seen as puncta at the cell wall junctions of outer root cells

overlying emerging LRP at different stages (arrowheads). PDLP5-GFP signal and intensity are represented by the blue-to-white rainbow filter; high-intensity signal was used as a way to determine PD puncta compared to background signal noise. White dashed arcs represent the size and direction of emerging LRPs. Note the accumulation of PDLP5-GFP in cell-cell junctions prior to separation (solid arrows), and the complete loss of puncta signal within these walls post-separation (empty arrows). Scale bars, 20 μm. **C**, model of PDLP5 in overlying En, Co, and Epi cell junctions during LRP emergence. Red puncta in the model represent PDLP5-GFP signals associated with the PD within the cells over emerging LRP; note their absence from separated cell walls.

3.3.7 *PDLP5* Upregulation can Restrict Intercellular Trafficking of GFP in Root Tissues

The function of PDLP5 in closing root PD had not been directly tested. Thus, we designed transgenic lines of a tissue-specific promoter expressing intercellular fluorescent markers, to examine whether *PDLP5* upregulation can affect cell-to-cell trafficking in *Arabidopsis* roots. The promoter of *Casparian Strip Membrane Protein 1* (*CASP1*) was chosen for its high specificity to the root endodermis, allowing easy observation of cell-to-cell movement from a single tissue layer into neighboring layers.

Prior to testing PDLP5 functionality, several experiments were performed to gain insight into PD trafficking from the root endodermal layer. First, the lines *CASP1pro:ER-YFP* and *CASP1pro:GFP* were produced and examined using confocal microscopy. ER-YFP is trapped within the ER and cannot move cell-to-cell, so YFP signal is only visible where the promoter is active, whereas free GFP (27 kDa) can move between cells through PD. *CASP1pro:ER-YFP* confirmed that the cloned *CASP1* promoter is highly specific to the endodermis, as shown previously (Roppolo et al., 2011) (Fig 3.11A). In contrast, *CASP1pro:GFP* showed that the free GFP

moved from the endodermis into the adjacent pericycle and cortex layers, as well as slightly farther longitudinally toward the root tip than its typical area of expression (Fig 3.11B).

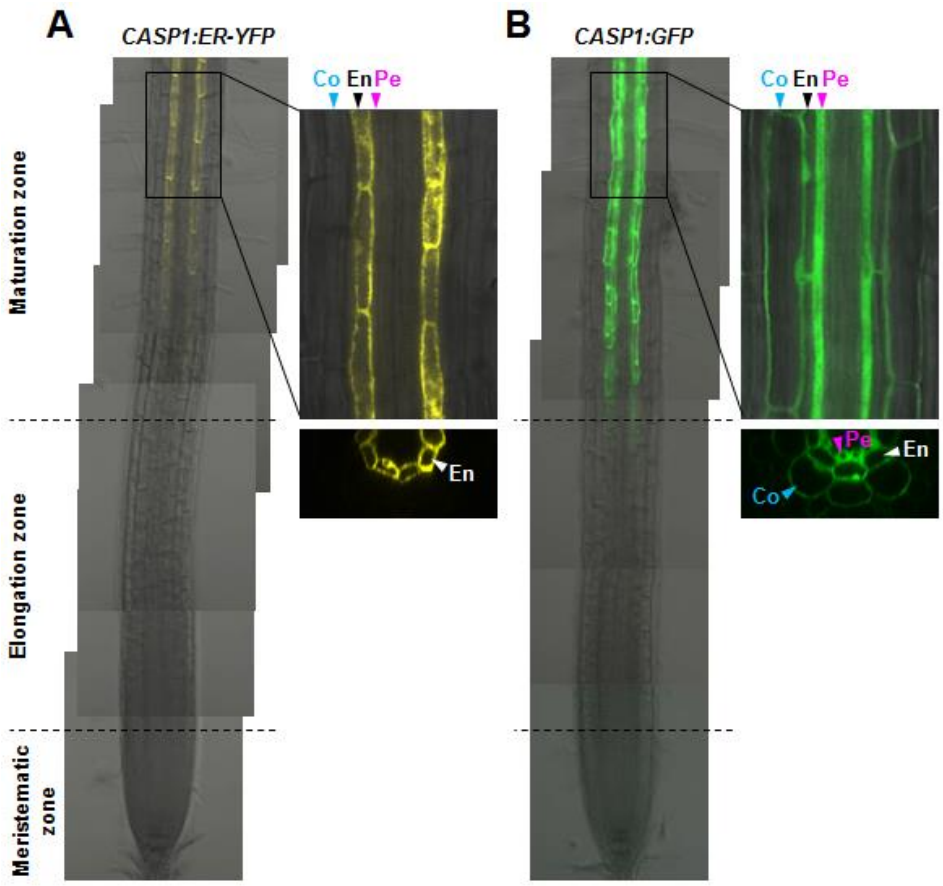

Figure 3.11: GFP expressed under the root endodermis-specific promoter CASP1 can diffuse into adjacent root tissue layers in normal conditions.
A, *CASP1pro:ER-YFP* proves that *CASP1* promoter is active above the elongation zone in the Casparian strip and is highly specific to only the endodermis (En). **B**, *CASP1pro:GFP* allows free GFP to diffuse longitudinally slightly closer to elongation zone, as well as laterally into the cortex (Co) and pericycle (Pe).

Next, *CASP1pro:PDLP5-GFP* was compared to *CASP1pro:TMV-MP-GFP*, a non-cell-autonomous PD marker protein derived from the *Tobacco mosaic virus*

(TMV). As expected, PDLP5-GFP in *CASP1pro:PDLP5-GFP* plants was localized to PD within the endodermal layer only (Fig 3.12A). In contrast, in *CASP1pro:TMV-MP-GFP*, TMV-MP-GFP not only marked PD in endodermal cells, but also moved into and marked PD within the adjacent pericycle and cortex tissue as well (Fig 3.12B); however, movement of the 57 kDa TMV-MP-GFP was not limited to only one adjacent tissue layer in each direction but more penetrant to the vasculature.

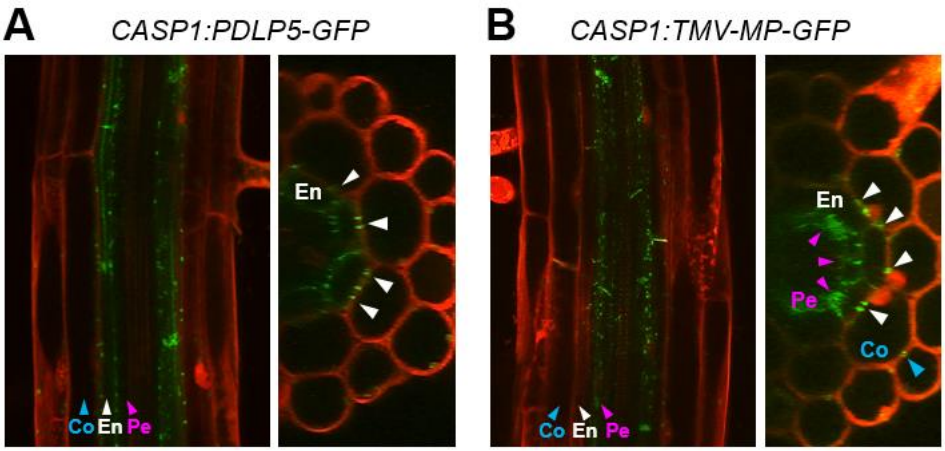

Figure 3.12: PDLP5 protein cannot move between root tissue layers.
A, *CASP1pro:PDLP5-GFP* retains PDLP5-GFP fully within PD in the endodermis (En). **B**, *CASP1pro:TMV-MP-GFP* allows TMV-MP-GFP to move into the neighboring pericycle (Pe) and cortex (Co) tissues. Cell walls stained with propidium iodide (red) in A and B.

Next, we examined how *PDLP5* affected molecular diffusion from the root endodermis. Treatments of shoot tissue had previously shown that SA could cause PD closure via *PDLP5* upregulation (Wang et al., 2013), and treatment of *PDLP5pro:GUS* roots with SA demonstrated that *PDLP5* promoter activity greatly increased in roots after SA treatment (Fig 3.7). Therefore, SA was used to attempt to close root PD via *PDLP5* upregulation. The roots of *CASP1pro:ER-YFP*,

CASP1pro:GFP, and *CASP1pro:GFP x pdlp5-1* were treated with 100 µM SA and imaged 24 hrs later on the confocal microscope (Fig 3.13A). The *CASP1pro:ER-YFP* intensity and location did not change, proving that SA treatment had no effect on the *CASP1* promoter itself (Fig 3.13A row 1). However, free GFP diffusion from the endodermis into the cortex was prevented in about 78% of SA-treated *CASP1pro:GFP* samples, while all mock-treated *CASP1pro:GFP* seedlings had unaltered GFP diffusion (Fig 3.13A row 2, and C). Similarly, GFP movement from endodermis to cortex was prevented in 73% of *CASP1pro:GFP x pdlp5-1* seedlings post-SA treatment, while mock-treated GFP movement was unaltered (Fig 3.13A row 3, and C). Surprisingly, unlike in shoot tissue, SA seems to close root PD independently of *PDLP5*.

In order to test PD closure via direct *PDLP5* upregulation in roots, the estradiol-inducible *pER8:PDLP5* line was crossed into *CASP1pro:GFP*. The roots of *CASP1pro:ER-YFP* and *pER8:PDLP5 x CASP1pro:GFP* F1 seedlings grown vertically on agar plates were either sprayed with 10 µM estradiol or mock-treated with water, and observed 24 hrs later with confocal microscopy (Fig 3.13B). Estradiol had no impact on CASP1 promoter activity or location, as expected (Fig 3.13B row 1). Inducing *PDLP5* with estradiol treatment prevented GFP diffusion into the cortex in about 87% of the *pER8:PDLP5 x CASP1pro:GFP* seedlings, whereas GFP movement was unaltered in mock-treated samples (Fig 3.13B row 2, and C). This result indicates that PDLP5 can close PD in *Arabidopsis* roots to prevent diffusion of molecules from the endodermis into the cortex.

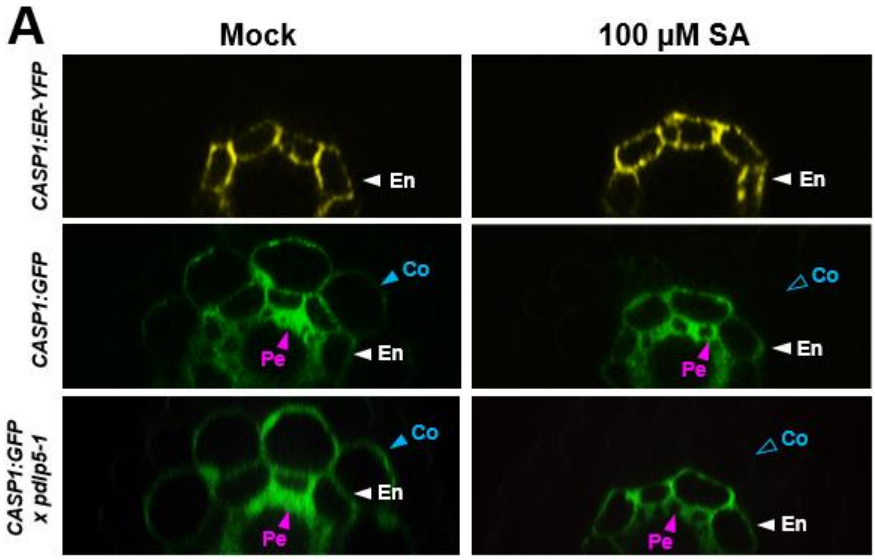

C

	# seedlings w/ GFP Co movement / # total seedlings		
	Mock-treated	100 µM SA	10 µM estradiol
CASP1:GFP	31/31 (100%)	8/36 (22%)	---
CASP1:GFP x pdlp5-1	12/12 (100%)	7/26 (27%)	---
CASP1:GFP x pER8:PDLP5	20/20 (100%)	---	3/17 (18%)

Figure 3.13: PDLP5 upregulation prevents GFP movement from endodermis into cortex.
A, SA treatment restricts GFP movement from root endodermis into cortex independently of PDLP5. The roots of 6-day old vertically-grown seedlings of *CASP1pro:ER-YFP*, *CASP1pro:GFP*, and *CASP1pro:GFP x pdlp5-1*, were submerged in water or 100 µM SA on plates for 5 min, then liquid was removed and seedlings were grown vertically for 24 hrs more. **B**, Estradiol treatment of *pER8:PDLP5 x CASP1pro:GFP* restricts GFP diffusion from the root endodermis into cortex. The roots of 6-day old vertically-grown seedlings of *CASP1pro:ER-YFP* and *pER8:PDLP5 x CASP1pro:GFP* were submerged in water or 10 µM estradiol on

plates for 5 min, then liquid was removed and seedlings were grown vertically for 24 hrs more. **A** and **B**, filled arrowheads indicate GFP is present in root layer, empty arrowheads indicate GFP is no longer present in root layer; En, endodermis; Co, cortex; Pe, pericycle. **C**, Table showing the number of mock-treated or treated seedlings with GFP movement into cortex, 24 hrs post-treatment.

Note that GFP diffusion into the pericycle was not reduced or eliminated after either SA or estradiol treatments (Fig 3.13A and B). From a technical standpoint, this could be due to prevention of SA or estradiol diffusion into the root endodermis by the Casparian strip. However, it is also possible that the PD of different root layers, or at different cell-cell junctions within the same root layer, are regulated differently in response to certain treatments or endogenous signals. Still, the results from this section provide experimental evidence that *PDLP5* upregulation reduces GFP movement in certain root cell junctions.

3.3.8 PDLP5 Modulates Auxin Accumulation in LRP-Overlying Cells

Auxin moves from the developing LRP into the overlying cells, where it is strongly concentrated by the actions of auxin influx carriers like *LAX3*. However, the hormone is small enough that it could passively diffuse through open PD. Thus, we hypothesized that perhaps PDLP5 acts to close PD in the LRP-overlying cells to prevent auxin diffusion out of them. To accurately determine the *in vivo* extent of auxin diffusion from LRP-overlying tissues in WT, *pdlp5-1*, and *PDLP5OE*, the nucleus-localizing fluorescent auxin sensor *DR5:3VENUS* was crossed into each background and monitored during gravitropically-induced LRP growth. 27 hrs post-gravitropism was chosen for analysis because at this time-point, root bend LRP in all backgrounds would be in the stage IV-V range of development, with similar sizes, and auxin would be accumulating within the overlying cortical (Co) cells. Earlier time-

points were not used because the endodermal and LRP nuclei expressing 3VENUS were difficult to distinguish (Fig 3.14A).

Confocal z-stack imaging was used to count *DR5:3VENUS*-expressing Co cell nuclei overlying the root-bend LRP at 27 hpg in each background. Greater numbers of Co cells with nuclear 3VENUS signal were present in *DR5:3VENUS x pdlp5-1* roots compared to the parental line in the WT background. In contrast, fewer overall 3VENUS nuclei were detectable in overlying Co cells in *DR5:3VENUS x PDLP5OE* roots (Fig 3.14B). Box plot analysis revealed that while 50% of WT seedlings had 3-5 overlying Co cells expressing *DR5:3VENUS*. This range was skewed higher in the *pdlp5-1* mutants, with 50% of seedlings having 4-5 *DR5:3VENUS*-expressing Co cells, and skewed lower in *PDLP5OE*, with 50% of seedlings having only 2-4 *DR5:3VENUS*-expressing Co cells (Fig 3.14C). These results support our hypothesis that PDLP5 is required to prevent auxin diffusion out of LRP-overlying cells during root emergence.

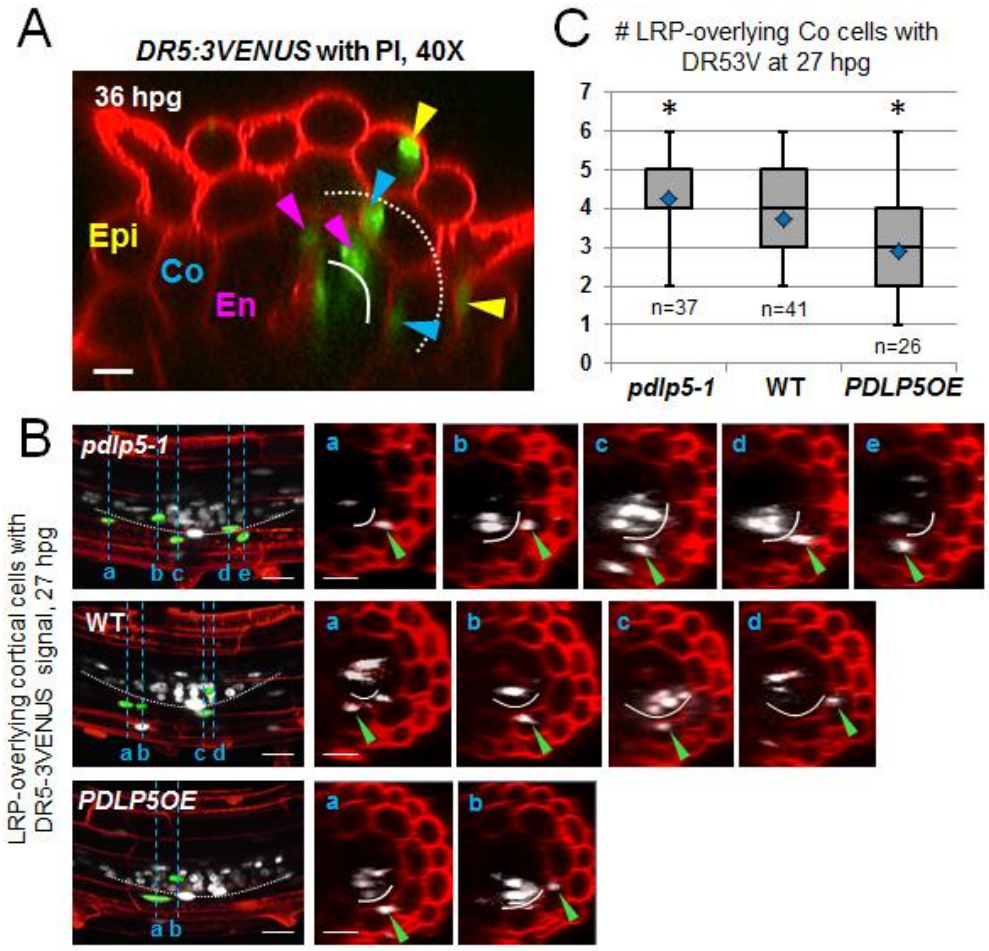

Figure 3.14: *PDLP5* expression inversely influences the range of auxin sensor *DR5:3VENUS* activity in LRP-overlying tissue.
A, Representative image of a PI-stained 36 hpg root bend LRP in *DR5:3VENUS*, shown as a single latitudinal cross-section from a confocal z-stack image. The solid white curve outlines the portion of the LRP visible within this single cross-section; the dotted white curve represents the maximum size of the LRP from the whole confocal image. Arrowheads indicate *DR5:3VENUS*-expressing LRP-overlying cells (green nuclei) visible within this single image: yellow, epidermis; blue, cortex; pink, endodermis. Scale bar, 20 μm. **B**, Representative confocal images of PI-stained 27 hpg root bend LRP from *DR5:3VENUS* expressed in WT (middle row), *pdlp5-1* (top row), and *PDLP5OE* (bottom row). The leftmost panels in each row are 115.4 μm-thick 3D maximum intensity projections, showing representative images of *DR5:3VENUS* signal in the nuclei of 27 hpg root bend LRP (approximately stage IV) and surrounding cells in each background. In the leftmost panels, the overall shape of each LRP is shown as a dotted white curve; LRP-overlying cortical nuclei expressing *DR5:3VENUS* are pseudo-colored green, to highlight their 3D positions, while all

other *DR5:3VENUS*-expressing nuclei are white. The vertical blue dotted lines in the leftmost panels represent the locations of the cross-sectional planes shown in the other panels to the right in each row, with letters corresponding to each cross-section. Each cross-section is through the nucleus of an LRP-overlying cortical cell expressing *DR5:3VENUS* (marked by green arrowheads in the panels to the right); the solid white curves outline the portion of the LRP visible in each cross-section. Scale bars, 20 μm. **C**, Box plot showing quantification of the number of LRP-overlying Co cells with *DR5:3VENUS* signal at 27 hpg in each background. Asterisks, statistical significance determined by student T-test ($P<0.05$) on three biological repeats.

3.3.9 PDLP5 Regulates the Timing and Location of *LAX3* Expression in LRP-Overlying Cells

To determine whether auxin responses in LRP-overlying cells were affected by *PDLP5*, *LAX3pro:LAX3-YFP* was crossed into *pdlp5-1* and *PDLP5OE* backgrounds. *LAX3* is a key component of LRP emergence, as described in previous sections, and its promoter is spatiotemporally activated by auxin in LRP-overlying cortical (Co) cells (Swarup et al., 2008; Peret et al., 2013). *LAX3pro:LAX3-YFP x pdlp5* and *LAX3pro:LAX3-YFP x PDLP5OE* seedlings were induced gravitropically and compared to the parental *LAX3:LAX3-YFP* line at several points during a 14-36 hr time course. LAX3-YFP appeared earlier in the LRP-overlying Co cells of the *pdlp5-1* background compared to WT, even rarely appearing at 16 hpg (Fig 3.15A). Overall, the greatest differences between lines could be seen at 22 hpg, when almost two-fold more *pdlp5-1* seedlings had LAX3-YFP Co signal than WT, while none of the *PDLP5OE* had yet shown Co signal (Fig 3.15A and B). In fact, though Co LAX3-YFP signal began to appear at 24 hpg in *PDLP5OE*, it was still consistently delayed compared to WT until 36 hpg (Fig 3.15A and C). These results are consistent with the hypothesis that PDLP5 negatively regulates auxin diffusion into LRP-overlying cells, in order to control the proper timing of LR emergence genes like *LAX3*.

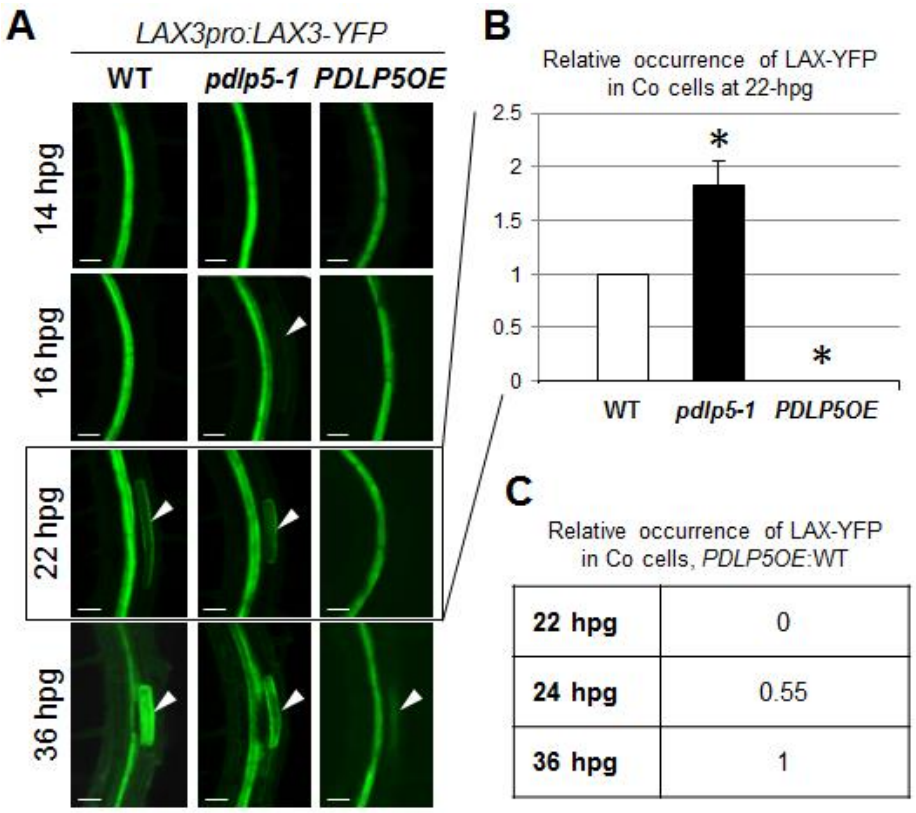

Figure 3.15: *PDLP5* expression inversely influences the timing of auxin-dependent gene *LAX3* expression in LRP-overlying cortical cells.
A, Representative confocal images taken from WT, *pdlp5-1*, and *PDLP5OE* seedlings expressing *LAX3pro:LAX3-YFP*. Images were taken at the LRP-emerging region in the root bend 14 hrs through 36 hrs post-gravistimulation (hpg). Arrowheads, LAX3-YFP in Co cells overlying newly-developing LRP. Scale bars, 50 µm. **B**, Quantification of relative occurrence of LAX3-YFP signal in LRP-overlying Co cells at 22 hpg (for full data, see Appendix Tables C1 and C2). Asterisk, statistical significance determined by student T-test ($P<0.01$). Bars, standard deviation. $n\geq30$ per seedling line. **C**, Quantification of relative occurrence of LAX3-YFP signal in LRP-overlying Co cells of *PDLP5OE* compared to WT (for full data, see App Table C1).

To test whether the increased diffusion of auxin in *pdlp5-1* could impact the *LAX3* zone of expression, seedlings of *LAX3pro:LAX3-YFP* and *LAX3pro:LAX3-YFP x pdlp5-1* were induced gravitropically, and the number of root bend LRP-overlying Co cells with LAX3-YFP signal was quantified between 26-36 hpg in each line. In

LAX3pro:LAX3-YFP, over 65% seedlings had detectable LAX3-YFP signal in 2-3 Co cells, and only 25% seedlings showed LAX3-YFP expression in 4-5 Co-cells (Fig 3.16A and B). In contrast, 45% of *LAX3pro:LAX3-YFP x pdlp5-1* seedlings showed detectable LAX3-YFP signal in 2-3 Co cells, but over 50% showed LAX3-YFP signal in 4-5 Co cells (Fig 3.16A and B). Furthermore, while only 25% of *LAX3pro:LAX3-YFP* seedlings showed LAX3-YFP expression in three Co cell files, 40% of *LAX3pro:LAX3-YFP x pdlp5-1* seedlings showed LAX3-YFP expression in three Co cell files (Fig 3.16A and C).

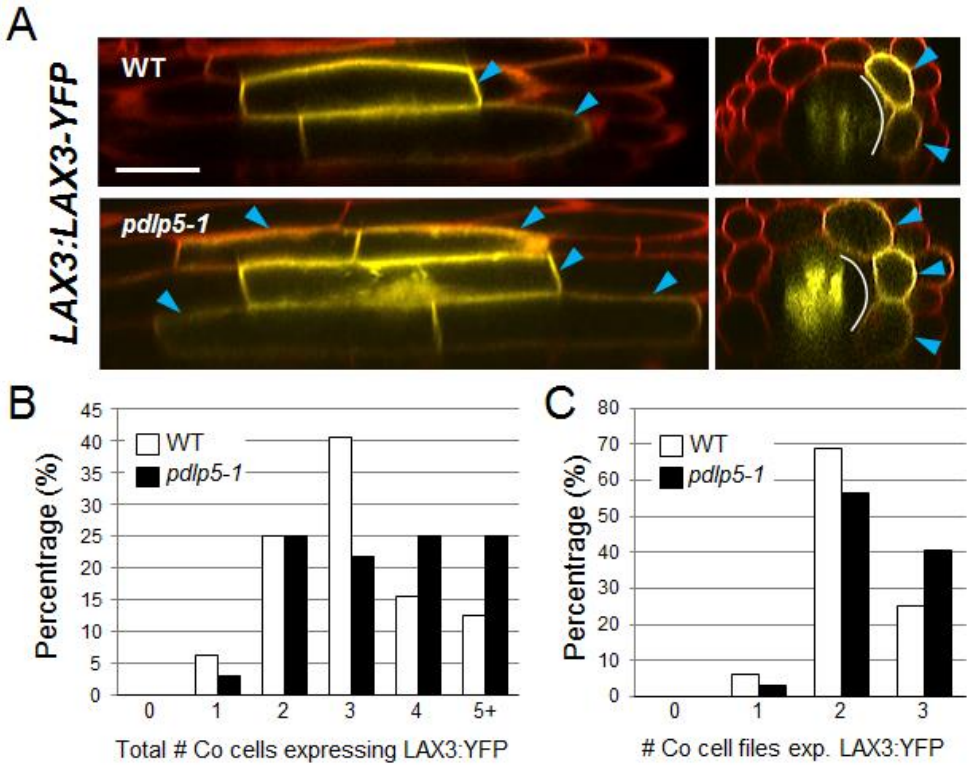

Figure 3.16: *PDLP5* expression inversely influences the range of *LAX3* expression in LRP-overlying cortical cells.
A, Representative cross-sectional images of *LAX3pro:LAX3-YFP* expression in root bend LRP-overlying cortical (Co) cells in the WT and *pdlp5-1* backgrounds. Blue arrowheads point to overlying Co cells with LAX3-YFP signal; white curves outline

the LRP. Scale bar, 50 µm. **B**, Graph showing the percentage of total seedlings with certain numbers of LRP-overlying Co cells expressing *LAX3pro:LAX3-YFP* in WT and *pdlp5-1* backgrounds, 26-36 hpg. **C**, Graph showing the percentage of total seedlings with certain numbers of LRP-overlying cortical cell files expressing *LAX3pro:LAX3-YFP* in WT and *pdlp5-1* backgrounds, 26-36 hpg. n=32 for WT and *pdlp5-1* in **B** and **C**.

Collectively, the results from this and previous sections support the hypothesis that *PDLP5* is expressed in LRP-overlying tissue to restrict auxin diffusion through PD, thereby maintaining the auxin distribution in the correct LRP-overlying cells, as well as the proper timing of auxin-dependent gene expression.

3.4 Discussion

Given that *PDLP5pro:GUS* is still expressed strongly in LRP-overlying endodermal cells in *shy2-2* roots (Fig 3.9), it seems *PDLP5* expression in the endodermis is either partially or fully independent of the *SHY2*-regulated endodermal cell separation pathway. There is currently very little data about endodermal transcriptional regulators other than *SHY2* that function during LRP emergence. The only other confirmed as of this writing is *At*MYB93, but while the expression domain of this transcription factor is highly specific to the LRP-overlying endodermal cells, its expression there occurs independently of auxin accumulation (Gibbs et al., 2014). Further research is needed to reveal new candidates for control of *PDLP5* endodermal expression.

When LRI does not occur, as in *arf7arf19* mutants, no *PDLP5pro:GUS* staining is visible in LRP-overlying endodermal cells (see Appendix C2). However, as long as LRI is attempted, even if the process is hindered or ultimately aborted, as in *iaa28-1* and *slr-1*, the brief auxin maximum within the FCs stimulates *PDLP5*

expression in the overlying endodermis (Fig 3.9, Appendix C2), and so it seems that early *PDLP5* expression is controlled by the auxin-dependent pathway that triggers LRI. Additionally, it seems possible that the auxin-dependent pathway controlling the cell separation of the LRP-overlying cortical and epidermal tissue cells could also control *PDLP5* expression in those cells, due to the expression timing and pattern of *PDLP5pro:GUS* there (Fig 3.5D). Currently, the auxin-dependent transcription factors that activate *PDLP5* in the overlying cells during LRI and LRP emergence are unknown. However, *ARF19* is a likely candidate for future study, given that the *PDLP5* promoter was found to have ARF19 binding sites (analysis performed by Malcolm Bennett lab, data not shown). Based on these collective results, I have devised a hypothesized model for the auxin-dependent pathways controlling *PDLP5* expression during LRI and LRP emergence (Fig 3.17).

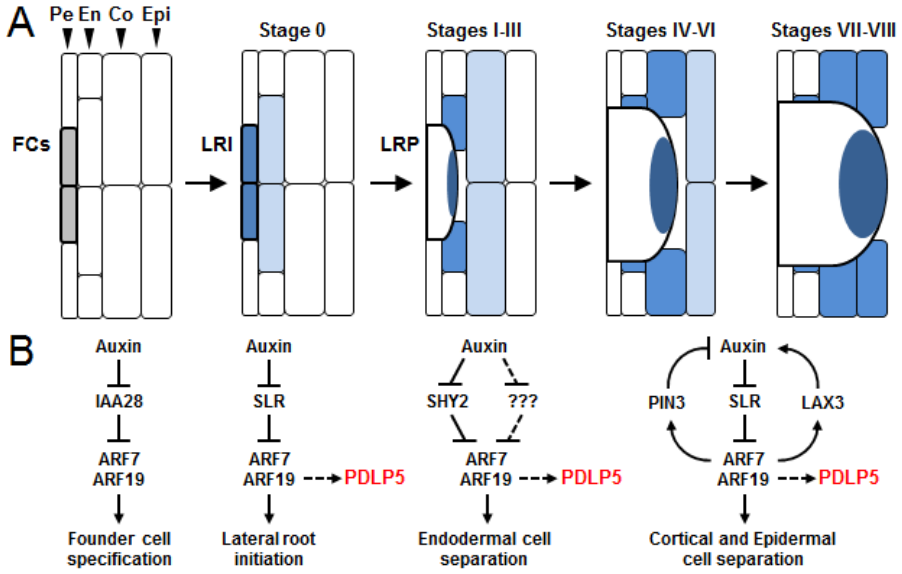

Figure 3.17: Model of the hypothetical auxin-dependent pathways controlling *PDLP5* expression during lateral root initiation (LRI) and lateral root primordium (LRP) emergence.

A, Representative stages of LR development. Light blue to dark blue within the cells indicates increasing auxin accumulation. **B**, The known pathways controlling each stage of LR development and emergence. Dashed arrows indicate the hypothesized pathways regulating *PDLP5* expression.

The experimental data presented in the Results section are consistent with the model whereby PDLP5 closes PD in LRP-overlying cells, to prevent the diffusion of auxin or auxin-related signals that promote cell-separation during LRP emergence. This hypothesis would be further supported by evidence showing that the LRP-overlying cells specifically had restricted PD during the same period that the *PDLP5* promoter activity is active. Our current working hypothesis (Fig 3.18) is that the auxin carriers *PIN3* and *LAX3*, which share very similar expression patterns to *PDLP5* during LRP emergence (Swarup et al., 2008; Marhavy et al., 2013), work together with PDLP5 to maintain the balance of auxin in LRP-overlying cells through a combination of auxin influx/efflux and PD closure.

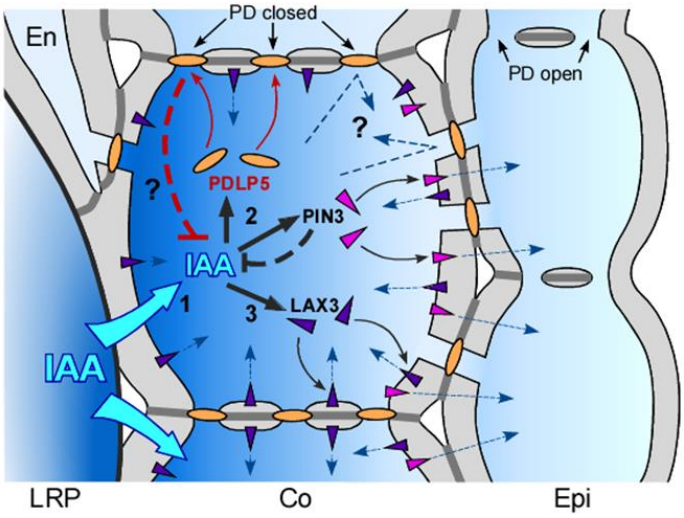

Figure 3.18: Model for the possible role of PDLP5-regulated PD closure in LRP-overlying cells during lateral root emergence.

Within these cells, a **darkening blue gradient** indicates an increasing auxin maximum, and the **blue dashed arrows** indicate the direction of auxin movement. The LRP shown in the model is late stage 3/pre-stage 4, having already grown through the endodermal (En) layer, and is now entering the LRP-overlying cortical (Co) cells. Auxin (indole acetic acid, IAA) is transported into the Co cells (**step 1**) and induces expression of PDLP5 (orange ovals) and PIN3 (pink triangles) (**step 2**), followed by LAX3 (purple triangles) expression when the auxin concentration is high enough (**step 3**). PIN3 efflux from the Co cells maintains the flow of auxin into adjacent overlying epidermal cells, and LAX3 influx into Co cells allows them to reach the auxin threshold required to induce cell wall remodeling enzyme expression. PDLP5 hypothetically contributes to this process by tightly sealing the PD to prevent auxin diffusion (**upper right question mark**), thus ensuring containment of the auxin maxima to only the overlying Co cells. The increased LRP emergence rate in *pdlp5-1* mutants could be explained by the involvement of PDLP5 in a negative auxin feedback pathway (**upper left question mark**).

PDLP5 may negatively feedback regulate auxin pathway such that an auxin-sensing mechanism within the LRP-overlying tissue would stimulate more auxin to be targeted to these cells when the concentration is too low. Based on this speculation, auxin diffusion out of the overlying cells through the open PD of the *pdlp5-1* background would trigger more auxin to be targeted to the area, which diffuses, and so on, creating a positive feedback loop that accelerates both LRP growth and the activation of overlying cell separation pathways.

REFERENCES

An, C., and Mou, Z. (2011). Salicylic acid and its function in plant immunity. J Integr Plant Biol **53,** 412-428.

Armengot, L., Marques-Bueno, M.M., and Jaillais, Y. (2016). Regulation of polar auxin transport by protein and lipid kinases. J Exp Bot **67,** 4015-4037.

Atkinson, J.A., Rasmussen, A., Traini, R., Voss, U., Sturrock, C., Mooney, S.J., Wells, D.M., and Bennett, M.J. (2014). Branching out in roots: uncovering form, function, and regulation. Plant Physiol **166,** 538-550.

Bayer, E., Thomas, C., and Maule, A. (2008). Symplastic domains in the Arabidopsis shoot apical meristem correlate with PDLP1 expression patterns. Plant Signal Behav **3,** 853-855.

Bel, A.J.E.v., and Kesteren, W.J.P.v. (1999). Plasmodesmata : structure, function, role in cell communication. (Berlin ; New York: Springer).

Benitez-Alfonso, Y., Faulkner, C., Pendle, A., Miyashima, S., Helariutta, Y., and Maule, A. (2013). Symplastic Intercellular Connectivity Regulates Lateral Root Patterning. Developmental Cell **26,** 136-147.

Benkova, E., Michniewicz, M., Sauer, M., Teichmann, T., Seifertova, D., Jurgens, G., and Friml, J. (2003). Local, efflux-dependent auxin gradients as a common module for plant organ formation. Cell **115,** 591-602.

Bhalerao, R.P., Eklof, J., Ljung, K., Marchant, A., Bennett, M., and Sandberg, G. (2002). Shoot-derived auxin is essential for early lateral root emergence in Arabidopsis seedlings. Plant Journal **29,** 325-332.

Blilou, I., Xu, J., Wildwater, M., Willemsen, V., Paponov, I., Friml, J., Heidstra, R., Aida, M., Palme, K., and Scheres, B. (2005). The PIN auxin efflux facilitator network controls growth and patterning in Arabidopsis roots. Nature **433,** 39-44.

Bruggeman, Q., Raynaud, C., Benhamed, M., and Delarue, M. (2015). To die or not to die? Lessons from lesion mimic mutants. Frontiers in Plant Science **6,** 24.

Brunkard, J.O., and Zambryski, P.C. (2016). Plasmodesmata enable multicellularity: new insights into their evolution, biogenesis, and functions in development and immunity. Curr Opin Plant Biol **35,** 76-83.

Bruno, L., Pacenza, M., Forgione, I., Lamerton, L.R., Greco, M., Chiappetta, A., and Bitonti, M.B. (2017). In Arabidopsis thaliana Cadmium Impact on the Growth of Primary Root by Altering SCR Expression and Auxin-Cytokinin Cross-Talk. Front Plant Sci **8,** 1323.

Burch-Smith, T.M., Stonebloom, S., Xu, M., and Zambryski, P.C. (2011). Plasmodesmata during development: re-examination of the importance of primary, secondary, and branched plasmodesmata structure versus function. Protoplasma **248,** 61-74.

Carella, P., Isaacs, M., and Cameron, R.K. (2015). Plasmodesmata-located protein overexpression negatively impacts the manifestation of systemic acquired resistance and the long-distance movement of Defective in Induced Resistance1 in Arabidopsis. Plant Biol (Stuttg) **17,** 395-401.

Casimiro, I., Marchant, A., Bhalerao, R.P., Beeckman, T., Dhooge, S., Swarup, R., Graham, N., Inze, D., Sandberg, G., Casero, P.J., and Bennett, M. (2001). Auxin transport promotes Arabidopsis lateral root initiation. Plant Cell **13,** 843-852.

Chandra-Shekara, A.C., Navarre, D., Kachroo, A., Kang, H.G., Klessig, D., and Kachroo, P. (2004). Signaling requirements and role of salicylic acid in HRT- and rrt-mediated resistance to turnip crinkle virus in Arabidopsis. Plant J **40,** 647-659.

Christensen, S.K., Dagenais, N., Chory, J., and Weigel, D. (2000). Regulation of auxin response by the protein kinase PINOID. Cell **100,** 469-478.

Clough, S.J., and Bent, A.F. (1998). Floral dip: a simplified method for Agrobacterium-mediated transformation of Arabidopsis thaliana. Plant J **16,** 735-743.

Cui, W., and Lee, J.Y. (2016). Arabidopsis callose synthases CalS1/8 regulate plasmodesmal permeability during stress. Nature Plants **2**.

De Rybel, B., Audenaert, D., Xuan, W., Overvoorde, P., Strader, L.C., Kepinski, S., Hoye, R., Brisbois, R., Parizot, B., Vanneste, S., Liu, X., Gilday, A., Graham, I.A., Nguyen, L., Jansen, L., Njo, M.F., Inze, D., Bartel, B., and Beeckman, T. (2012). A role for the root cap in root branching revealed by the non-auxin probe naxillin. Nat Chem Biol **8,** 798-805.

De Rybel, B., Vassileva, V., Parizot, B., Demeulenaere, M., Grunewald, W., Audenaert, D., Van Campenhout, J., Overvoorde, P., Jansen, L., Vanneste, S., Moller, B., Wilson, M., Holman, T., Van Isterdael, G., Brunoud, G., Vuylsteke, M., Vernoux, T., De Veylder, L., Inze, D., Weijers, D., Bennett, M.J., and Beeckman, T. (2010). A novel aux/IAA28 signaling cascade activates GATA23-dependent specification of lateral root founder cell identity. Curr Biol **20,** 1697-1706.

De Smet, I., Tetsumura, T., De Rybel, B., Frei dit Frey, N., Laplaze, L., Casimiro, I., Swarup, R., Naudts, M., Vanneste, S., Audenaert, D., Inze, D., Bennett, M.J., and Beeckman, T. (2007). Auxin-dependent regulation of lateral root positioning in the basal meristem of Arabidopsis. Development **134,** 681-690.

Dettmer, J., and Friml, J. (2011). Cell polarity in plants: when two do the same, it is not the same. Curr Opin Cell Biol **23,** 686-696.

Dhonukshe, P. (2009). Cell polarity in plants: Linking PIN polarity generation mechanisms to morphogenic auxin gradients. Commun Integr Biol **2,** 184-190.

Dhonukshe, P., Huang, F., Galvan-Ampudia, C.S., Mahonen, A.P., Kleine-Vehn, J., Xu, J., Quint, A., Prasad, K., Friml, J., Scheres, B., and Offringa, R. (2010). Plasma membrane-bound AGC3 kinases phosphorylate PIN auxin carriers at TPRXS(N/S) motifs to direct apical PIN recycling. Development **137,** 3245-3255.

Dhonukshe, P., Tanaka, H., Goh, T., Ebine, K., Mahonen, A.P., Prasad, K., Blilou, I., Geldner, N., Xu, J., Uemura, T., Chory, J., Ueda, T., Nakano, A., Scheres, B., and Friml, J. (2008). Generation of cell polarity in plants links endocytosis, auxin distribution and cell fate decisions. Nature **456,** 962-966.

Dhonukshe, P., Tanaka, H., Goh, T., Ebine, K., Mahonen, A.P., Prasad, K., Blilou, I., Geldner, N., Xu, J., Uemura, T., Chory, J., Ueda, T., Nakano, A., Scheres, B., and Friml, J. (2014). Retraction: Generation of cell polarity in plants links endocytosis, auxin distribution and cell fate decisions. Nature **511,** 370-370.

Dubrovsky, J.G., Doerner, P.W., Colon-Carmona, A., and Rost, T.L. (2000). Pericycle cell proliferation and lateral root initiation in Arabidopsis. Plant Physiol **124,** 1648-1657.

Dubrovsky, J.G., Sauer, M., Napsucialy-Mendivil, S., Ivanchenko, M.G., Friml, J., Shishkova, S., Celenza, J., and Benkova, E. (2008). Auxin acts as a local morphogenetic trigger to specify lateral root founder cells. Proc Natl Acad Sci U S A **105,** 8790-8794.

Eckardt, N.A. (2014). A Useful Model of Auxin Transport in the Root Apex. The Plant Cell **26,** 843-843.

Ehlers, K., and Kollmann, R. (2001). Primary and secondary plasmodesmata: structure, origin, and functioning. Protoplasma **216,** 1-30.

Enders, T.A., and Strader, L.C. (2015). Auxin activity: Past, present, and future. Am J Bot **102,** 180-196.

Falk, A., Feys, B.J., Frost, L.N., Jones, J.D.G., Daniels, M.J., and Parker, J.E. (1999). EDS1, an essential component of R gene-mediated disease resistance in Arabidopsis has homology to eukaryotic lipases. Proceedings of the National Academy of Sciences of the United States of America **96,** 3292-3297.

Faulkner, C., Petutschnig, E., Benitez-Alfonso, Y., Beck, M., Robatzek, S., Lipka, V., and Maule, A.J. (2013). LYM2-dependent chitin perception limits molecular flux via plasmodesmata. Proc Natl Acad Sci U S A **110,** 9166-9170.

Feraru, E., and Friml, J. (2008). PIN polar targeting. Plant Physiol **147,** 1553-1559.

Feraru, E., Feraru, M.I., Kleine-Vehn, J., Martiniere, A., Mouille, G., Vanneste, S., Vernhettes, S., Runions, J., and Friml, J. (2011). PIN polarity maintenance by the cell wall in Arabidopsis. Curr Biol **21,** 338-343.

Ferreira, P.C., Hemerly, A.S., Engler, J.D., van Montagu, M., Engler, G., and Inze, D. (1994). Developmental expression of the arabidopsis cyclin gene cyc1At. Plant Cell **6,** 1763-1774.

Feys, B.J., Moisan, L.J., Newman, M.A., and Parker, J.E. (2001). Direct interaction between the Arabidopsis disease resistance signaling proteins, EDS1 and PAD4. EMBO J **20,** 5400-5411.

Feys, B.J., Wiermer, M., Bhat, R.A., Moisan, L.J., Medina-Escobar, N., Neu, C., Cabral, A., and Parker, J.E. (2005). Arabidopsis SENESCENCE-ASSOCIATED GENE101 stabilizes and signals within an ENHANCED DISEASE SUSCEPTIBILITY1 complex in plant innate immunity. Plant Cell **17,** 2601-2613.

Friml, J., Wisniewska, J., Benkova, E., Mendgen, K., and Palme, K. (2002a). Lateral relocation of auxin efflux regulator PIN3 mediates tropism in Arabidopsis. Nature **415,** 806-809.

Friml, J., Benkova, E., Blilou, I., Wisniewska, J., Hamann, T., Ljung, K., Woody, S., Sandberg, G., Scheres, B., Jurgens, G., and Palme, K. (2002b). AtPIN4 mediates sink-driven auxin gradients and root patterning in Arabidopsis. Cell **108,** 661-673.

Fukaki, H., Tameda, S., Masuda, H., and Tasaka, M. (2002). Lateral root formation is blocked by a gain-of-function mutation in the SOLITARY-ROOT/IAA14 gene of Arabidopsis. Plant J **29,** 153-168.

Fukaki, H., Nakao, Y., Okushima, Y., Theologis, A., and Tasaka, M. (2005). Tissue-specific expression of stabilized SOLITARY-ROOT/IAA14 alters lateral root development in Arabidopsis. Plant J **44,** 382-395.

Galweiler, L., Guan, C., Muller, A., Wisman, E., Mendgen, K., Yephremov, A., and Palme, K. (1998). Regulation of polar auxin transport by AtPIN1 in Arabidopsis vascular tissue. Science **282,** 2226-2230.

Gao, Q.M., Zhu, S., Kachroo, P., and Kachroo, A. (2015). Signal regulators of systemic acquired resistance. Front Plant Sci **6,** 228.

Garcia, A.V., Blanvillain-Baufume, S., Huibers, R.P., Wiermer, M., Li, G., Gobbato, E., Rietz, S., and Parker, J.E. (2010). Balanced nuclear and cytoplasmic activities of EDS1 are required for a complete plant innate immune response. PLoS Pathog **6,** e1000970.

Garcion, C., Lohmann, A., Lamodiere, E., Catinot, J., Buchala, A., Doermann, P., and Metraux, J.P. (2008). Characterization and biological function of the ISOCHORISMATE SYNTHASE2 gene of Arabidopsis. Plant Physiol **147,** 1279-1287.

Garner, C.M., Kim, S.H., Spears, B.J., and Gassmann, W. (2016). Express yourself: Transcriptional regulation of plant innate immunity. Semin Cell Dev Biol **56,** 150-162.

Geldner, N., Friml, J., Stierhof, Y.D., Jurgens, G., and Palme, K. (2001). Auxin transport inhibitors block PIN1 cycling and vesicle trafficking. Nature **413,** 425-428.

Geldner, N., Anders, N., Wolters, H., Keicher, J., Kornberger, W., Muller, P., Delbarre, A., Ueda, T., Nakano, A., and Jurgens, G. (2003). The

Arabidopsis GNOM ARF-GEF mediates endosomal recycling, auxin transport, and auxin-dependent plant growth. Cell **112,** 219-230.

Gibbs, D.J., Voss, U., Harding, S.A., Fannon, J., Moody, L.A., Yamada, E., Swarup, K., Nibau, C., Bassel, G.W., Choudhary, A., Lavenus, J., Bradshaw, S.J., Stekel, D.J., Bennett, M.J., and Coates, J.C. (2014). AtMYB93 is a novel negative regulator of lateral root development in Arabidopsis. New Phytol **203,** 1194-1207.

Glazebrook, J., Rogers, E.E., and Ausubel, F.M. (1996). Isolation of Arabidopsis mutants with enhanced disease susceptibility by direct screening. Genetics **143,** 973-982.

Goh, T., Joi, S., Mimura, T., and Fukaki, H. (2012a). The establishment of asymmetry in Arabidopsis lateral root founder cells is regulated by LBD16/ASL18 and related LBD/ASL proteins. Development **139,** 883-893.

Goh, T., Kasahara, H., Mimura, T., Kamiya, Y., and Fukaki, H. (2012b). Multiple AUX/IAA-ARF modules regulate lateral root formation: the role of Arabidopsis SHY2/IAA3-mediated auxin signalling. Philos Trans R Soc Lond B Biol Sci **367,** 1461-1468.

Goldsmith, M.H.M. (1977). The Polar Transport of Auxin. Annual Review of Plant Physiology **28,** 439-478.

Gonzalez-Carranza, Z.H., Elliott, K.A., and Roberts, J.A. (2007). Expression of polygalacturonases and evidence to support their role during cell separation processes in Arabidopsis thaliana. J Exp Bot **58,** 3719-3730.

Grant, M., and Lamb, C. (2006). Systemic immunity. Curr Opin Plant Biol **9,** 414-420.

Habets, M.E., and Offringa, R. (2014). PIN-driven polar auxin transport in plant developmental plasticity: a key target for environmental and endogenous signals. New Phytol **203,** 362-377.

Han, X., Hyun, T.K., Zhang, M., Kumar, R., Koh, E.J., Kang, B.H., Lucas, W.J., and Kim, J.Y. (2014). Auxin-callose-mediated plasmodesmal gating is essential for tropic auxin gradient formation and signaling. Dev Cell **28,** 132-146.

Hepler, P.K. (1982). Endoplasmic-Reticulum in the Formation of the Cell Plate and Plasmodesmata. Protoplasma **111,** 121-133.

Huang, F., Zago, M.K., Abas, L., van Marion, A., Galvan-Ampudia, C.S., and Offringa, R. (2010). Phosphorylation of conserved PIN motifs directs Arabidopsis PIN1 polarity and auxin transport. Plant Cell **22,** 1129-1142.

Ingram, P., Dettmer, J., Helariutta, Y., and Malamy, J.E. (2011). Arabidopsis Lateral Root Development 3 is essential for early phloem development and function, and hence for normal root system development. Plant J **68,** 455-467.

Jagadeeswaran, G., Raina, S., Acharya, B.R., Maqbool, S.B., Mosher, S.L., Appel, H.M., Schultz, J.C., Klessig, D.F., and Raina, R. (2007). Arabidopsis GH3-LIKE DEFENSE GENE 1 is required for accumulation of salicylic acid,

activation of defense responses and resistance to Pseudomonas syringae. Plant J **51,** 234-246.

Jirage, D., Tootle, T.L., Reuber, T.L., Frost, L.N., Feys, B.J., Parker, J.E., Ausubel, F.M., and Glazebrook, J. (1999). Arabidopsis thaliana PAD4 encodes a lipase-like gene that is important for salicylic acid signaling. Proc Natl Acad Sci U S A **96,** 13583-13588.

Kankanala, P., Czymmek, K., and Valent, B. (2007). Roles for rice membrane dynamics and plasmodesmata during biotrophic invasion by the blast fungus. Plant Cell **19,** 706-724.

Kitakura, S., Vanneste, S., Robert, S., Lofke, C., Teichmann, T., Tanaka, H., and Friml, J. (2011). Clathrin mediates endocytosis and polar distribution of PIN auxin transporters in Arabidopsis. Plant Cell **23,** 1920-1931.

Kleine-Vehn, J., Huang, F., Naramoto, S., Zhang, J., Michniewicz, M., Offringa, R., and Friml, J. (2009). PIN auxin efflux carrier polarity is regulated by PINOID kinase-mediated recruitment into GNOM-independent trafficking in Arabidopsis. Plant Cell **21,** 3839-3849.

Kleine-Vehn, J., Wabnik, K., Martiniere, A., Langowski, L., Willig, K., Naramoto, S., Leitner, J., Tanaka, H., Jakobs, S., Robert, S., Luschnig, C., Govaerts, W., Hell, S.W., Runions, J., and Friml, J. (2011). Recycling, clustering, and endocytosis jointly maintain PIN auxin carrier polarity at the plasma membrane. Mol Syst Biol **7,** 540.

Korbei, B., and Luschnig, C. (2011). Cell polarity: PIN it down! Curr Biol **21,** R197-199.

Kovrizshnykh, V.V., Omelyanchuk, N.A., Pasternak, T.P., and Mironova, V.V. (2015). The key role of PIN proteins in auxin transport in Arabidopsis thaliana Roots. Russian Journal of Genetics: Applied Research **5,** 279-285.

Kragler, F. (2013). Plasmodesmata: intercellular tunnels facilitating transport of macromolecules in plants. Cell Tissue Res **352,** 49-58.

Křeček, P., Skůpa, P., Libus, J., Naramoto, S., Tejos, R., Friml, J., and Zažímalová, E. (2009). The PIN-FORMED (PIN) protein family of auxin transporters. Genome Biology **10,** 249.

Kuai, X., MacLeod, B.J., and Despres, C. (2015). Integrating data on the Arabidopsis NPR1/NPR3/NPR4 salicylic acid receptors; a differentiating argument. Front Plant Sci **6,** 235.

Kumpf, R.P., Shi, C.L., Larrieu, A., Sto, I.M., Butenko, M.A., Peret, B., Riiser, E.S., Bennett, M.J., and Aalen, R.B. (2013). Floral organ abscission peptide IDA and its HAE/HSL2 receptors control cell separation during lateral root emergence. Proc Natl Acad Sci U S A **110,** 5235-5240.

Langowski, L., Wabnik, K., Li, H., Vanneste, S., Naramoto, S., Tanaka, H., and Friml, J. (2016). Cellular mechanisms for cargo delivery and polarity maintenance at different polar domains in plant cells. Cell Discov **2,** 16018.

Laskowski, M., and ten Tusscher, K.H. (2017). Periodic Lateral Root Priming: What Makes It Tick? The Plant Cell **29,** 432-444.

Lee, J.Y., Yoo, B.C., Rojas, M.R., Gomez-Ospina, N., Staehelin, L.A., and Lucas, W.J. (2003). Selective trafficking of non-cell-autonomous proteins mediated by NtNCAPP1. Science **299,** 392-396.

Lee, J.Y., Wang, X., Cui, W., Sager, R., Modla, S., Czymmek, K., Zybaliov, B., van Wijk, K., Zhang, C., Lu, H., and Lakshmanan, V. (2011). A plasmodesmata-localized protein mediates crosstalk between cell-to-cell communication and innate immunity in Arabidopsis. Plant Cell **23,** 3353-3373.

Lee, M.W., Jelenska, J., and Greenberg, J.T. (2008). Arabidopsis proteins important for modulating defense responses to Pseudomonas syringae that secrete HopW1-1. Plant J **54,** 452-465.

Leyser, O. (2010). The power of auxin in plants. Plant Physiol **154,** 501-505.

Lim, G.H., Shine, M.B., de Lorenzo, L., Yu, K., Cui, W., Navarre, D., Hunt, A.G., Lee, J.Y., Kachroo, A., and Kachroo, P. (2016). Plasmodesmata Localizing Proteins Regulate Transport and Signaling during Systemic Acquired Immunity in Plants. Cell Host Microbe **19,** 541-549.

Liu, Y., Xu, M., Liang, N., Zheng, Y., Yu, Q., and Wu, S. (2017). Symplastic communication spatially directs local auxin biosynthesis to maintain root stem cell niche in Arabidopsis. Proc Natl Acad Sci U S A **114,** 4005-4010.

Lorrain, S., Vailleau, F., Balague, C., and Roby, D. (2003). Lesion mimic mutants: keys for deciphering cell death and defense pathways in plants? Trends Plant Sci **8,** 263-271.

Mano, Y., and Nemoto, K. (2012). The pathway of auxin biosynthesis in plants. J Exp Bot **63,** 2853-2872.

Manohar, M., Tian, M., Moreau, M., Park, S.W., Choi, H.W., Fei, Z., Friso, G., Asif, M., Manosalva, P., von Dahl, C.C., Shi, K., Ma, S., Dinesh-Kumar, S.P., O'Doherty, I., Schroeder, F.C., van Wijk, K.J., and Klessig, D.F. (2014). Identification of multiple salicylic acid-binding proteins using two high throughput screens. Front Plant Sci **5,** 777.

Marchant, A., Bhalerao, R., Casimiro, I., Eklof, J., Casero, P.J., Bennett, M., and Sandberg, G. (2002). AUX1 promotes lateral root formation by facilitating indole-3-acetic acid distribution between sink and source tissues in the Arabidopsis seedling. Plant Cell **14,** 589-597.

Marhavy, P., Vanstraelen, M., De Rybel, B., Zhaojun, D., Bennett, M.J., Beeckman, T., and Benkova, E. (2013). Auxin reflux between the endodermis and pericycle promotes lateral root initiation. EMBO J **32,** 149-158.

Martiniere, A., Lavagi, I., Nageswaran, G., Rolfe, D.J., Maneta-Peyret, L., Luu, D.T., Botchway, S.W., Webb, S.E., Mongrand, S., Maurel, C., Martin-Fernandez, M.L., Kleine-Vehn, J., Friml, J., Moreau, P., and Runions, J. (2012). Cell wall constrains lateral diffusion of plant plasma-membrane proteins. Proc Natl Acad Sci U S A **109,** 12805-12810.

Mashiguchi, K., Tanaka, K., Sakai, T., Sugawara, S., Kawaide, H., Natsume, M., Hanada, A., Yaeno, T., Shirasu, K., Yao, H., McSteen, P., Zhao, Y.,

Hayashi, K., Kamiya, Y., and Kasahara, H. (2011). The main auxin biosynthesis pathway in Arabidopsis. Proc Natl Acad Sci U S A **108,** 18512-18517.

Mauch-Mani, B., and Slusarenko, A.J. (1996). Production of Salicylic Acid Precursors Is a Major Function of Phenylalanine Ammonia-Lyase in the Resistance of Arabidopsis to Peronospora parasitica. Plant Cell **8,** 203-212.

Michniewicz, M., Zago, M.K., Abas, L., Weijers, D., Schweighofer, A., Meskiene, I., Heisler, M.G., Ohno, C., Zhang, J., Huang, F., Schwab, R., Weigel, D., Meyerowitz, E.M., Luschnig, C., Offringa, R., and Friml, J. (2007). Antagonistic regulation of PIN phosphorylation by PP2A and PINOID directs auxin flux. Cell **130,** 1044-1056.

Moreno-Risueno, M.A., Van Norman, J.M., Moreno, A., Zhang, J., Ahnert, S.E., and Benfey, P.N. (2010). Oscillating gene expression determines competence for periodic Arabidopsis root branching. Science **329,** 1306-1311.

Mou, Z., Fan, W., and Dong, X. (2003). Inducers of plant systemic acquired resistance regulate NPR1 function through redox changes. Cell **113,** 935-944.

Muller, A., Guan, C., Galweiler, L., Tanzler, P., Huijser, P., Marchant, A., Parry, G., Bennett, M., Wisman, E., and Palme, K. (1998). AtPIN2 defines a locus of Arabidopsis for root gravitropism control. EMBO J **17,** 6903-6911.

Neuteboom, L.W., Ng, J.M., Kuyper, M., Clijdesdale, O.R., Hooykaas, P.J., and van der Zaal, B.J. (1999). Isolation and characterization of cDNA clones corresponding with mRNAs that accumulate during auxin-induced lateral root formation. Plant Mol Biol **39,** 273-287.

Okada, K., Ueda, J., Komaki, M.K., Bell, C.J., and Shimura, Y. (1991). Requirement of the Auxin Polar Transport System in Early Stages of Arabidopsis Floral Bud Formation. Plant Cell **3,** 677-684.

Okrent, R.A., Brooks, M.D., and Wildermuth, M.C. (2009). Arabidopsis GH3.12 (PBS3) conjugates amino acids to 4-substituted benzoates and is inhibited by salicylate. J Biol Chem **284,** 9742-9754.

Okushima, Y., Fukaki, H., Onoda, M., Theologis, A., and Tasaka, M. (2007). ARF7 and ARF19 regulate lateral root formation via direct activation of LBD/ASL genes in Arabidopsis. Plant Cell **19,** 118-130.

Omelyanchuk, N.A., Kovrizhnykh, V.V., Oshchepkova, E.A., Pasternak, T., Palme, K., and Mironova, V.V. (2016). A detailed expression map of the PIN1 auxin transporter in Arabidopsis thaliana root. BMC Plant Biol **16 Suppl 1,** 5.

Oparka, K.J. (1993). Signalling via plasmodesmata--the neglected pathway. Semin Cell Biol **4,** 131-138.

Oparka, K.J., Prior, D.A.M., and Wright, K.M. (1995). Symplastic Communication between Primary and Developing Lateral Roots of Arabidopsis-Thaliana. Journal of Experimental Botany **46,** 187-197.

Orman-Ligeza, B., Parizot, B., de Rycke, R., Fernandez, A., Himschoot, E., Van Breusegem, F., Bennett, M.J., Perilleux, C., Beeckman, T., and Draye, X.

(2016). RBOH-mediated ROS production facilitates lateral root emergence in Arabidopsis. Development **143,** 3328-3339.

Overvoorde, P., Fukaki, H., and Beeckman, T. (2010). Auxin control of root development. Cold Spring Harb Perspect Biol **2,** a001537.

Pallas, J.A., Paiva, N.L., Lamb, C., and Dixon, R.A. (1996). Tobacco plants epigenetically suppressed in phenylalanine ammonia-lyase expression do not develop systemic acquired resistance in response to infection by tobacco mosaic virus. Plant Journal **10,** 281-293.

Pape, S., Thurow, C., and Gatz, C. (2010). The Arabidopsis PR-1 promoter contains multiple integration sites for the coactivator NPR1 and the repressor SNI1. Plant Physiol **154,** 1805-1818.

Parker, J.E., Holub, E.B., Frost, L.N., Falk, A., Gunn, N.D., and Daniels, M.J. (1996). Characterization of eds1, a mutation in Arabidopsis suppressing resistance to Peronospora parasitica specified by several different RPP genes. Plant Cell **8,** 2033-2046.

Parry, G., Calderon-Villalobos, L.I., Prigge, M., Peret, B., Dharmasiri, S., Itoh, H., Lechner, E., Gray, W.M., Bennett, M., and Estelle, M. (2009). Complex regulation of the TIR1/AFB family of auxin receptors. Proc Natl Acad Sci U S A **106,** 22540-22545.

Peret, B., Larrieu, A., and Bennett, M.J. (2009). Lateral root emergence: a difficult birth. J Exp Bot **60,** 3637-3643.

Peret, B., Li, G., Zhao, J., Band, L.R., Voss, U., Postaire, O., Luu, D.T., Da Ines, O., Casimiro, I., Lucas, M., Wells, D.M., Lazzerini, L., Nacry, P., King, J.R., Jensen, O.E., Schaffner, A.R., Maurel, C., and Bennett, M.J. (2012a). Auxin regulates aquaporin function to facilitate lateral root emergence. Nat Cell Biol **14,** 991-998.

Peret, B., Swarup, K., Ferguson, A., Seth, M., Yang, Y., Dhondt, S., James, N., Casimiro, I., Perry, P., Syed, A., Yang, H., Reemmer, J., Venison, E., Howells, C., Perez-Amador, M.A., Yun, J., Alonso, J., Beemster, G.T., Laplaze, L., Murphy, A., Bennett, M.J., Nielsen, E., and Swarup, R. (2012b). AUX/LAX genes encode a family of auxin influx transporters that perform distinct functions during Arabidopsis development. Plant Cell **24,** 2874-2885.

Peret, B., Middleton, A.M., French, A.P., Larrieu, A., Bishopp, A., Njo, M., Wells, D.M., Porco, S., Mellor, N., Band, L.R., Casimiro, I., Kleine-Vehn, J., Vanneste, S., Sairanen, I., Mallet, R., Sandberg, G., Ljung, K., Beeckman, T., Benkova, E., Friml, J., Kramer, E., King, J.R., De Smet, I., Pridmore, T., Owen, M., and Bennett, M.J. (2013). Sequential induction of auxin efflux and influx carriers regulates lateral root emergence. Mol Syst Biol **9,** 699.

Perrine-Walker, F.M., and Jublanc, E. (2014). The localization of auxin transporters PIN3 and LAX3 during lateral root development in Arabidopsis thaliana. Biologia Plantarum **58,** 778-782.

Petrasek, J., and Friml, J. (2009). Auxin transport routes in plant development. Development **136,** 2675-2688.

Prasad, K., and Dhonukshe, P. (2013). Polar Auxin Transport: Cell Polarity to Patterning. In Polar Auxin Transport, R. Chen and F. Baluška, eds (Berlin, Heidelberg: Springer Berlin Heidelberg), pp. 25-44.

Qi, J., and Greb, T. (2017). Cell polarity in plants: the Yin and Yang of cellular functions. Curr Opin Plant Biol **35,** 105-110.

Raven, J.A. (1975). TRANSPORT OF INDOLEACETIC ACID IN PLANT CELLS IN RELATION TO pH AND ELECTRICAL POTENTIAL GRADIENTS, AND ITS SIGNIFICANCE FOR POLAR IAA TRANSPORT. New Phytologist **74,** 163-172.

Reed, R.C., Brady, S.R., and Muday, G.K. (1998). Inhibition of auxin movement from the shoot into the root inhibits lateral root development in Arabidopsis. Plant Physiol **118,** 1369-1378.

Reinhardt, H., Hachez, C., Bienert, M.D., Beebo, A., Swarup, K., Voss, U., Bouhidel, K., Frigerio, L., Schjoerring, J.K., Bennett, M.J., and Chaumont, F. (2016). Tonoplast Aquaporins Facilitate Lateral Root Emergence. Plant Physiol **170,** 1640-1654.

Robert, H.S., and Friml, J. (2009). Auxin and other signals on the move in plants. Nat Chem Biol **5,** 325-332.

Rogg, L.E., Lasswell, J., and Bartel, B. (2001). A gain-of-function mutation in IAA28 suppresses lateral root development. Plant Cell **13,** 465-480.

Roppolo, D., De Rybel, B., Denervaud Tendon, V., Pfister, A., Alassimone, J., Vermeer, J.E., Yamazaki, M., Stierhof, Y.D., Beeckman, T., and Geldner, N. (2011). A novel protein family mediates Casparian strip formation in the endodermis. Nature **473,** 380-383.

Rubery, P.H., and Sheldrake, A.R. (1974). Carrier-mediated auxin transport. Planta **118,** 101-121.

Rutschow, H.L., Baskin, T.I., and Kramer, E.M. (2011). Regulation of solute flux through plasmodesmata in the root meristem. Plant Physiol **155,** 1817-1826.

Sachs, T. (1981). The Control of the Patterned Differentiation of Vascular Tissues. In Advances in Botanical Research, H.W. Woolhouse, ed (Academic Press), pp. 151-262.

Sachs, T. (1986). Cellular interactions in tissue and organ development. Symp Soc Exp Biol **40,** 181-210.

Sachs, T. (1991). Cell polarity and tissue patterning in plants. Development **113,** 83-93.

Sager, R., and Lee, J.Y. (2014). Plasmodesmata in integrated cell signalling: insights from development and environmental signals and stresses. J Exp Bot **65,** 6337-6358.

Sauer, M., Robert, S., and Kleine-Vehn, J. (2013). Auxin: simply complicated. J Exp Bot **64,** 2565-2577.

Sauer, M., Balla, J., Luschnig, C., Wisniewska, J., Reinohl, V., Friml, J., and Benkova, E. (2006). Canalization of auxin flow by Aux/IAA-ARF-dependent feedback regulation of PIN polarity. Genes Dev **20,** 2902-2911.

Serghini, M.A., Ritzenthaler, C., and Pinck, L. (1989). A rapid and efficient 'miniprep' for isolation of plasmid DNA. Nucleic Acids Res **17,** 3604.

Sevilem, I., Yadav, S.R., and Helariutta, Y. (2015). Plasmodesmata: channels for intercellular signaling during plant growth and development. Methods Mol Biol **1217,** 3-24.

Shamrai, S.N. (2014). Plant immune system: Basal immunity. Cytology and Genetics **48,** 258-271.

Sherwin, J.E., and Purves, W.K. (1969). Tryptophan as an auxin precursor in cucumber seedlings. Plant Physiol **44,** 1303-1309.

Spoel, S.H., and Dong, X. (2008). Making sense of hormone crosstalk during plant immune responses. Cell Host Microbe **3,** 348-351.

Spoel, S.H., Mou, Z., Tada, Y., Spivey, N.W., Genschik, P., and Dong, X. (2009). Proteasome-mediated turnover of the transcription coactivator NPR1 plays dual roles in regulating plant immunity. Cell **137,** 860-872.

Steinmann, T., Geldner, N., Grebe, M., Mangold, S., Jackson, C.L., Paris, S., Galweiler, L., Palme, K., and Jurgens, G. (1999). Coordinated polar localization of auxin efflux carrier PIN1 by GNOM ARF GEF. Science **286,** 316-318.

Swarup, K., Benkova, E., Swarup, R., Casimiro, I., Peret, B., Yang, Y., Parry, G., Nielsen, E., De Smet, I., Vanneste, S., Levesque, M.P., Carrier, D., James, N., Calvo, V., Ljung, K., Kramer, E., Roberts, R., Graham, N., Marillonnet, S., Patel, K., Jones, J.D., Taylor, C.G., Schachtman, D.P., May, S., Sandberg, G., Benfey, P., Friml, J., Kerr, I., Beeckman, T., Laplaze, L., and Bennett, M.J. (2008). The auxin influx carrier LAX3 promotes lateral root emergence. Nat Cell Biol **10,** 946-954.

Swarup, R., and Peret, B. (2012). AUX/LAX family of auxin influx carriers-an overview. Front Plant Sci **3,** 225.

Swarup, R., Friml, J., Marchant, A., Ljung, K., Sandberg, G., Palme, K., and Bennett, M. (2001). Localization of the auxin permease AUX1 suggests two functionally distinct hormone transport pathways operate in the Arabidopsis root apex. Genes Dev **15,** 2648-2653.

Swarup, R., Kramer, E.M., Perry, P., Knox, K., Leyser, H.M., Haseloff, J., Beemster, G.T., Bhalerao, R., and Bennett, M.J. (2005). Root gravitropism requires lateral root cap and epidermal cells for transport and response to a mobile auxin signal. Nat Cell Biol **7,** 1057-1065.

Swarup, R., Kargul, J., Marchant, A., Zadik, D., Rahman, A., Mills, R., Yemm, A., May, S., Williams, L., Millner, P., Tsurumi, S., Moore, I., Napier, R., Kerr, I.D., and Bennett, M.J. (2004). Structure-function analysis of the presumptive Arabidopsis auxin permease AUX1. Plant Cell **16,** 3069-3083.

Tanaka, H., Dhonukshe, P., Brewer, P.B., and Friml, J. (2006). Spatiotemporal asymmetric auxin distribution: a means to coordinate plant development. Cell Mol Life Sci **63,** 2738-2754.

Tanaka, H., Kitakura, S., Rakusova, H., Uemura, T., Feraru, M.I., De Rycke, R., Robert, S., Kakimoto, T., and Friml, J. (2013). Cell polarity and patterning by PIN trafficking through early endosomal compartments in Arabidopsis thaliana. PLoS Genet **9,** e1003540.

Teale, W.D., Paponov, I.A., and Palme, K. (2006). Auxin in action: signalling, transport and the control of plant growth and development. Nat Rev Mol Cell Biol **7,** 847-859.

Thomas, C.L., Bayer, E.M., Ritzenthaler, C., Fernandez-Calvino, L., and Maule, A.J. (2008). Specific targeting of a plasmodesmal protein affecting cell-to-cell communication. PLoS Biol **6,** e7.

Tian, Q., and Reed, J.W. (1999). Control of auxin-regulated root development by the Arabidopsis thaliana SHY2/IAA3 gene. Development **126,** 711-721.

Ulmasov, T., Murfett, J., Hagen, G., and Guilfoyle, T.J. (1997). Aux/IAA proteins repress expression of reporter genes containing natural and highly active synthetic auxin response elements. Plant Cell **9,** 1963-1971.

van Berkel, K., de Boer, R.J., Scheres, B., and ten Tusscher, K. (2013). Polar auxin transport: models and mechanisms. Development **140,** 2253-2268.

Van Norman, J.M. (2015). Root system patterning: auxin synthesis at the root periphery. Curr Biol **25,** R460-462.

Van Norman, J.M., Xuan, W., Beeckman, T., and Benfey, P.N. (2013). To branch or not to branch: the role of pre-patterning in lateral root formation. Development **140,** 4301-4310.

Van Norman, J.M., Zhang, J., Cazzonelli, C.I., Pogson, B.J., Harrison, P.J., Bugg, T.D., Chan, K.X., Thompson, A.J., and Benfey, P.N. (2014). Periodic root branching in Arabidopsis requires synthesis of an uncharacterized carotenoid derivative. Proc Natl Acad Sci U S A **111,** E1300-1309.

Vanneste, S., De Rybel, B., Beemster, G.T., Ljung, K., De Smet, I., Van Isterdael, G., Naudts, M., Iida, R., Gruissem, W., Tasaka, M., Inze, D., Fukaki, H., and Beeckman, T. (2005). Cell cycle progression in the pericycle is not sufficient for SOLITARY ROOT/IAA14-mediated lateral root initiation in Arabidopsis thaliana. Plant Cell **17,** 3035-3050.

Vermeer, J.E., and Geldner, N. (2015). Lateral root initiation in Arabidopsis thaliana: a force awakens. F1000Prime Rep **7,** 32.

Vermeer, J.E., von Wangenheim, D., Barberon, M., Lee, Y., Stelzer, E.H., Maizel, A., and Geldner, N. (2014). A spatial accommodation by neighboring cells is required for organ initiation in Arabidopsis. Science **343,** 178-183.

Vidhyasekaran, P. (2015). Salicylic Acid Signaling in Plant Innate Immunity. In Plant Hormone Signaling Systems in Plant Innate Immunity (Dordrecht: Springer Netherlands), pp. 27-122.

Vilches-Barro, A., and Maizel, A. (2015). Talking through walls: mechanisms of lateral root emergence in Arabidopsis thaliana. Curr Opin Plant Biol **23,** 31-38.

Vissenberg, K., Oyama, M., Osato, Y., Yokoyama, R., Verbelen, J.P., and Nishitani, K. (2005). Differential expression of AtXTH17, AtXTH18, AtXTH19 and AtXTH20 genes in Arabidopsis roots. Physiological roles in specification in cell wall construction. Plant Cell Physiol **46,** 192-200.

Voigt, C.A., and Somerville, S.C. (2009). Callose in Biotic Stress (Pathogenesis) Biology, biochemistry and molecular biology of callose in plant defence: callose deposition and turnover in plant-pathogen interactions. Chemistry, Biochemistry, and Biology of (1-->3)-Beta-Glucans and Related Polysaccharides**,** 525-562.

Wagner, S., Stuttmann, J., Rietz, S., Guerois, R., Brunstein, E., Bautor, J., Niefind, K., and Parker, J.E. (2013). Structural basis for signaling by exclusive EDS1 heteromeric complexes with SAG101 or PAD4 in plant innate immunity. Cell Host Microbe **14,** 619-630.

Wang, G.F., Seabolt, S., Hamdoun, S., Ng, G., Park, J., and Lu, H. (2011). Multiple roles of WIN3 in regulating disease resistance, cell death, and flowering time in Arabidopsis. Plant Physiol **156,** 1508-1519.

Wang, X., Sager, R., Cui, W., Zhang, C., Lu, H., and Lee, J.Y. (2013). Salicylic acid regulates Plasmodesmata closure during innate immune responses in Arabidopsis. Plant Cell **25,** 2315-2329.

Warren, R.F., Merritt, P.M., Holub, E., and Innes, R.W. (1999). Identification of three putative signal transduction genes involved in R gene-specified disease resistance in Arabidopsis. Genetics **152,** 401-412.

Weller, B., Zourelidou, M., Frank, L., Barbosa, I.C., Fastner, A., Richter, S., Jurgens, G., Hammes, U.Z., and Schwechheimer, C. (2017). Dynamic PIN-FORMED auxin efflux carrier phosphorylation at the plasma membrane controls auxin efflux-dependent growth. Proc Natl Acad Sci U S A **114,** E887-E896.

Westfall, C.S., Sherp, A.M., Zubieta, C., Alvarez, S., Schraft, E., Marcellin, R., Ramirez, L., and Jez, J.M. (2016). Arabidopsis thaliana GH3.5 acyl acid amido synthetase mediates metabolic crosstalk in auxin and salicylic acid homeostasis. Proc Natl Acad Sci U S A **113,** 13917-13922.

Widhalm, J.R., and Dudareva, N. (2015). A familiar ring to it: biosynthesis of plant benzoic acids. Mol Plant **8,** 83-97.

Wiermer, M., Feys, B.J., and Parker, J.E. (2005). Plant immunity: the EDS1 regulatory node. Current Opinion in Plant Biology **8,** 383-389.

Wildermuth, M.C., Dewdney, J., Wu, G., and Ausubel, F.M. (2001). Isochorismate synthase is required to synthesize salicylic acid for plant defence. Nature **414,** 562-565.

Wilmoth, J.C., Wang, S., Tiwari, S.B., Joshi, A.D., Hagen, G., Guilfoyle, T.J., Alonso, J.M., Ecker, J.R., and Reed, J.W. (2005). NPH4/ARF7 and ARF19

promote leaf expansion and auxin-induced lateral root formation. Plant J **43,** 118-130.

Won, C., Shen, X., Mashiguchi, K., Zheng, Z., Dai, X., Cheng, Y., Kasahara, H., Kamiya, Y., Chory, J., and Zhao, Y. (2011). Conversion of tryptophan to indole-3-acetic acid by TRYPTOPHAN AMINOTRANSFERASES OF ARABIDOPSIS and YUCCAs in Arabidopsis. Proc Natl Acad Sci U S A **108,** 18518-18523.

Wu, S., Shan, L., and He, P. (2014). Microbial signature-triggered plant defense responses and early signaling mechanisms. Plant Sci **228,** 118-126.

Wu, S., O'Lexy, R., Xu, M., Sang, Y., Chen, X., Yu, Q., and Gallagher, K.L. (2016). Symplastic signaling instructs cell division, cell expansion, and cell polarity in the ground tissue of Arabidopsis thaliana roots. Proc Natl Acad Sci U S A **113,** 11621-11626.

Wu, Y., Zhang, D., Chu, J.Y., Boyle, P., Wang, Y., Brindle, I.D., De Luca, V., and Despres, C. (2012). The Arabidopsis NPR1 protein is a receptor for the plant defense hormone salicylic acid. Cell Rep **1,** 639-647.

Xu, J., Hofhuis, H., Heidstra, R., Sauer, M., Friml, J., and Scheres, B. (2006). A molecular framework for plant regeneration. Science **311,** 385-388.

Xu, X.M., and Jackson, D. (2010). Lights at the end of the tunnel: new views of plasmodesmal structure and function. Curr Opin Plant Biol **13,** 684-692.

Xuan, W., Audenaert, D., Parizot, B., Moller, B.K., Njo, M.F., De Rybel, B., De Rop, G., Van Isterdael, G., Mahonen, A.P., Vanneste, S., and Beeckman, T. (2015). Root Cap-Derived Auxin Pre-patterns the Longitudinal Axis of the Arabidopsis Root. Curr Biol **25,** 1381-1388.

Yadav, S.R., Yan, D., Sevilem, I., and Helariutta, Y. (2014). Plasmodesmata-mediated intercellular signaling during plant growth and development. Front Plant Sci **5,** 44.

Zazimalova, E., Murphy, A.S., Yang, H., Hoyerova, K., and Hosek, P. (2010). Auxin transporters--why so many? Cold Spring Harb Perspect Biol **2,** a001552.

Zhang, J., Nodzynski, T., Pencik, A., Rolcik, J., and Friml, J. (2010a). PIN phosphorylation is sufficient to mediate PIN polarity and direct auxin transport. Proc Natl Acad Sci U S A **107,** 918-922.

Zhang, X., Chen, S., and Mou, Z. (2010b). Nuclear localization of NPR1 is required for regulation of salicylate tolerance, isochorismate synthase 1 expression and salicylate accumulation in Arabidopsis. J Plant Physiol **167,** 144-148.

Zhao, Y. (2010). Auxin biosynthesis and its role in plant development. Annu Rev Plant Biol **61,** 49-64.

Zhao, Y. (2012). Auxin biosynthesis: a simple two-step pathway converts tryptophan to indole-3-acetic acid in plants. Mol Plant **5,** 334-338.

Zhao, Y. (2014). Auxin biosynthesis. Arabidopsis Book **12,** e0173.

Zhu, S., Jeong, R.D., Venugopal, S.C., Lapchyk, L., Navarre, D., Kachroo, A., and Kachroo, P. (2011). SAG101 forms a ternary complex with EDS1 and

PAD4 and is required for resistance signaling against turnip crinkle virus. PLoS Pathog **7,** e1002318.

Zolman, B.K., Nyberg, M., and Bartel, B. (2007). IBR3, a novel peroxisomal acyl-CoA dehydrogenase-like protein required for indole-3-butyric acid response. Plant Mol Biol **64,** 59-72.

Appendix A

MATERIALS AND METHODS FOR CHAPTERS 2 AND 3

A.1 Plant Cultivation in Soil

Arabidopsis seed was sown directly onto moist soil (Sunshine Mix 1, SunGro Horticulture). Pots with seeds were covered with clear lids and placed into 4°C for 2 day stratification in the dark. Pots were then transferred to controlled environment chambers (Conviron®), and plants were grown under long day conditions (16 h day/8 hr night, 20°C, 60% humidity, with 130 µmol/m^2s light intensity). Lids were removed post-germination (5-7 days). Soil was watered via subirrigation, with 1.5 tsp solid Gnatrol® WDG (Valent BioSciences) per 8 L water, every watering except weeks 4 and 8, when fertilizer was used. Seeds were collected by placing dried siliques over clean white paper and squeezing gently to break apart siliques and release seeds.

A.2 Seed Sterilization and Growth on Plates

Approximately 20-100 µL of Arabidopsis seeds were poured into 1.5 mL Eppendorf tubes. Seeds were washed first with 1 mL 3% bleach solution for 5 min, centrifuged, bleach removed, then rinsed 3 times each (as above) with 1 mL autoclaved Milli-Q® H2O. Sterilized seeds in water were placed in 4°C for 2 day stratification in the dark. To grow on plates, seeds were drawn into a sterile 1 mL pipette tip, and placed upon solid 1% Caisson Labs Phytoblend™ agar media containing 0.5X PhytoTechnology Laboratories® Mushirage and Skoog (MS) by carefully touching tip of pipette to surface of agar, allowing cohesion to pull out seeds

one by one in very small droplets of water (after 12 hr, excess water has been absorbed into agar). Plates were then moved to controlled environment chamber and grown horizontally (0.7% agar) or vertically (1.0% agar), under 24 hr light conditions (22°C, 60% humidity, with 130 umol/m2s light intensity).

A.3 Primer Tables

Table A1 Primers used for RT-PCR expression analyses

Template	**Purpose**	**Primer names and sequences (5'→3')**
Ubiquitin (At3G62250) cDNA	Detect UBQ transcript expression	Fw: Lpr136: GGAAGACCATAACCCTTGAGGTTG Rv: Lpr151: TCTTAGCACCACCACGGAGA
PDLP5 (At1G70690) cDNA	Detect PDLP5 transcript expression	Fw: Lpr665: CCGCTACGCCAACTTCACAG Rv: Lpr723: CTTCTCTCCTTCATGACCAAAGT
PR1 (At2G14610) cDNA	Detect PR1 transcript expression	Fw: Lpr882: GAAAACTTAGCCTGGGGTAGC Rv: Lpr883: TTCATTAGTATGGCTTCTCGTTCA
PR2 (At3G57260) cDNA	Detect PR2 transcript expression	Fw: Lpr891: GAGTGTGGAAAACGCAAAGAC Rv: Lpr890: GACTGTCGATCTGGATGAAACA
WRKY6 (At1G62300) cDNA	Detect WRKY6 transcript expression	Fw: Lpr976: CTAATGGTTCCAATCCTTCC Rv: Lpr977: GTTGTTTCCTTCGCCGTC
SAG13 (At2G29350) cDNA	Detect SAG13 transcript expression	Fw: Lpr927: CAAGATGGAGTCTTGGAGGCA Rv: Lpr928: AGGAAAAACCGTTAACAGTGG

Table A2 Primers used for genotyping

Template	**Purpose**	**Target**	**Primer names and sequences (5'→3')**
eds1-2 x 35S:PDLP5 genomic DNA	Confirm eds1 mutant homozygosity	WT EDS1	Fw: Lpr1038: GTTAGCAACTCGATACCGCAGATTAGTTG Rv: Lpr1040: GAAGCAAGTGTTCTAATAGCTTAAATACTCC

		eds1-2 mutation	Fw: Lpr1039: GTTAGCAACTCGATACCGCAGATTAGTTA Rv: Lpr1073b: CTGTTATTTCATCCATCATATAGTCTCGCAGAGG
ics1 x 35S:PDLP 5 genomic DNA	Confirm ics1 mutant homozygosity	ics1 (sid2-1) mutation	Fw: Lpr1042: TGCAAGAGTGCAACATCTATATTCTC Rv: Lpr1044: CTGCCCTAGTTACAACCCGAAAAGGC
npr1-1 x 35S:PDLP 5 genomic DNA	Confirm npr1 mutant homozygosity	WT NPR1	Fw: Lpr1035: AATCCGAGGGGATATACGGTGCTTC Rv: Lpr1037: CCATTGGTTCAAATTGTTACAACATTTGTTTGAA GCACACC
		npr1-1 mutation	Fw: Lpr1036: AATCCGAGGGGATATACGGTGCTTT Rv: Lpr1037 (as above)
NahG x 35S:PDLP 5 genomic DNA	Confirm NahG transgene	NahG transgene	Fw: Lpr1076b: ACTGGAACTCTGCCGCTA Rv: Lpr1077b: TGAGTTACTAGGGCGTCG
pdlp5-1 genomic DNA	Confirm pdlp5-1 TDNA insertion homozygosity	WT PDLP5	Fw: Lpr853: TGGATCTTACAGGACAGGTGG Rv: Lpr852: TTTGCATAGACGAAAAACATGG
		pdlp5-1 T-DNA insert	Fw: Lpr853 (as above) Rv: Lpr417: GCCTTTTCAGAAATGGATAAATAGCCTTGCTTCC

Table A3 Primers used for cloning

Template	**Purpose**	**Primer names and sequences (5'→3')**
Plasmid "PDLP5 in pdGN"	Clone blunt-ended PDLP5	Fw: Lpr026: CCTTCGCAAGACCCTTCCTCT Rv: Lpr696: ACTGTCGACTCATTTACACCATTTCTCATCTTGTAATTT TCTACAAC
Genomic DNA from Arabidopsis Col-0	Clone CASP1 promoter with NotI/AscI R.E. sites	Fw: Lpr1428: GAAGATCTGCGGCCGCTTAATCTGCATAAAAGTGAGT ATGAG Rv: Lpr1429: CCGCTCGAGGCGCTTTCTCTTGCAATTGGGGTTTAAAA G
Plasmid "PDLP5:GUS in pRita"	Clone PDLP5 promoter with NotI/AscI	Fw: Lpr1303: GAAGATCTGCGGCCGCAAACAAAACATATCTCAATTT CATGAC Rv: Lpr1304:

	R.E. sites	CCGCTCGAGGCGCGCCGGTTACTTTTTGTTTTGAGAGATAGAG
Plasmid "pdYC"	Clone ER-YFP with HDEL sequence and XhoI/XbaI R.E. sites	PCR#1: Fw: Lpr1337: CTCATCTTTTCACTTCTCCTATCATTATCCTCGGCCGTGAGCAAGGGCGAGGAGCT Rv: Lpr1338: AATCTAGATTAAAGCTCATCATGCTTGTATAGCTCGTCCATGCCG PCR#2: Fw: Lpr1336: GACTCGAGAATGAAGACTAATCTTTTTCTCTTTCTCATCTTTTCACTTCT Rv: Lrp1338 (as above)
Plasmid "P30 TMV-MP-GFP in pdGN"	Clone TMV-MP-GFP with XhoI/XbaI R.E. sites	Fw: Lpr1559: CATTAAAGCAGGACTCTAGAGGCCGCTTTACTTGT Rv: Lpr1560: ACGCTCGAGAATTCTCAACTC

A.4 PCR Program Tables

Table A4 Conditions for genotyping for presence of mutations

Initial Denaturation	Denaturation	Primer	Extension	Denaturation	Primer	Extension	Final Extension	Hold
94°C	94°C	52°C	72°C	94°C	60°C	72°C	72°C	4°C
5 min	1 min	2 min	6 min	1 min	2 min	6 min	7 min	Forever
1 cycle	3 cycles			27 cycles			1 cycle	

Table A5 Conditions for cloning tissue-specific promoters from genomic DNA

Initial Denaturation	Denaturation	Primer	Extension	Denaturation	Primer	Extension	Final Extension	Hold
98°C	98°C	60°C	72°C	94°C	66°C	72°C	72°C	4°C
30 sec	10 sec	10 sec	3 min	10 sec	10 sec	3 min	7 min	Forever
1 cycle	5 cycles			25 cycles			1 cycle	

A.5 Plant Genotypes Used in Thesis

Table A6 Plants used in Thesis Chapter 2. Accession is Col-0 unless otherwise noted.

Mutant or Transgenic Name	AGI Code	Purpose	Source	Reference	Note
eds1-2	At3G48090	Knock-out mutation in EDS1, to see how loss of this critical upstream SA pathway signaling gene affects PDLP5 expression and SA feedback	H. Bais lab, UD	Falk et al., 1999	In Ler background
pad4-1	At3G52430	Knock-out mutation in PAD4, to see how loss of this critical upstream SA pathway signaling gene affects PDLP5 expression and SA feedback	H. Bais lab, UD	Jirage et al., 1999	
ics1 (sid2-2/eds16-1)	At1G74710	Knock-out mutation in ICS1, to see how loss of this critical SA biosynthesis gene affects PDLP5 expression and SA feedback	H. Bais lab, UD	(Wildermuth et al., 2001)	
npr1-1	At1G64280	Knock-out mutation in NPR1, to see how loss of this critical downstream SA pathway transcription factor affects PDLP5 expression and SA feedback	H. Bais lab, UD	Cao et al., 1994	
NahG	N/A	Express the SA-degrading NahG enzyme, to determine whether observed phenotypic changes are related to SA accumulation	X. Dong lab, Duke U	Bowling et al., 1997	
pdlp5-1	At1G70690	Severe knockdown of PDLP5, to observe its effect on plant genotype and	ABRC	Lee et al., 2011	

		signaling pathways			
35S:PDLP5		Overexpress PDLP5, to observe its effect on plant genotype and signaling pathways	J.Y. Lee lab	Lee et al., 2011	
pER8:PDLP5		Highly induce PDLP5 expression using an estradiol promoter, to observe its effect on plant genotype and signaling pathways	This study		

Table A7 Plants used in Thesis Chapter 3. Accession is Col-0 unless otherwise noted.

Mutant or Transgenic Name	AGI Code	Purpose	Source	Reference	Note
pdlp5-1	At1G70690	Study the root phenotype of this severe knockdown PDLP5 mutant	ABRC	Lee et al., 2011	T-DNA insertion SAIL_46_E06
35S:PDLP5 (PDLP5OE)		Study the root phenotype of this strong PDLP5 overexpressor	J.Y.Lee lab, UD	Lee et al., 2011	
PDLP5pro:GUS		Find the plant tissue with strong PDLP5 promoter activity using histochemical staining	J.Y.Lee lab, UD	Lee et al., 2011	
PDLP5pro:PDLP5-GFP		Study PDLP5 localization in tissues where its promoter is naturally expressed	This study		
DR5:GUS	N/A	Locate areas of high auxin accumulation in fixed tissue	J.Y.Lee lab, UD	Ulmasov et al., 1997	
DR5:3VENUS		Locate areas of high auxin accumulation in live tissue	Malcolm Bennet lab, U of Nottingham	Brunoud et al., 2012	
LAX3pro:GUS	At1G77690	Find the plant tissue with strong LAX3 promoter activity using histochemical staining	Malcolm Bennet lab, U of Nottingham	(Swarup et al., 2008)	

LAX3pro:LAX 3-YFP		Study the plant tissue with strong LAX3 promoter activity using live cell confocal imaging	Malcolm Bennet lab, U of Nottingham	(Swarup et al., 2008)	
iaa28-1	At5G25890	Study PDLP5 promoter activity in this gain-of-function lateral root mutant	B. Bartel lab, Rice U	Rogg et al., 2001	In Ws backgrou nd
shy2-2	At1G04240		J.W.Reed lab, UNC-CH	Tian et al., 2002	In Ler backgrou nd
CASP1pro:ER-YFP	At2G36100	Confirm CASP1 promoter specificity	This study		
CASP1pro:GFP		Study symplasmic diffusion from endodermal tissue	This study		
CASP1pro:PDLP5-GFP		Study PDLP5 localization within endodermal tissue	This study		
CASP1pro:TMV-MP-GFP		Study active symplasmic transport out of endodermal tissue	This study		

A.6 Plant Treatments

Table A8 Hormone treatment concentrations

Hormone	**[Stock solution] in DMSO**	**[Treatment] in H2O**	**Reference**
Auxin (1-Napthaleneacetic acid)	10 µM	1 µM; 0.1 µM	Mei et al., 2012
Salicylic acid	200 mM	100 µM	Lee et al., 2011
Jasmonic acid	100 mM	50 µM	Hentrich et al., 2013
Abscisic acid	10 mM	10 µM	Yoon et al., 2010
Cytokinin (6-Benzylaminopurine)	10 mM	1 µM	Bai and DeMason, 2007
Auxin inhibitor (N-1-Napthylphthalmic acid)	10 µM	5 µM	Casimiro et al., 2001
17-β-estradiol	100 mM	10 µM	

Appendix B

SUPPLEMENTAL MATERIALS FOR CHAPTER 2

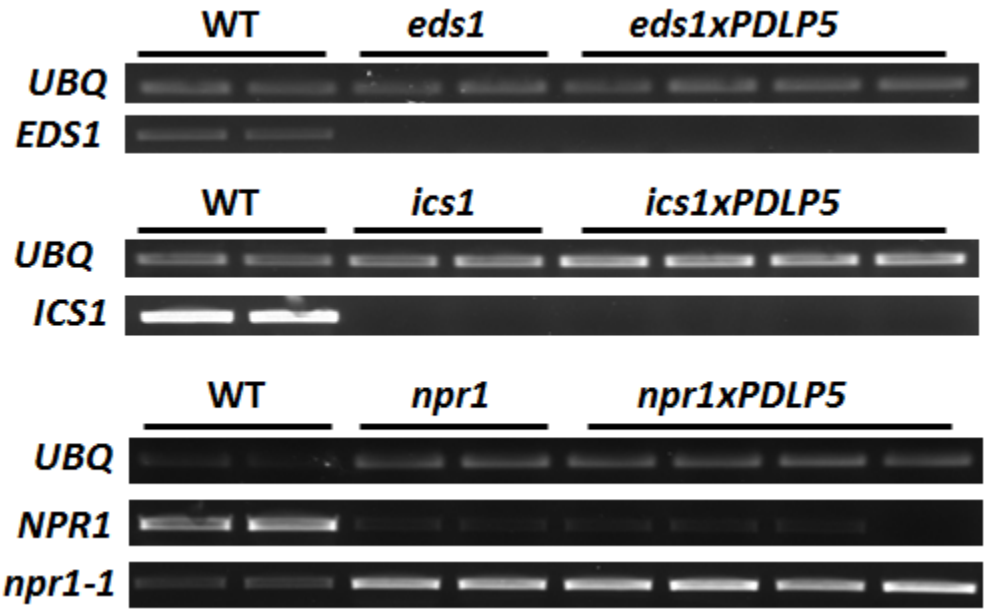

Figure B1: Genotyping of SA mutants crossed with *35S:PDLP5*.
Gene-specific primers were used to confirm the homozygosity of the SA pathway gene mutations in each cross; *eds1* and *ics1* lack transcript expression, while *npr1-1* has a point mutation that can be distinguished from *NPR1* with certain primers, as shown here.

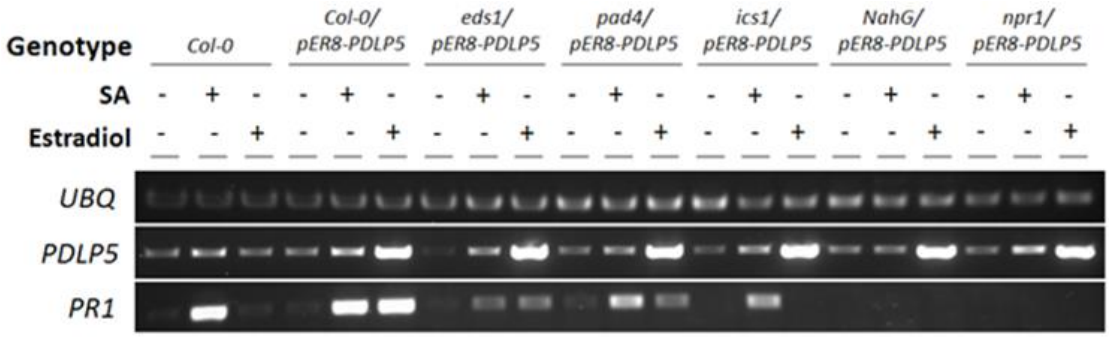

Figure B2: Gel data from estradiol-induced pER8:PDLP5 crossed with SA pathway mutants.
Representative gel used for semi-quantitative RT-PCR comparing PR1 expression after SA or estradiol treatment in the different genetic backgrounds shown above (from Fig 2.7).

Table B1 List of important defense and cell death genes co-expressed with *PDLP5*

Gene name	Function	References
Isochorismate synthase 1 (ICS1)	Salicylic acid biosynthesis	11
Phytoalexin deficient 4 (PAD4)	Regulates SA basal immunity with partner EDS1	10
Enhanced disease-susceptibility 1B (EDS1B; At3g48080)	Functions redundantly with characterized gene EDS1 (At3g48090)	17
Enhanced disease-susceptibility (EDS5)	Homologous with members of the MATE (multidrug and toxin extrusion) transporter family	39
Pathogenesis related 1 (PR1)	Molecular marker for SA induction	40
Avr-phB susceptible 3 (PBS3), or HopW1-1-interacting protein 3 (Win3)	Conjugates 4-substituted benzoates; contributes to the accumulation of SA during defense	19, 41
Syntaxin family member (SYP122)	Double mutant of proteins in SNARE machinery, accumulates high SA	42
Flavin-dependent monooxygenase 1 (FMO1)	EDS1-dependent SA-independent regulator of resistance and cell death at infection sites	43, 44

Glutaredoxin family member 13	Plays a key role in protection against photo-oxidative stress	45, 46
TGA1 transcription factor	Interacts with NPR1 during downstream SA defense signaling	9
WRKY22	Transcription factor regulating darkness-induced senescence	4
Senescence-associated gene 13 (SAG13)	Molecular marker upregulated during leaf senescence	28

Appendix C

SUPPLEMENTAL MATERIALS FOR CHAPTER 3

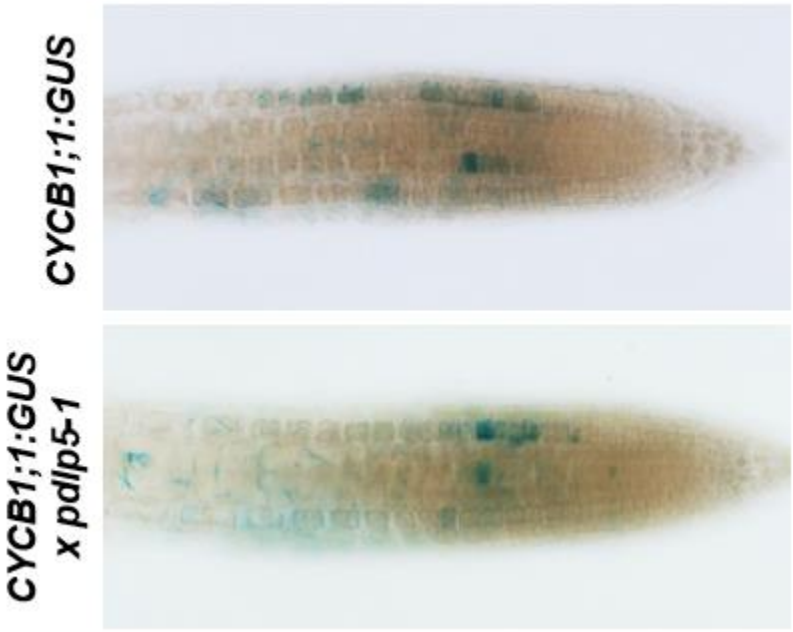

Figure C1: There are no differences in growth rates between WT and *pdlp5-1* root tips.
The cell division marker *CYCB1;1:GUS* has been used previously to show root tip growth upregulation. However, when *CYCB1;1:GUS* was expressed in homozygous *pdlp5-1* mutants, no differences were observed compared to *CYCB1;1:GUS* in WT.

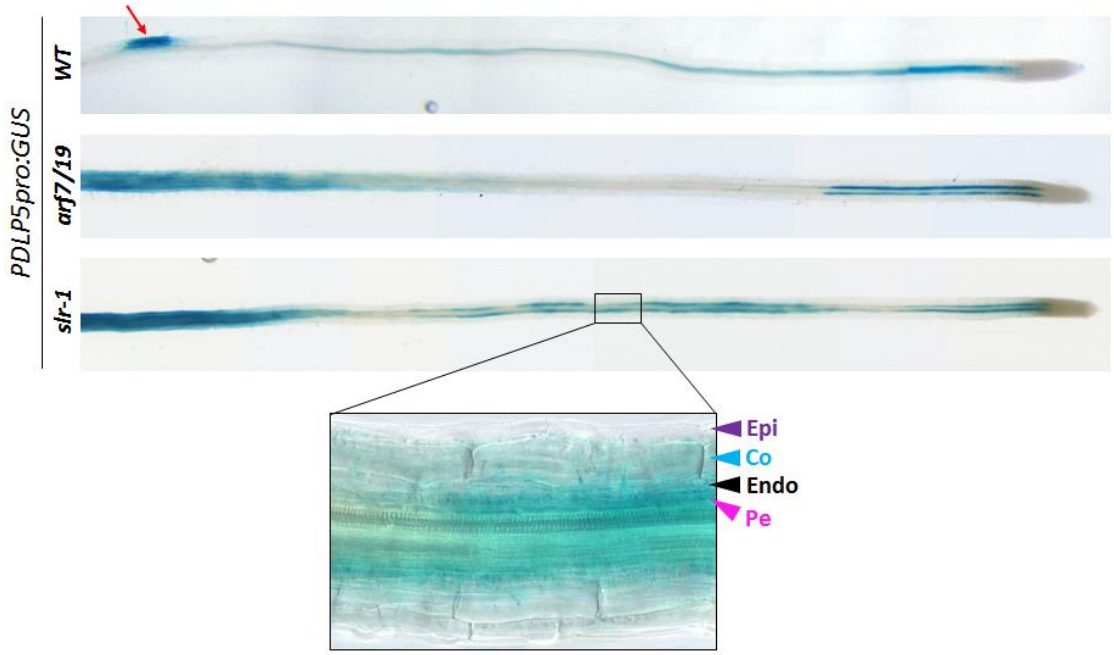

Figure C2: Lateral root initiation must be attempted for *PDLP5* expression to be induced in LRP-overlying cells.
14 dpg seedlings of the above crosses were GUS-stained 4 hrs, cleared overnight in 70% ethanol, then viewed at 5X and 40X mag. In WT, LRP formed and developed, with *PDLP5pro:GUS* in overlying cells as expected (upper row). In *arf7arf19*, no initial LRP cell divisions were observed, and no *PDLP5pro:GUS* was induced (middle row). In *slr-1*, no LRP formed, and no initial divisions were observed. However, it has previously been observed that given enough time (or when heterozygous), LRP initiation can be observed (Fukaki et al., 2002), even if LRP are aborted before the first divisions are complete. This could explain why *PDLP5pro:GUS* can be observed in the endodermis of the root zone where LRP initiation typically occurs (bottom row). Careful observation of *slr-1* under 40X showed no LRP divisions in the pericycle, a phenotype which differs from shy2-2, where the first divisions do still occur prior to LRP abortion. These data support the idea that, as long as LRP initiation is attempted, the auxin targeted to LRP founder cells can induce *PDLP5* in the overlying endodermal tissue.

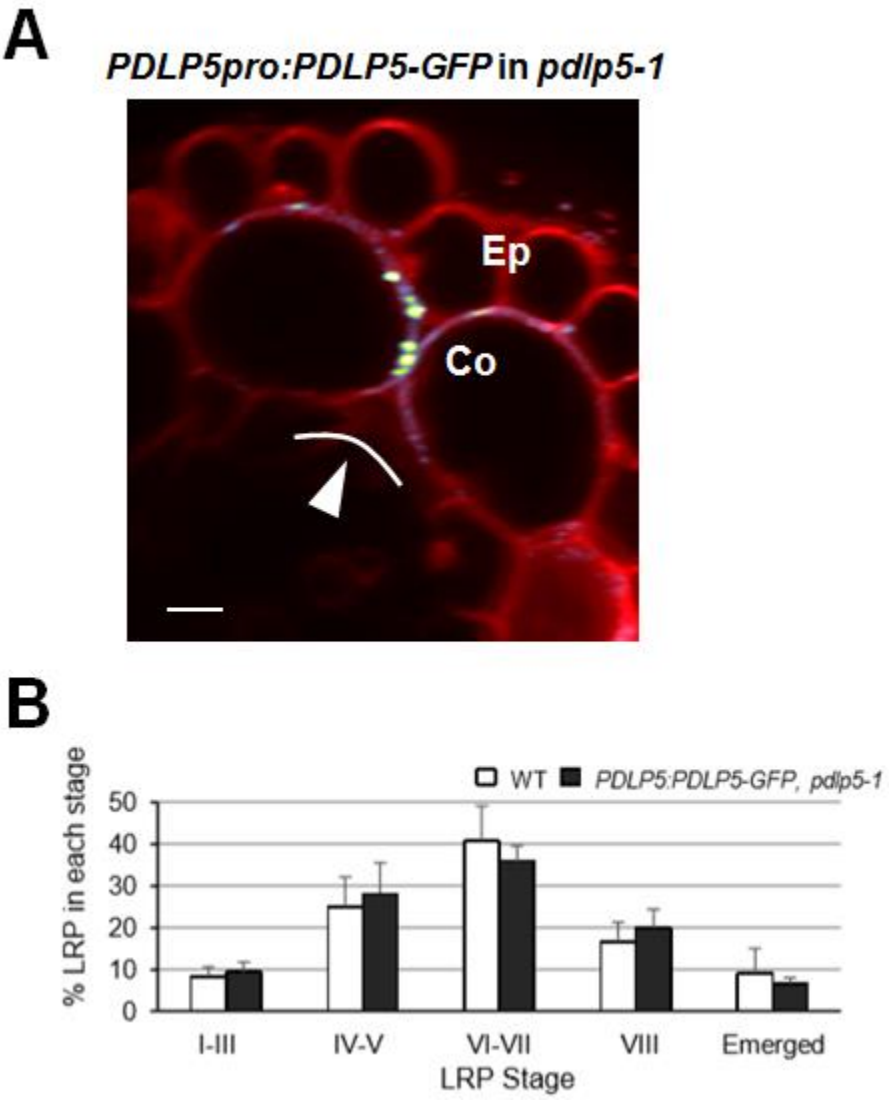

Figure C3: PDLP5-GFP has equivalent behavior to untagged PDLP5 protein.
A, PDLP5-GFP localizes to PD puncta in the *pdlp5-1* background, as it does it WT. **B**, PDLP5pro:PDLP5-GFP restores the WT LRP emergence rate in *pdlp5-1*.

Table C1 Quantification of seedlings expressing *LAX3pro:LAX3-YFP* in overlaying Co cells at 22 hours post-gravitropic stimulation.

Repeats	**WT**	***pdlp5-1***	***PDLP5OE***	***pdlp5-1*:WT**	***PDLP5OE*:WT**
Set 1	6/23 (26%)	9/20 (45%)	0/21 (0%)	1.73	0
Set 2	5/43 (12%)	10/40 (25%)	0/23 (0%)	2.08	0
Set 3	7/34 (21%)	13/37 (35%)	0/24 (0%)	1.67	0
Total # of seedlings	100	97	68		
Average	18%	33%	0%	1.83	0

Table C2 *LAX3pro:LAX3:YFP* cortical signal in *PDLP5OE* at 24 and 36 hours post-gravitropic response.

Repeats	**WT (24 hpg)**	***PDLP5OE* (24 hpg)**	***PDLP5OE*:WT (24 hpg)**	***PDLP5OE*:WT (36 hpg)**
Set 1	11/31 (36%)	4/27 (15%)	0.42	1
Set 2	22/30 (73%)	15/30 (50%)	0.68	1
Total # of seedlings	61	57		
Average	55%	33%	0.55	1

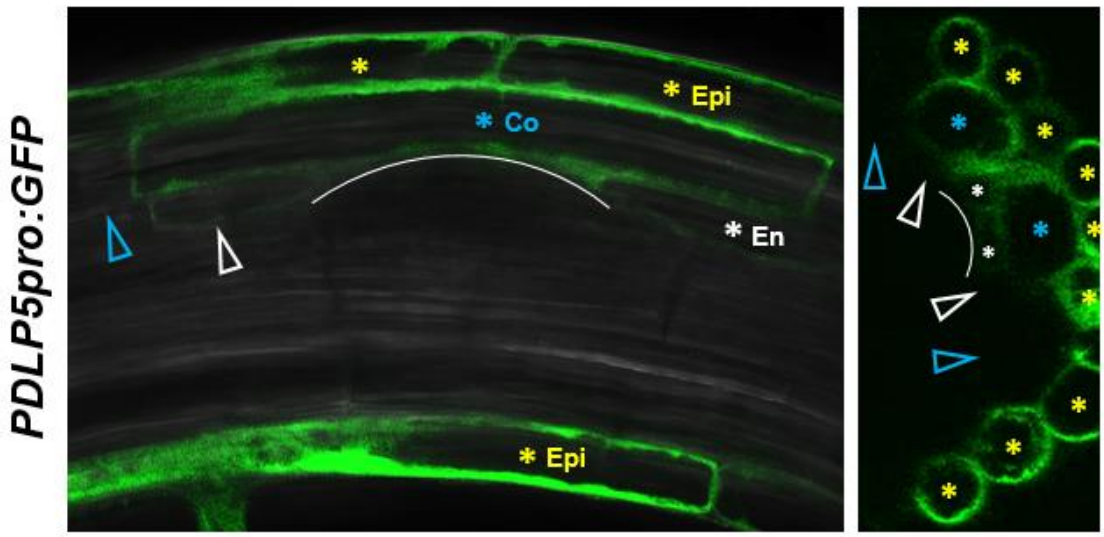

Figure C4: Free GFP does not move out of LRP-overlying endodermal and cortical cells in *PDLP5pro:GFP* roots.
Diffusible GFP is still restricted in only the overlying cells, suggesting PD closure in these cells. En, endodermis; Co, cortex; Epi, epidermis. Asterisks indicate cells with *PDLP5pro:GFP* expression; Empty arrowheads indicate the lack of GFP diffusion into neighboring cells. Images taken from one successful T2 line of *PDLP5pro:GFP*, and must be supported by data from multiple lines created in future research.

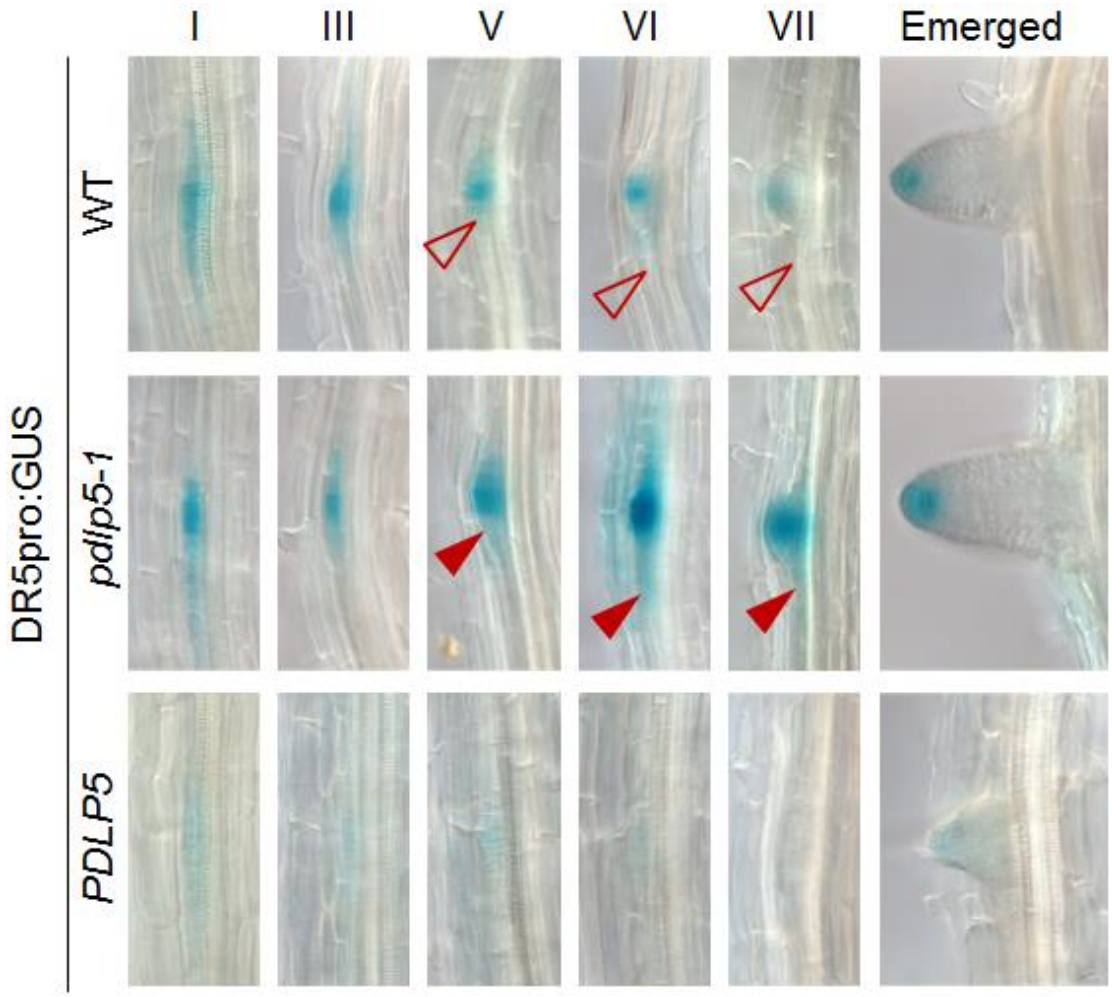

Figure C5: The range of auxin sensor *DR5:GUS* within LRP can be influenced by PDLP5 expression.
Seven-day-old Arabidopsis seedlings expressing *DR5:GUS* were GUS-stained for 25 minutes and observed under the microscope after clearing in 85% lactic acid for 2 hrs. Filled-in red arrowheads indicate observed increase of GUS spread from auxin maxima in pdlp5-1 compared to WT (empty red arrowheads). Note as well the overall decrease in GUS staining within LRP in the *PDLP5OE* background; this could be due to repressed auxin signaling via negative feedback by *PDLP5*, or due to side-effects of the SA hyper-accumulation within this background. Images taken from multiple experiments, but these effects are not always present.

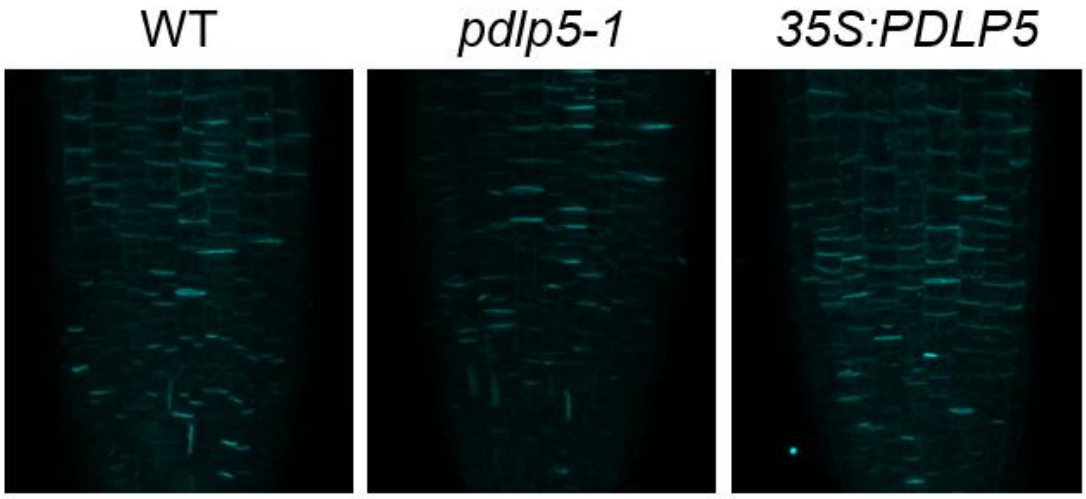

Figure C6: No overall differences in callose deposition in the roots of WT, *pdlp5-1*, and *35S:PDLP5*.
These aniline blue staining results seem to indicate that *PDLP5* expression may not effect overall callose levels in the roots as it does in shoots. Though there is a small chance that PDLP5 does not restrict root PD via callose deposition, it is more probable that more sensitive callose detection methods are required instead.